Peak and Power Reduction in Multicarrier Communication Systems

Andgart, Niklas

2005

Peak and Power Reduction in Multicarrier Communication Systems

Niklas Andgart

LUND UNIVERSITY

Ph.D. Thesis, November 25, 2005

Niklas Andgart
Department of Information Technology
Lund University
Box 118
S-221 00 Lund, Sweden
e-mail: niklas.andgart@it.lth.se
http://www.it.lth.se/

ISBN: 91-7167-035-1
ISRN: LUTEDX/TEIT-05/1032-SE

Abstract

Broadband multicarrier communication suffers from a large signal span, causing problems in both wireless and wireline systems. This is commonly referred to as a high peak to average ratio (PAR), and leads to a high power consumption, which is an important limitation in many communication systems.

This thesis puts focus on PAR reduction for wireline communication systems, in particular for the multicarrier-based DSL family. Special interest is put on the tone reservation method, where some subcarriers are used to construct a peak-canceling signal in counterphase to the signal peaks. A part of the thesis investigates properties of this method, in particular the proper placement of these subcarriers.

Applying PAR reduction in existing DSL systems raises the issue of standard compliance. This puts a number of requirements on the PAR algorithms. The thesis examines what can realistically be achieved in existing systems, with special attention given to the impact of a limited PSD mask. We derive bounds on achievable performance, address the optimization criterion, analyze implementational trade-offs, and describe guidelines for system design. For the system engineer, early indications of realistic performance can then be deduced for different designs, without need for extensive simulations for each parameter choice.

Implementation of the reduction algorithms, with the PSD mask taken into account, may efficiently be done with a proposed active-set based algorithm. The complexity is demonstrated to be well below 100 MIPS.

Contents

Preface

The work documented in this thesis has been supported and partially funded by Vinnova, through the Eureka MIDAS A110 project; by Ericsson AB; and by the Swedish Research Council. The work has been carried out in connection to these organizations, as well as in connection to TeliaSonera; the MUSE project of the European Union's 6th framework; and the Eureka BANITS project.

The thesis consists of an introduction and nine included papers. These are two journal papers, four conference contributions, and one internal report within peak to average ratio reduction, in addition to two conference contributions related to other aspects of DSL communication systems.

Note that in 2003, I changed my last name from Petersson to Andgart.

I Niklas Petersson, Albin Johansson, Per Ödling, and Per Ola Börjesson, "Analysis of tone selection for PAR reduction," in *Proc. International Conference on Information, Communications & Signal Processing*, (Singapore), Oct. 2001.

II Niklas Petersson, Albin Johansson, Per Ödling, and Per Ola Börjesson, "A performance bound on PSD-constrained PAR reduction," in *Proc. International Conference on Communications*, (Anchorage, Alaska, USA), pp. 3498–3502, May 2003.

III Niklas Andgart, Brian Krongold, Per Ödling, Albin Johansson, and Per Ola Börjesson, "PSD-constrained PAR reduction for DMT/OFDM," *EURASIP Journal on Applied Signal Processing*, vol. 2004, no. 10, pp. 1498–1507, Aug. 2004.

IV Niklas Andgart, Per Ödling, Albin Johansson, and Per Ola Börjesson, "Designing tone reservation PAR reduction," accepted for publication in *EURASIP Journal on Applied Signal Processing*.

V Per Ödling, Niklas Petersson, Albin Johansson, and Per Ola Börjesson, "How much PAR to bring to the party?," in *Proc. Nordic Signal Processing Symposium*, (Tromsø–Trondheim, Norway), Oct. 2002.

VI Karl Werner, Niklas Larsson, Niklas Andgart, Thomas Magesacher, Tore André, Torbjörn Randahl, and Per Ödling, "Moving the PAR reduction criterion into the line driver," in *Proc. European Signal Processing Conference*, (Vienna, Austria), Sept. 2004.

VII N. Andgart, T. Magesacher, P. Ödling, and P. O. Börjesson, "Implementation notes for PAR reduction," Internal report, Lund University, Lund, Sweden, Dec. 2003.

VIII Daniel Landström, Niklas Petersson, Per Ödling, and Per Ola Börjesson, "OFDM frame synchronization for dispersive channels," in *Proc. International Symposium on Signal Processing and its Applications*, (Kuala Lumpur, Malaysia), Aug. 2001.

IX Werner Henkel, Georg Tauböck, Per Ödling, Per Ola Börjesson, Niklas Petersson, and Albin Johansson, "The cyclic prefix of OFDM/DMT – an analysis," in *Proc. International Zurich Seminar on Broadband Communications*, (Zurich, Switzerland), Feb. 2002.

Acknowledgments

I first met my two supervisors, Professor Per Ola Börjesson and Professor Per Ödling, in 1999, just before leaving for my Master's thesis at University of California at Berkeley. The discussions with Per Ola and Per in the early summer of 1999, and the friendly atmosphere along with the people at Vehicle Dynamics Lab in Berkeley led me to start graduate studies upon my return to Sweden.

Since the spring of 2000, I have worked with Per Ola and Per, first at the department of Electroscience, and later at the department of Information Technology. During this whole time, Per Ola has generously shared his broad knowledge and research experience, as well as given inspiring ideas about new angles of the research. Per, being my other supervisor, makes a great team together with Per Ola. With Per, I have had numerous valuable discussions about ideas, how to carry out the research and, not the least, how to present it. Per's broad contact network with industry has given useful insights in what the research should aim at.

I would also like to thank all past and present colleagues, both in the signal processing group as well as in the departments of Electroscience and Information Technology. In particular, I would like to thank Dr. Daniel Landström and Thomas Magesacher for all discussions and joint work.

During my PhD studies, we have had a cooperation with the Access Signal Processing Laboratory at Ericsson AB. Working in this environment—there combining industrial and academic perspectives—has given birth to

interesting research aspects. At Ericsson I have worked a lot with Albin Johansson, who in parallel to his Ericsson work also is a part-time graduate student. Albin's engagement and broad industrial knowledge has been most useful in the research. Among other people in the lab, I want to mention Dr. Robert Baldemair, Tore André and Dr. Jaume Rius I Riu for interesting discussions, and Henrik Almeida for providing the possibility to take part in Ericsson's R&D.

After my licentiate thesis in November 2002, I got the opportunity to cooperate with Dr. Brian Krongold who acted as opponent on the thesis, and in 2004, I visited him a number of months at Cubin Lab at Melbourne University. In addition to this I have also had the opportunity to visit Forschungszentrum Telekommunikation Wien in Austria.

Finally, my warm thanks go to my parents for all support during all years, and to Anna and our son, for all their love and encouragement.

Niklas

October 2005

1

Introduction

Information and communication are two of the words that characterize today's society. With the continuously improving techniques for information transmission, people can communicate more, faster, cheaper, and in new ways. This, in turn, leads to an even larger demand for even better techniques. Over the years, many different communication schemes have emerged, suitable for different scenarios. Whether the intended application is phone conversation or web browsing, originating from mobile or fixed locations, with emphasis on high speed or reliable transmission, different solutions have been suggested, to match the requirements and limitations in each case.

What most schemes have in common, independent of the scenario, is the *digital* representation of the information. The rapid improvement of fast and cheap digital processing power, better use of the resources, and interference robustness, make digital communication the dominating choice in new communication systems.

In this thesis, we focus on digital communication over copper telephone lines, so called *digital subscriber lines* (DSL). These methods give the possibility of using cheap lines (normally pre-existing and paid for since long) to provide high-speed communication. A suitable technique for this environment is *multicarrier modulation*.

This first chapter will give an introduction to multicarrier systems, and to problems arising due to the high signal peaks in these systems. Some

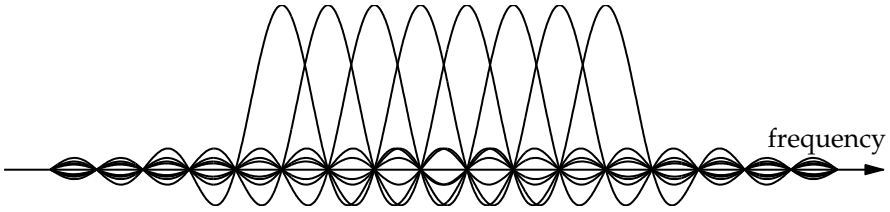

Figure 1.1: Placement of subcarriers for an OFDM system with $N = 8$ subcarriers. The zero crossings of the sinc-shaped frequency function lead to orthogonality between the subcarriers.

approaches to handle signal peaks are summarized, and in the end of the chapter, we view one of the methods in more detail. This method, tone reservation, will remain in focus throughout the thesis.

1.1 Multicarrier systems

Communication by multicarrier modulation has in the recent years become a widely spread basis for data communication. Today, wireless systems using multicarrier modulation span from wireless personal networks, such as IEEE 802.11a [1] and Hiperlan 2 [2], to broadcast radio and television using the DAB [3] and DVB-T standards [4]. For wireline systems, the technique has gained much interest by the increasing use of *digital subscriber lines* (DSL) [5], providing broadband access on existing telephone lines. Multicarrier systems are usually referred to as *orthogonal frequency division multiplexing* (OFDM) for the wireless case, and *discrete multitone* (DMT) for wireline applications.

1.1.1 The multicarrier concept

Multicarrier systems efficiently use the available frequency band by dividing it into N different subcarriers. Normally, placing carriers tightly would cause interference between the carriers due to the slow decay of the sidelobes, but when placed at proper distance from each other, the orthogonality in the receiver is maintained between the subcarriers, see Figure 1.1. Looking at the top of the main lobe of one of the subcarriers, the spectrum (when taken over an appropriate time window) of all of the $N - 1$ other subcarriers will have a zero crossing at this frequency. Either increasing or decreasing the subcarrier spacing would introduce *intercarrier interference* (ICI).

The use of efficient FFT algorithms and improvements in digital signal processing circuitry have made it possible to easily implement multicarrier

modulation techniques [6–9], as the IFFT operation efficiently places the subcarriers at the desired distance from each other, without need for many different oscillators. In the small frequency interval occupied by each subcarrier, the channel frequency response is essentially constant and can be considered as a flat fading channel with additive noise. This will simplify the channel equalization, as this can be implemented by a simple division in the frequency domain.

For certain applications, the channel characteristics can be considered static over several symbols. This is especially the case in wireline systems, where these characteristics vary slowly. The channel can then be efficiently used by letting the power on each of the subchannels be determined by their respective resulting *signal to noise ratio* (SNR). In order to use the channel as efficiently as possible, so called water filling should be applied, distributing more power to good channels (high channel SNR), and less power to bad channels [10, 11]. Similarly, the number of bits per subcarrier, the bitloading, can easily be varied between the subcarriers depending on their individual SNR:s [12].

1.1.2 Communication block-scheme

The basic parts of a typical OFDM or DMT system are shown in Figure 1.2. Starting with an information sequence at the beginning of the data path in the upper left of the figure, the first block in the block diagram maps the information bits to weights on the different subcarriers. Typically some kind of QAM constellation is used, where the number of bits per subcarrier depends on the system and the effective SNR. In noisy wireless systems, lower size constellations such as 4-QAM (2 bits) may be used, while wireline systems with very high SNR, such as *asymmetric digital subscriber line* (ADSL), use up to 15 bits per subcarrier [13]. This data representation in the frequency domain is transformed into the time domain by an N-point IFFT. By this transformation, the data will be assigned to orthogonal subcarriers.

To prevent consecutive symbols from disturbing each other through *intersymbol interference* (ISI) in a dispersive channel, a cyclic prefix can be added to the signal in the digital domain, after the IFFT. A copy of the last selected number of samples, 32 out of 512 in ADSL systems [13], is concatenated in front of the original data signal. The copied end of the data signal will, by the channel impulse response, affect the received signal in the beginning of the symbol. This will then make the linear convolution performed by the channel act as a circular convolution seen from the system. In the frequency domain, the circular convolution corresponds to element-wise multiplications, which will give the possibility to easily implement channel equalization on the receiver side. Since the different subcarriers can be considered as flat fading channels, the equalization can be implemented as

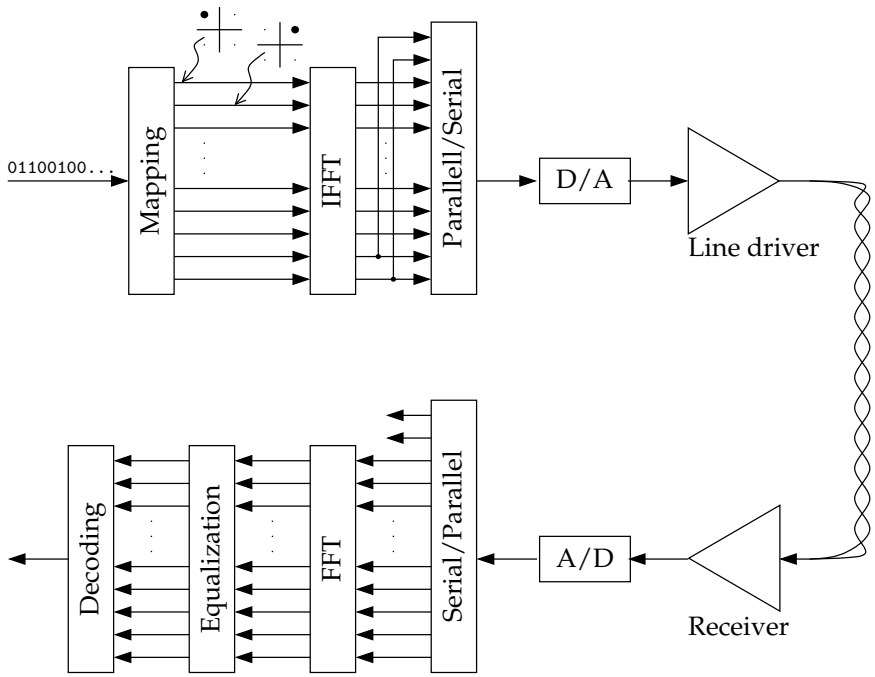

Figure 1.2: Block diagram of a multicarrier system with cyclic prefix.

a complex division by the channel's frequency function evaluated a that frequency. Using the cyclic prefix, both ISI and ICI can be totally avoided. By exploiting the correlation introduced by the cyclic prefix, this information can in addition be used to synchronize the timing and frequency offset of the OFDM symbol [14–17], Paper VIII [18].

The signal after the addition of the cyclic prefix is the digital representation of the signal to be transmitted over the analog channel. In a DSL system, the signal passes through upsampling and digital transmit filters to the D/A converter, and after that also analog filters. The digital and analog transmit filters, not shown in Figure 1.2, guarantee that the spectral masks are fulfilled. Finally, the signal is passed to the line driver, which is the power amplifier closest to the cable. It is this line driver and its limitations that will cause much of the problems that will be dealt with in this thesis.

The channel used in DSL systems is a twisted copper pair loop between the central office and the customer. Compared to wireless systems, this channel is stationary, making it possible to perform measurements on the

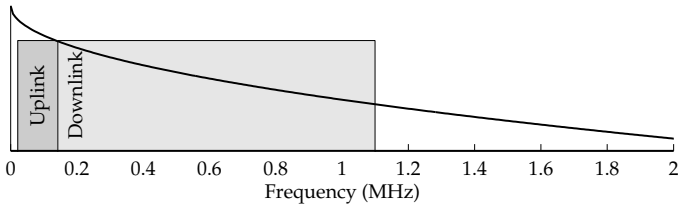

Figure 1.3: The lowest part of the spectrum is reserved for the analog telephone services. The lower parts of the remaining subcarriers are used for uplink transmission, leaving the largest number of subcarriers to downlink transmission. The decaying curve illustrates the better channel characteristics on low frequencies.

system during the start-up phase in order to measure what constellation sizes should be used on different channels. In wireless systems, different subcarriers normally carry the same number of bits, which is not the case in broadband wireline systems, where there is a large difference between the channel characteristics of the two ends of the spectrum.

Since the DMT signal is transmitted in baseband, the signal $x(t)$ transmitted on the line must be real-valued, thereby imposing a requirement for the IFFT output $x[n]$. In the frequency domain, this corresponds to Hermitian symmetry, meaning that only half of the N subcarriers can be used. This limit corresponds to the Nyquist frequency; transmitting above half the sampling frequency cannot be done maintaining the possibility to reconstruct the signal [19].

The ADSL system, described by the ITU-T standard [13], uses $N = 512$ subcarriers, with a spacing of 4.3125 kHz. This places the highest used subcarrier (number 255) at 1.1 MHz. In the frequency plan, the lowest regions are reserved for the analog telephone system, see Figure 1.3. This was what the twisted copper pairs originally were intended for [20], and it still has its own frequency portion allowing coexistence with newer digital systems. The remaining part of the spectrum is divided into up- and downlink, and we mainly consider the downlink part of an ADSL loop. Then, carriers number 33–255 are used, leaving the low part of the frequency band for analog telephony and uplink ADSL.

1.1.3 Power consumption

One of the main limiting factors in many of today's telecommunication devices is power consumption. Power consumption limits stand-by time and talk-time in cellular phones. It also limits the degree of integration in many devices. The level of integration is a very important factor in determining

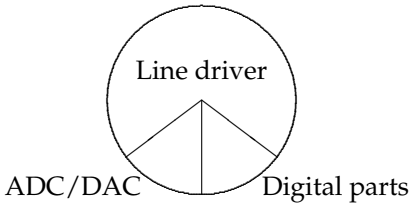

Figure 1.4: Power distribution in an ADSL transceiver.

cost, but if you make the devices too small, they become too warm and burn up, because the power dissipation is too high per unit of area or volume. A trend in system design is to reduce power consumption in analog parts by handling as much as possible in the digital domain. The field of PAR reduction is fueled by this trend.

In a wireless system, the advantage of reducing power consumption is obvious. A more power-efficient system leads to longer standby and operation times, or smaller and lighter handheld devices. For wireline approaches, the advantages are perhaps at first sight not as clear. Here the problem is not to *supply* the unit with power, but rather how to *dissipate* the power. What the end-customer has to pay for ADSL is much determined by the cost that the telecommunications operator has, which, in turn, depends on the level of integration of the central-office end (CO) modem. Space requirements, maintenance, and price of the modem per line all depend on how many lines of ADSL that fit onto a single line card. The number of lines per line card is limited by the power consumption of the line card and its ability to dissipate this power.

For ADSL transceivers, the development of digital processing has led to a situation where the digital parts of the system, all parts before the D/A converter in Figure 1.2, stands for as little as about 15%[1] of the total power consumption, see Figure 1.4. About the same amount is consumed by analog-to-digital and digital-to-analog converters. Meanwhile, the power efficiency of the analog front-end has not undergone as rapid an improvement, causing the line driver to be responsible for the major part, about 70%, of the total power consumption. It is clear that much effort could be spent in the digital processing, if this would lower the power dissipation in the line driver. However, knowing that we should focus on the line driver, we need to figure out how we can reduce its power consumption. It turns out that this essentially is determined by the line driver supply voltage. In turn, this depends on the properties of the input signal. If the signal has a high

[1]The numbers are depending on target hardware.

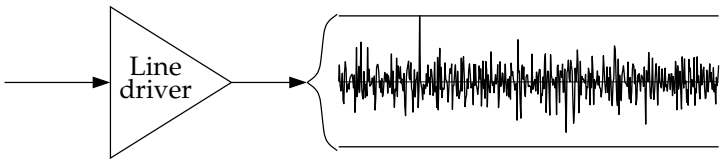

Figure 1.5: Region in which the line driver has to be linear in order not to distort the signal.

dynamic range, the line driver and its supply voltage will have to be dimensioned to achieve linear amplification in the whole span, see Figure 1.5. (This will also impact the choice of D/A converter, which then needs to operate over a wider range.) Modifying the data signal to have lower peak levels, without affecting the data transmission quality, will give the opportunity to reduce the supply voltage to the line driver, thus saving power.

1.2 Peak to average ratio

The previous section showed the importance of the amplitude span of the data signal. The desired situation would be when the signal has a low peak value, allowing a lower supply voltage to the system, but at the same time a high average power, giving high SNR and thereby high bitrate. However, one of the problems with multicarrier modulation is that the resulting data signal has large amplitude variations.

1.2.1 Multicarrier signal dynamics

The IFFT block performing the conversion from frequency domain to time domain is the main cause of the wide signal dynamics. Due to the data dependence, each one of the subcarriers can be considered to have independent amplitude and phase, given by X_k. The IFFT operation,

$$x[n] = \frac{1}{\sqrt{N}} \sum_{k=0}^{N-1} X_k e^{j2\pi nk/N}, \tag{1.1}$$

then gives the value of sample $x[n]$ as a sum of a large number independent terms. Since the terms are independent, although not having identical distributions, the Lyapunov condition of the central limit theorem can be used [21]. Then it can be shown that the distribution of $x[n]$ approaches a Gaussian random variable [22]. That this also holds in the time-continuous case has been shown in [23].

1.2.2 Definition of PAR

The desired situation with a low amplitude span, and a high SNR resulting from a high average power, leads to a natural approach of looking at the ratio between these two factors, the *peak to average ratio* (PAR), which is a measurement of the amplitude variation of a signal. As a basic definition of the peak to average ratio of a zero-mean signal, we use the following expression where we consider a time interval $\mathcal{T}$:

$$\mathrm{PAR}\{x(t), \mathcal{T}\} = \frac{\max\limits_{t\in\mathcal{T}} |x(t)|^2}{\sigma^2}. \tag{1.2}$$

In the denominator, σ^2 denotes the variance of $x(t)$, $E(|x(t)|^2)$, when viewing $x(t)$ as a random signal. The notations *peak to average power ratio* (PAPR) and for passband signals also *peak to mean envelope power ratio* (PMEMR) are sometimes seen in the literature, having the same meaning as PAR. Another measure of the dynamics of the signal is the *crest factor* (CF), where $\mathrm{CF} = \sqrt{\mathrm{PAR}}$, showing the relationship in amplitude rather than working in the power domain.

Depending on the kind of signal, the time interval $\mathcal{T}$ may be defined in different ways. If the signal is physically limited or in some other way guaranteed to never exceed a certain level, the observation interval $\mathcal{T}$ can be chosen arbitrarily long. However, let us consider the multicarrier signal. The maximum signal peak that can be generated is when all subcarriers line up constructively on the same position. Using $N/2$ subcarriers, each having amplitude A, this would result in a signal peak of height $AN/2$. With an average power per subcarrier of $A^2/2$, we would then have a maximum PAR of

$$\frac{\left(\frac{AN}{2}\right)^2}{\frac{N}{2}\cdot\frac{A^2}{2}} = N. \tag{1.3}$$

For an ADSL system with $N = 512$, this corresponds to a PAR level as high as $10\log_{10} 512 = 27\,\mathrm{dB}$ (crest factor 22.6). However, this high value occurs only when all tones line up in phase at the same sample, an event with a very small probability. In this case, the PAR is better viewed in a probabilistic sense, *i.e.*, the probability of the signal exceeding a certain level during a limited time interval $\mathcal{T}$. Similarly, if we consider a true Gaussian signal, there is a probability of having arbitrarily high signal peaks and the PAR has to be viewed in this statistical sense. Commonly, the interval $\mathcal{T}$ will be chosen as one symbol interval. We will then obtain the *symbol clip probability*: the probability that the PAR in (1.2) is above a certain level during one symbol period.

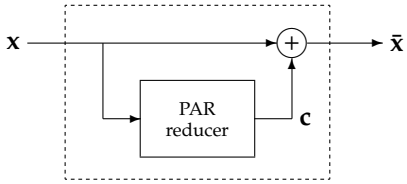

Figure 1.6: Additive PAR reduction, where a PAR reduction signal, $\mathbf{c}$, is added to counteract the peaks in $\mathbf{x}$.

1.3 PAR reduction methods

Considered as one of the main drawbacks with multicarrier modulation, the PAR problem has received significant interest. In this section, some different methods to address the problem are summarized. Since we put special focus on DSL systems, we choose to divide the algorithms into two groups according to their suitability for this application: *transparent* and *non-transparent*, depending on whether they can be implemented in standardized systems.

1.3.1 Transparent methods

The transparent methods can be implemented in existing standards. If the transmitter incorporates one of the schemes, the receiver does not have to know about its existence. Similarly, the receiver can use a method unknown to the transmitter.

A PAR-reduced signal $\bar{\mathbf{x}}$, which should have a low amplitude span, is transmitted instead of the original data signal $\mathbf{x}$. We can view the creation of $\bar{\mathbf{x}}$ as an additive PAR reduction method, see Figure 1.6, where a reduction signal $\mathbf{c}$ is added to the data signal. Either this reduction signal is explicitly generated and added by an algorithm, such as *tone reservation* or *active constellation extension*, or follows implicitly as the difference between $\mathbf{x}$ and $\bar{\mathbf{x}}$ when clipping the signal $\mathbf{x}$. In either case, what is important is that the receiver can decode the information as it was before the PAR reduction, *i.e.*, that the added reduction signal $\mathbf{c}$ is essentially *transparent* to the receiver.

In order for the resulting signal $\bar{\mathbf{x}}$ to be limited in amplitude, the reduction signal $\mathbf{c}$ must follow the shape of the data signal. If the data signal has a high peak at one location, the reduction signal must have a low value there. Figure 1.7 shows an example where the symbol $\mathbf{x}$ represented by the solid line is to be PAR-reduced. If the reduction signal then is within the shaded area, the resulting signal will be within the desired span. The figure shows the available freedom in the creation of the reduction signal. This signal has to approximate the main look of the peaks, not the whole data signal, and it also needs to avoid the creation of any unwanted peaks in new locations.

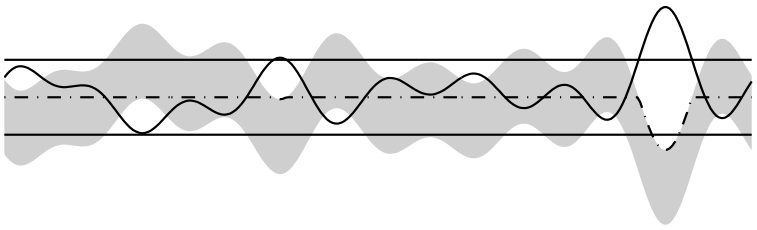

Figure 1.7: The shaded area shows the allowed region for the reduction signal **c** from Figure 1.6. In order to keep the resulting signal within the desired amplitude span between the two straight lines, the reduction signal is added to the data signal **x**, shown by the solid curve.

Clipping and noise shaping

A simple approach to PAR reduction is to basically clip the parts of the signal that are outside the allowed region. Using amplifiers with saturation levels below the signal span will automatically cause the signal to be clipped. In the model in Figure 1.6, this corresponds to a reduction signal equal to the negative of the parts of the signal peaks that are outside the allowed region; see the dash-dotted signal in Figure 1.7. This impulse-like reduction signal will lead to distortion of other subcarriers as well as out-of-band distortion if the clip is applied to an oversampled signal. Filtering can be applied to lower the out-of-band distortion and shape the in-band noise [24–26].

Clip mitigation on the receiver side

There is also a possibility of clips on the receiver side, for example when the A/D converter is saturated. Even though this clip also will lower the SNR of the received symbol, the properties of the clip can be estimated by measuring some of the unused subcarriers. If the correct position and amplitude of the clip is estimated, this distortion signal can be subtracted to reconstruct the signal before the clip [27]. This method can be applied to the receiver side, without transmitter knowledge. There may also be a possibility to correct for transmitter-side clips in the receiver [28, 29], although this approach is more sensitive for noise and channel modeling errors.

Tone reservation

The tone reservation method [27, 30, 31] takes advantage of the orthogonality between the different subcarriers. If the information bits are modulated

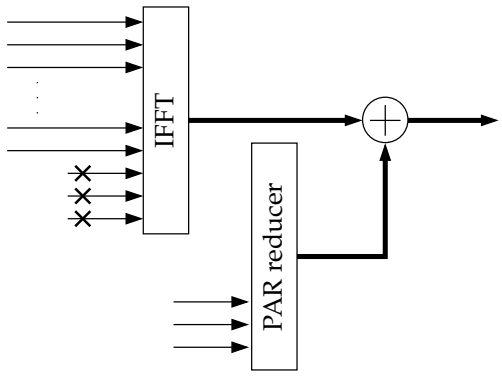

Figure 1.8: Tone reservation. Certain subcarriers are not used for transmitting data, but are instead used to create a reduction signal.

on certain subcarriers, other unused subcarriers can be used as a basis for the reduction signal, see Figure 1.8, avoiding any disturbance on the data-carrying tones.

The set of data-carrying subcarriers must be known to both the transmitter and receiver. On subcarriers not carrying data, the transmitter is free to create a reduction signal. Working with wireline transmission, there is often so strong attenuation on high subcarriers that these cannot be used. Otherwise, the transmitter can simply choose not to transmit data on certain tones, thereby sacrificing some data capacity in favor of PAR reduction, see Paper I [32] and Paper V [33]. Since the transmitter is free to decide the number of bits on the tones, this PAR reduction method is possible to include in present ADSL standards [13, 34, 35].

The construction of the reduction signal based on the reserved tones can be done in different ways, with different complexities. Either iterative approaches can be used [31, 36], or methods without several iterations on the full symbol [37, 38]. Some recent methods [39–41], see also Paper III [42], use a lower complexity linear programming approach based on the active set method [43].

Active constellation extension

With PAR reduction by active constellation extension [41, 44, 45], the points on the constellation boundary can be moved according to Figure 1.9 in order to create the reduction signal $\mathbf{c}$. The advantage with this method is that many subcarriers can be used for PAR reduction, while the decision regions for the receiver do not change. Thus, in order to include this reduction

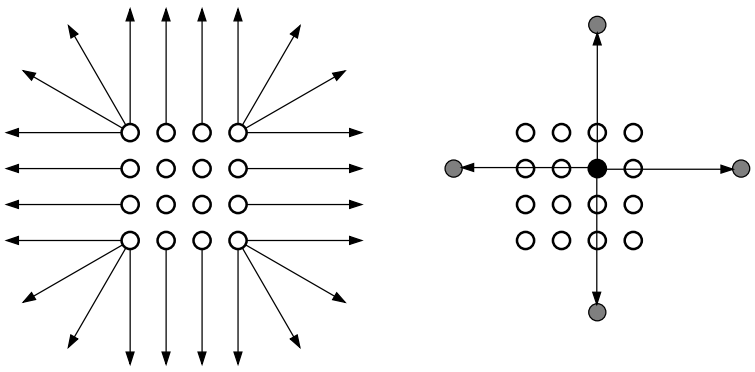

Figure 1.9: Active constellation extension (left) and tone injection (right).

method, neither receivers nor the standard have to be changed. However, the system could possibly be affected by the change of constellation points, since this affects the Euclidean distance metrics used in systems where soft decoding is employed. For systems having very large constellations, such as DSL systems, only a small part of the constellation points are placed on the edges and possible to move, so in these cases the reduction gain is not as good.

1.3.2 Non-transparent methods

These methods require new standardization and include a broader variety of PAR reduction algorithms. Typically, reduction algorithms that need the transmission of *side information* from one side to the other about what operations are performed on the data signal, or are based on a new coding concept, are placed in this category.

Scaling

A simple solution is a scaling operation. Symbols that have too high peaks are scaled by some factor between 0 and 1, in fixed or arbitrary steps [24]. For signal constellations with points of different magnitudes, e.g. QAM constellations with more than four signal points, the transmitter needs to convey side information about how the signal was scaled. The advantage with this method is the simplicity, but it suffers from lowered SNR due to the scaling.

Selected mapping & partial transmit sequences

In the selected mapping method, one single data vector can have multiple representations in the transmit signal. The signal is re-encoded if it has a too high peak after the IFFT [46, 47]. The frequency coefficients are shifted in phase by a fixed known phase transformation, and then the IFFT is performed once again. Since the phase transformation completely rearranges the time-domain signal, the probability that this second symbol now has a peak is practically the same as for the first symbol, and they can be considered as independent. This scheme can be iterated several times, but demands the complexity of an extra IFFT per iteration. Also, information about which transform is used has to be transmitted.

The partial transmit sequences method is similar to the previous, but divides the frequency vector into smaller blocks before applying the phase transformations [48, 49]. Thereby, some of the complexity of the several full IFFT operations can be avoided.

Tone injection

The tone injection method, presented in [31, 50], is similar to the active constellation extension, but not only the outer constellation points have alternative positions, see Figure 1.9. The receiver can perform a modulo operation (mod 4 in the figure) to map the points back to the original position.

This method can efficiently reduce PAR, since so many frequencies are used, but requires knowledge on the receiver side of how to decode the signal, as well as standardization changes. Like the active constellation extension, it demands extra IFFT operations, which implies an increased complexity.

Transmission of only low-PAR sequences

One way to reduce the PAR level of the signal is to be sure not to transmit any signals with high peak values. This can be achieved using block coders, where only those codewords that have low PAR are transmitted. This method can achieve very low PAR levels, for example using Golay complementary sequences [51–53]. Another method is the OFDM necklace approach found in [54], where combinatorial algorithms are used to generate the low-PAR sequences. Using any of these methods, the PAR is deterministically bounded to some value, rather than, in the previously described approaches, only having a low probability of exceeding a certain value. The disadvantage with these approaches is generally that the fraction of sequences with low PAR is small. This leads to a low code rate for the large symbols which typically exist in wireline systems.

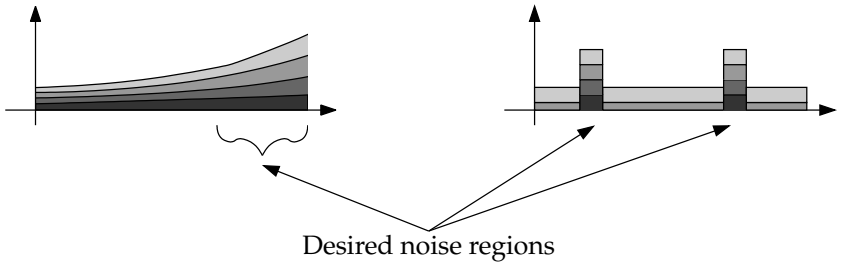

Figure 1.10: Moving distortion to desired frequency regions. Left: Noise shaping. Right: Tone reservation.

A promising candidate that guarantees a low PAR, while at the same time is not being limited to only small-scale systems, is a lattice-based transmission scheme suggested by [55, 56]. This diverges from the use of sinusoidal basis functions, so it is no longer a DMT system.

1.3.3 Comparing different schemes

The different reduction methods described here have their individual advantages and drawbacks. Some methods can be combined to build a system achieving better total reduction performance and it has been suggested that such a combination is the best choice [57].

In order to judge the performance of two different schemes, we need to have in mind that they affect the signal in different ways. In Figure 1.10, the schematic behavior of the distortion using a noise shaper (clipping followed by noise shaping) and tone reservation is depicted. The left part shows the resulting noise for four different clip levels when a noise shaper is used. The lower lines correspond to higher clip levels and as the clip level is decreased, the noise level increases in particular at the higher frequencies. The right part of the picture shows the behavior for tone reservation; here the noise is concentrated to the unused tones. For the two highest clip levels, there is no noise at the used frequencies — the PAR reduction is non-distorting, but as the clip level decreases, the noise will increase over the whole frequency band.

This clip noise should be considered when calculating how high bitrate the system can support given a certain system scenario and line driver supply voltage. However, to get from clip noise to bit rate, a thorough implementation of the coding chain in the transmitter and receiver is necessary, as the statistics of the clip noise is different between different reduction algo-

rithms [58]. When using PAR reduction algorithms, the shape of clips will not be the same as the shape of a clip when viewing an unreduced signal. For reduced signals, the clips will typically be smaller, but may occur more frequently than for an unreduced signal.

1.4 A closer look on tone reservation

Of the different PAR reduction approaches outlined in the previous section, we focus primarily on the tone reservation method introduced by Gatherer & Polley [27] and Tellado [30, 31]. This section will discuss definitions and optimization criteria when using tone reservation, and the included papers in the thesis go further in examining performance and implementation of the algorithm.

1.4.1 Mathematical model

We work with discrete-time signals, with an oversampling factor $L \geq 1$. Formulating a matrix notation for the reduction model, the addition of the reduction signal $\mathbf{c}$ in Figure 1.6 is written as

$$\bar{\mathbf{x}}_L = \mathbf{x}_L + \mathbf{c}_L = \mathbf{x}_L + \check{\mathbf{Q}}_L \check{\mathbf{C}}. \tag{1.4}$$

The $\check{\mathbf{Q}}_L$ matrix is an $NL \times 2U$ matrix with sine and cosine basis vectors for the frequencies specified by the U reserved tones. The $\check{\mathbf{C}}$ vector is determined by the reduction algorithm, giving the weight on each of the basis functions in $\check{\mathbf{Q}}_L$.

Which U tones to exclude from data transmission, and instead use for PAR reduction, is a choice for the system designer. Both reduction performance and data rate depend on this, which will be further analyzed in Papers I [32] and V [33]. As a general rule, a spread-out placement of the tones gives a better reduction performance, and certain structured choices, such as only choosing odd or even-numbered tones, can be shown to limit the reduction performance [59].

1.4.2 Definition of PAR for reduced signals

Following the definition of PAR in (1.2), the expression for the PAR of the reduced signal $\bar{\mathbf{x}}_L = \mathbf{x}_L + \mathbf{c}_L$ should include the power of the reduction signal in the denominator. However, if this were the case, a decrease in PAR level could be caused by an increase in the total power, without any reduction of the peak power. An example is shown in Figure 1.11, where the right,

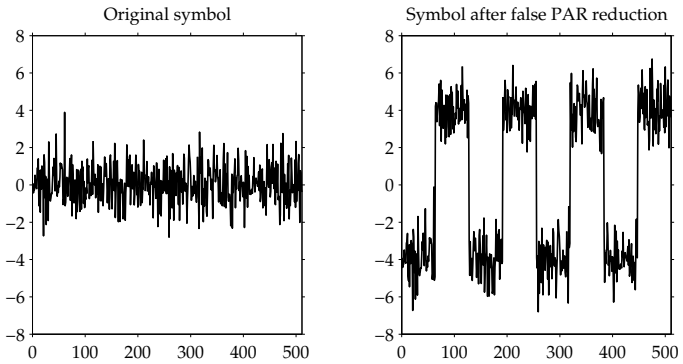

Figure 1.11: Example of false PAR reduction. The left unreduced symbol has a PAR level of 11.8 dB. After the addition of a large square wave, the right symbol would have a PAR level of only 4.3 dB, if the reduction signal is included in the denominator. Using the PAR definition from (1.5) gives a PAR level of 16.7 dB, which better reflects the increased peak magnitude.

PAR-reduced, signal would have a lower PAR value after the addition of a large square wave. Thus, we define the PAR after reduction as

$$\mathrm{PAR} = \frac{\max |\mathbf{x}_L + \mathbf{c}_L|^2}{\sigma^2}, \tag{1.5}$$

with σ^2 denoting the variance of the $\mathbf{x}_L$ vector. This is not a true peak to average ratio of a single signal, since it is a function of the signal both before and after reduction. This definition will, however, describe how much average signal power it is possible to use under a certain peak power constraint. If this PAR level can be lowered, we can use a higher average signal to a fixed peak level. Then the SNR on each frequency will increase, and thereby also the number of data bits per subcarrier, see Paper V [33].

1.4.3 Optimization criteria

Commonly, PAR or one of the other corresponding notations from Section 1.2.2 are used when combating the high signal dynamics. However, in Section 1.3.3, we saw that what is important for a system is the amount of distortion that is applied by, *e.g.*, clip noise. This raises the question whether it may be more appropriate to consider another metric than the PAR when using tone reservation.

Using the mathematical notation above, the minimization of the PAR can

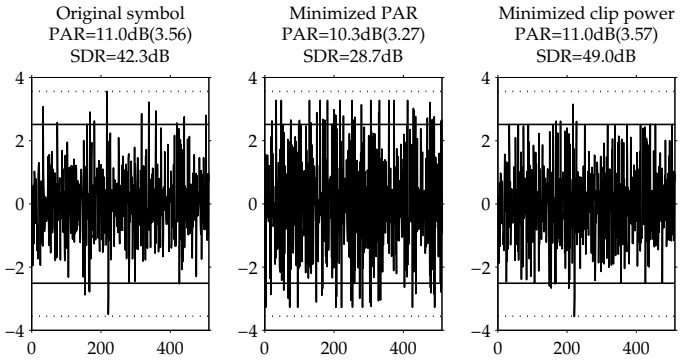

Figure 1.12: A symbol before and after PAR reduction with 10 contiguous tones and unconstrained reduction signal. No oversampling is used ($L = 1$). After minimization of the peak level the PAR value is a little bit lower, but the clipped power outside the solid lines is much higher, having a lower *signal-to-distortion ratio* (SDR). Compare to the rightmost symbol with minimized clip power.

be written as a linear program [31],

$$\begin{aligned} \underset{\check{\mathbf{C}}}{\text{minimize}} \quad & \gamma \\ \text{subject to} \quad & |\mathbf{x}_L + \check{\mathbf{Q}}_L \check{\mathbf{C}}| \leq \gamma\sigma, \end{aligned} \tag{1.6}$$

which has $2U + 1$ variables and $2NL$ constraints. The minimization of the clipped energy can be formulated as a quadratic program,

$$\begin{aligned} \underset{\check{\mathbf{C}}}{\text{minimize}} \quad & \mathbf{d}^T\mathbf{d} \\ \text{subject to} \quad & \mathbf{x}_L + \check{\mathbf{Q}}_L \check{\mathbf{C}} \leq \gamma_{\text{target}}\sigma - \mathbf{d}, \end{aligned} \tag{1.7}$$

with $\mathbf{d}$ denoting the distortion as the difference between the signals before and after the clip. This quadratic program has $N + 2U$ variables and $2NL$ constraints. With a much larger number of variables ($N \gg U$), this problem formulation has significantly higher complexity.

An example where there is a difference between minimizing PAR and minimizing clipped power can be seen in Figure 1.12. The leftmost unreduced symbol has a peak value that is higher than for the middle symbol, which is the same symbol after peak reduction with block-placed tones. However, if a clip level is chosen at the solid lines, the middle signal would have significantly higher clipped power. The signal to the right has the lowest clip power, but still a high PAR level. As seen, PAR reduction can in some cases increase the clip power. The reason for the bad result of this example is that the algorithm was pushed too hard with an unrealistic level

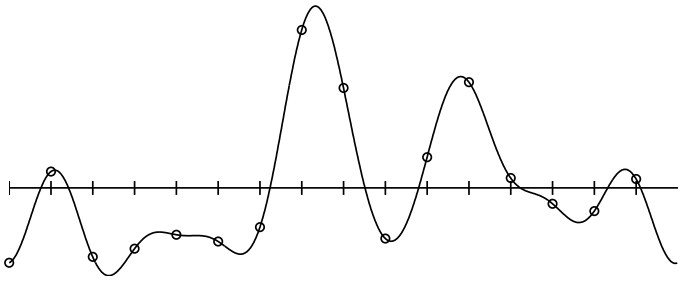

Figure 1.13: After oversampling, the signal has a peak value that is at least as high as before oversampling.

on the target PAR. Combining this with a bad selection of reduction tones may lead to unexpected results. However, with more realistic requirements on the algorithms, the resulting performance difference between the two approaches is small, and considering that this is a less complex operation, reduction of PAR is a realistic choice [59].

1.4.4 Peak regrowth

Looking only at the values of the sampled signal does not tell us that the signal in continuous-time, after the D/A converter and analog front-end, will have the same peak value. Consider Figure 1.13, where the peak value of the analog signal is higher than its sampled version. The peak value of the sampled signal only specifies a lower limit on the peak value of the analog signal.

To get a better control of the behavior between the sampling instants in the critically sampled signal, working on an oversampled signal is a viable option. An oversampling factor of 2 to 8 is commonly used [31, 41, 60]. The remaining peak regrowth in the analog signal after a certain level of oversampling can be bounded [61, 62] as

$$\max_{0 \le t \le T_{\text{sym}}} |x(t)| \;\le\; \frac{1}{\cos \frac{\pi}{2L}} \cdot \max_{0 \le n \le NL-1} |x[n/L]|, \tag{1.8}$$

where $x[n/L]$ denotes the L times oversampled signal. As an example, using 4 or 8 times oversampling, the maximum regrowth would be 0.69 dB or 0.17 dB, respectively. However, with oversampled signals, the dimensions of the problems increase, and thereby also the complexity of the reduction algorithms. Thus, a larger oversampling factor than necessary should be avoided.

The reconstruction shown in Figure 1.13 is based on a sinc interpolation, with no frequency content outside half the original sampling frequency. In

a practical implementation in a DSL system, the interpolation path often includes several steps with upsampling and filtering before the D/A converter, and an analog interpolation filter afterwards (see the appendix in Paper VII for an example of this). These filters present in the system can then be incorporated into the model and the reduction criterion [60,63]. For an even better correspondence to the true system behavior, the characteristics of the line driver could be taken into account, see Paper VI [64].

2

Summary of included papers

2.1 Tone reservation performance in DMT systems

Of the different PAR reduction approaches available to multicarrier systems, tone reservation [27, 30, 31] is the main focus in this work. The method is especially suitable to wireline communication systems, where the channel characteristics vary over the frequency band and a certain portion of the spectrum may show low communication performance. In standardized systems [13, 34, 35], there is also a possibility of incorporating this method transparently to the receiver side.

The tone reservation method is an additive reduction method, where a reduction signal $\mathbf{c}$ is added to the data signal $\mathbf{x}$, generating a resulting signal $\bar{\mathbf{x}}$; recapitulate Figure 1.6. The various parts of this thesis address the model in Figure 1.6, by answering a number of questions: Which signal $\mathbf{x}$ is the correct signal to apply PAR reduction to? How do we generate $\mathbf{c}$ in the best way? How can we be sure that the resulting signal $\bar{\mathbf{x}}$ gives a good representation of the true system behavior? What reduction can be achieved?

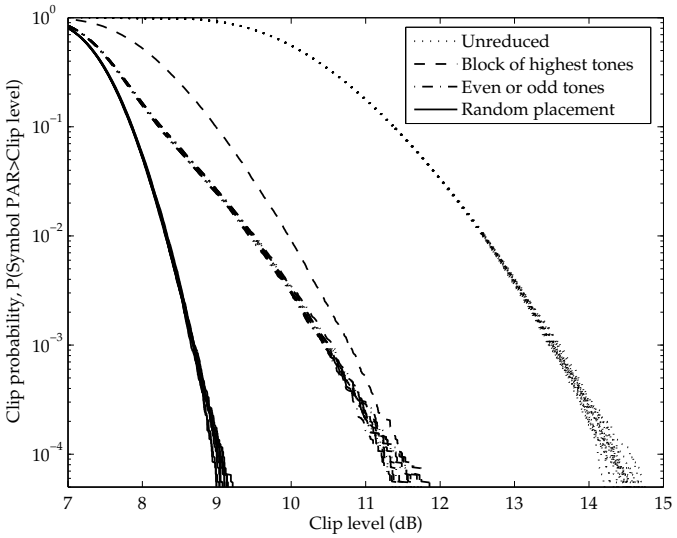

Figure 2.1: Symbol clip probability for different tone placement methods. 12 PAR reduction tones with unlimited added energy. For the random and purely odd/oven placements, 10 different placement realizations are shown.

2.1.1 Paper I: Analysis of Tone Selection for PAR Reduction

The reduction signal **c** is constructed from a set of subcarriers not used for data transmission. A natural question is how this set of reduction tones should be chosen.

This is what we start out with in Paper I [32], where the choice of reduction tones is examined. Since the number of alternative placements is large for a full-size system, a small system is evaluated with all possible tone set choices. It turns out that most of the placement choices make a good job, although some combinations with a strict ordering of the tones give worse performance. Simulations with full-size systems indicate as well that most of the alternatives tend to be acceptable, as long as some structured placements are avoided.

An example of PAR reduction performance is shown in Figure 2.1 (Figure 5 in Paper I), where 12 out of the 223 available tones are used for PAR reduction. The vertical axis shows the probability that a symbol has a peak value above the PAR level specified on the horizontal axis.

We see that the different randomly chosen tone sets perform better than the more properly ordered tone sets with either contiguous tones, or only even or odd tones. With only odd or only even tones, the second half of the

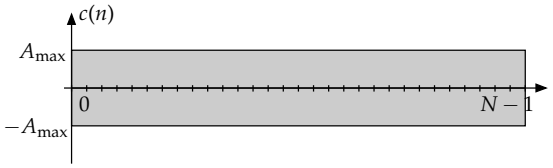

Figure 2.2: Limits for reduction signal in bound for PSD-constrained tone placement.

reduction signal will be a copy of the first half, which affects the reduction capabilities [31, 59].

The paper introduces a restriction on the magnitude of each reduction tone. Without this, violations of PSD masks may occur. For simplicity and to show the effects of this constraint, the restriction is set equal to the PSD level for the data-carrying tones. This leads to a case (shown in Figure 6 in Paper I) when the performance gain with a good tone set is almost disappeared. Essentially, only the number of tones then determines performance.

In the paper, also the situation when reduction is performed only down to a certain level is examined. Since what is measured in the PAR reduction is the worst case situations—the highest peaks that occur during a certain period of time—efforts should not be spent into improving already good results. Here the goal is to achieve a target PAR level with a minimum added reduction signal.

Although not answering all questions, this early paper observes phenomena that occur when applying tone reservation, and raises questions to be pursued in the following papers.

2.1.2 Paper II: A Performance Bound on PSD-Constrained PAR Reduction

The results in Paper I show that the performance is limited when introducing a strict PSD. Paper II [65] continues this investigation and derives a bound applicable for the PSD-constrained case. Since the magnitude for each reduction tone is limited, the size of the total reduction signal is limited to the sum of these individual magnitudes. By assuming that we can create an arbitrary reduction signal with a certain maximum magnitude $A_{\max}$, see Figure 2.2, all peaks up to a certain level can be reduced, and we end up with a bound on achievable reduction performance,

$$\gamma \geq Q^{-1}\left(\frac{1-(1-p_{\text{sym}})^{1/N}}{2}\right) - \frac{1}{\sigma}A_{\max}, \tag{2.1}$$

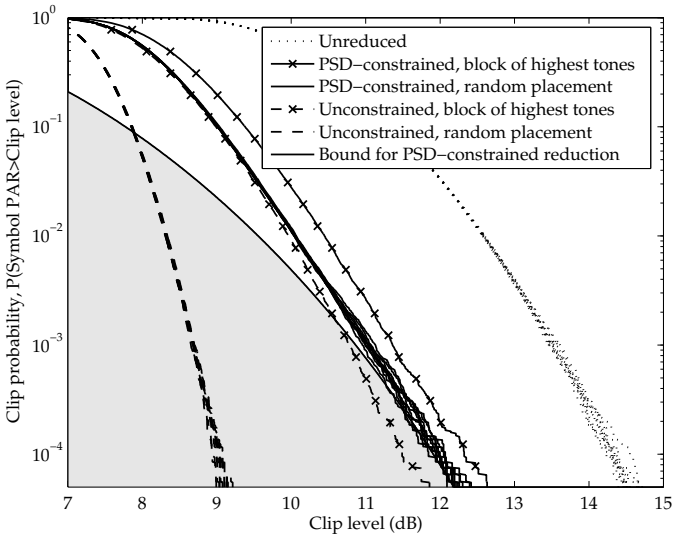

Figure 2.3: Symbol clip probability for tone sets with 12 randomly selected reduction tones. The bound for constrained power is shown as a solid line, and the simulations with PSD constraints can not go under this bound on average.

where γ denotes the minimum achievable PAR level, p_{sym} is the symbol clip probability, and σ is the variance of the signal[1].

The bound is shown with the shaded region in Figure 2.3 (Figure 5 in Paper II), also here for the case with the PSD limit the same as for the data-carrying tones. The unconstrained cases for block and random tones from Figure 2.1 are shown along with new simulations incorporating the bound. For this situation with 12 reduction tones, the bound seems to efficiently limit the reduction performance, and results for different number of tones are shown in Figure 2.4. We see that the bound sets the performance up to about 10 reduction tones, a region where the reduction tone magnitude is the limiting factor. After that, the choice of a good or bad tone placement starts to show importance, and the reduction performance is dependent on the degree of freedom in the tone set choice.

2.1.3 Paper III: PSD-Constrained PAR Reduction for DMT/OFDM

Papers I and II have used general-purpose linear programming algorithms

[1]The $Q(\cdot)$ function denotes the tail probability for a Gaussian random variable, $Q(x) = \frac{1}{\sqrt{2\pi}} \int_x^\infty e^{-x^2/2}\, dx$.

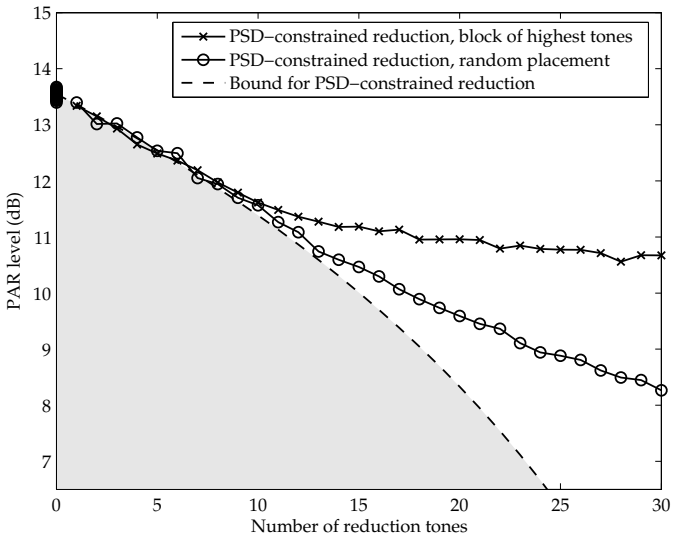

Figure 2.4: PAR level as a function of number of PAR reduction tones. The results are shown for a symbol clip probability of 10^{-3}. Up to 10 reduction tones, the difference between the placement methods is negligible, and the performance closely follows the bound.

to get the optimal solution of the linear PAR program. For implementation, an efficient algorithm is necessary, since often only a small delay may be allowed in the data transmission.

In Paper III [42], an active-set algorithm is used for PAR reduction under the PSD constraints. The active-set method [43] is an efficient scheme to solve linear programming problems, and was used for tone reservation PAR reduction in [63]. In Paper III, it is extended to incorporate also PSD constraints. The basic technique with active set based PAR-reduction is to start with the highest peak in the signal, and add a peak-canceling kernel until a new peak is balanced with the first one. Then, this new peak is included in the *active set*, and two kernels are added to reduce these two peaks equally, until a third peak is balanced, and so on.

The addition of PSD constraints to the reduction signal will alter the optimization problem and make this more challenging. Still having the same problem setup as in the unconstrained case, we now also have a set of quadratic constraints for each reduction tone. During the reduction, different tones may reach their constraints sooner than others, see Figure 2.5. At this point, there is a choice of how to handle the situation. Since this tone has

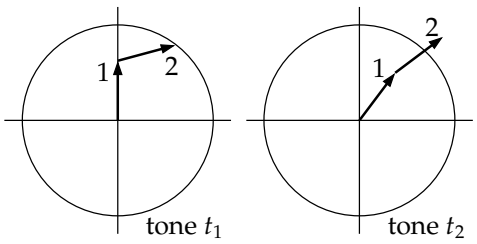

Figure 2.5: Addition of the tone weights for reduction of two different peaks can cause the PSD constraint to be reached on certain tones before others.

reached its constraint, we could continue with the remaining tones, until all tones are filled up, or we can accept the peak level that has been achieved.

Paper III proposes a low-complex solution, that stops the reduction process once one of the reduction tones hit the PSD constraint. This will lead to a suboptimal algorithm, but as can be seen from the results in the paper, the performance is rather good already after a few iterations and additional reduction may not be worth the efforts. The peak constraint from the first two papers is used also here, but the scenario is extended to also incorporate a 50% higher magnitude per tone.

Simulation results can be seen in Figure 2.6 (cf. Figure 8 in Paper III), where the unreduced signal is shown as well as reduction with 1 to 4 active set iterations. Two PAR level bounds are also shown: the lower solid line corresponds to (2.1), here shown as a maximal reduction of $A_{\max}$ from the simulated initial PAR value, and the dashed line shows reduction with an optimal algorithm. In the simulations, the first few iterations give the most, and after that, the gain for each iteration is smaller.

2.1.4 Paper IV: Designing Tone Reservation PAR Reduction

With Paper III developing algorithms suitable for the PSD-constrained tone reservation, Paper IV [66] moves focus from the algorithm-oriented level to a wider perspective—what is possible to achieve with tone reservation implemented in a system. The paper aims to lead a system designer to predict the performance for a given parameter setting, without having to simulate every parameter choice.

Papers I–III use a PSD constraint set at a certain level. Paper IV examines what could be possible to do in standardized ADSL2 or ADSL2+ systems. Following the standards, the PSD is limited to a level 10 dB below the data-carrying tones [34].

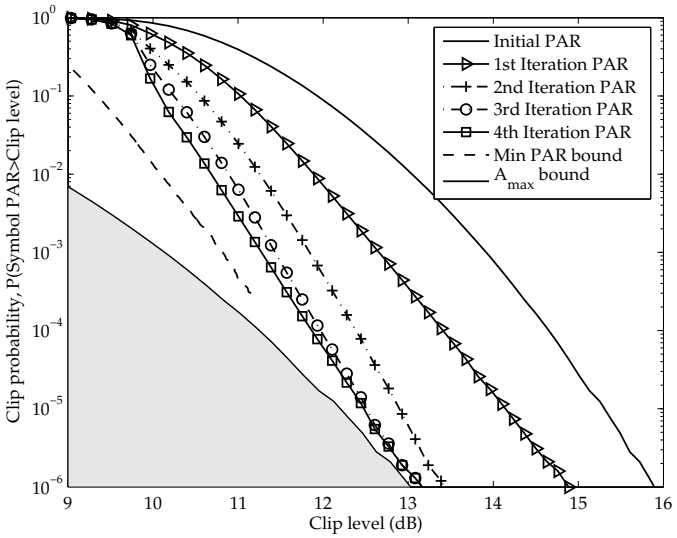

Figure 2.6: Symbol clip probability for the first four active set iterations with 12 random tones. The PSD constraint allows 50% higher magnitude per tone than for the data tones.

Obeying to a PSD constraint on the reduction tones as well as on the data tones, will as seen in Papers I–III result in a limited PAR reduction performance. Paper IV examines how strict this limitation really is—if the goal for PAR reduction is set at a moderate level, the algorithm would not have to be used often, and efforts could be saved to the symbols that need reduction. On the other hand, aiming too low will result in a weak reduction signal, in order not to exceed the limit on average.

For a correct description of the analog signal, the use of oversampled or time-continuous signals is of importance. The paper develops the following expression of the PAR for a continuous-time signal:

$$\text{Prob(clip at level } \gamma\sigma) = 1 - \exp\left(-\frac{N}{\sqrt{3}} e^{-\gamma^2/2}\right). \tag{2.2}$$

This approximation, tight except for very low PAR values, is based on Rice's level-crossing theorems [67,68] and incorporates the higher symbol PAR of a continuous-time or oversampled signal. Using this expression for the signal distribution, we can calculate the average PSD as a function of the specified target PAR level and maximum allowed magnitude per reduction tone.

This relationship is illustrated by the thick lines in Figure 2.7, where the average PSD is fixed to the maximum value ($-10\,\text{dB}$) specified by

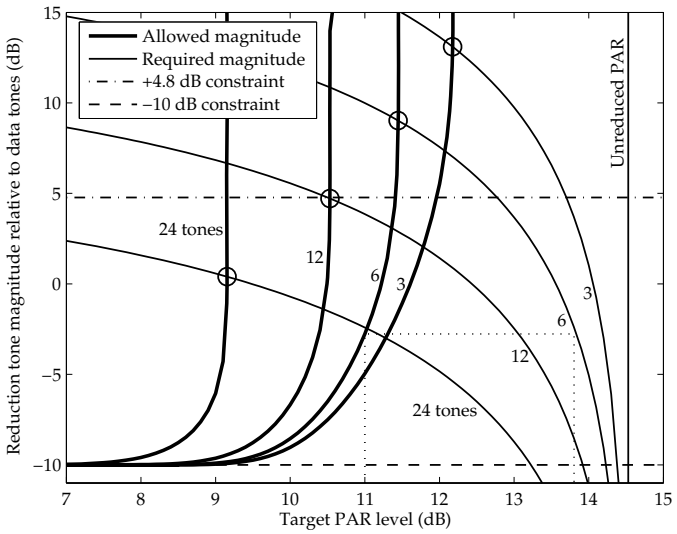

Figure 2.7: The thick solid lines starting from the bottom left corner and bending upwards show the maximum reduction tone magnitude allowed without exceeding the average PSD level, when aiming at the target PAR level shown on the horizontal axis. The solid lines starting from the bottom right show the PSD bound, indicating what reduction tone magnitude is needed to achieve the target PAR level on the horizontal axis. For both sets of bounds, the allowed points are on the right-hand sides.

the ADSL2 standard [34], and the maximum reduction tone magnitude is shown as a function of the target PAR level. From the right, the thick curves show reduction with 3, 6, 12 and 24 tones. Following the curves from the left, corresponding to a low target PAR level, almost all symbols need reduction and the maximum level has to be set close to $-10\,\mathrm{dB}$. With increasing target PAR levels, fewer symbols need reduction, and the maximum instantaneous magnitude may be set higher, thus allowing for a better PAR reduction. This is also verified by simulations shown in Figure 7 in Paper IV.

The thick curves tell how much can be put on the tones without exceeding the average PSD mask. However, access to a high instantaneous reduction signal is also important, as pointed out by the bound in (2.1) and Paper II. The leftmost thin curves in Figure 2.7 show what reduction tone magnitude is needed to achieve a certain target PAR. The four intersection points between the curves then show the optimum solution, if the bound is tight. As an example we can consider reduction with six tones, where we see that the optimum would be to choose $11.4\,\mathrm{dB}$. However, without insight

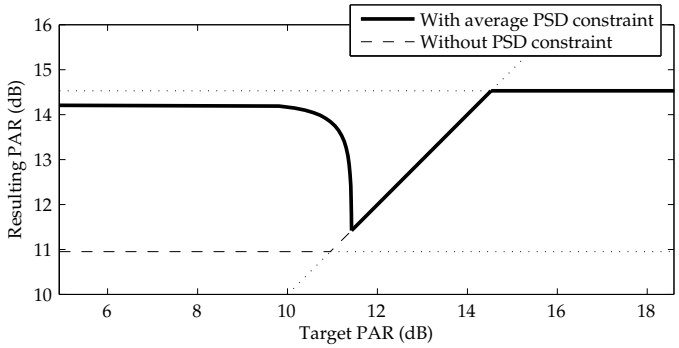

Figure 2.8: Relationship between target PAR and the resulting PAR level for reduction with 6 tones, with and without constraints on average reduction PSD.

into the problem, say that one would be tempted to aim at 11 dB. According to the dotted lines this give a maximum relative magnitude of -2.8 dB. Following this value to the right to the other bound, the lowest possible result is 13.8 dB. A robust choice for this situation could instead be to aim at a level slightly above 11.4 dB.

The relationship between target and resulting PAR levels is shown in Figure 2.8. Notable is the distinct optimum in achievable reduction performance, useful for system designers to be aware of.

We can now combine this bound based on the average PSD with a bound based on a fixed maximum tone magnitude, as used in Papers I–III. In Paper IV, the limit is derived by calculation of how much interference is reasonable to put on other users. With these two bounds, we obtain the regions shown in Figure 2.9. The performance increases faster when using a low number of tones, and shows a more moderate increase at higher number of reserved tones. Simulations for both ADSL2 and ADSL2+ confirm that the bounds give a good prediction of system performance.

2.2 When and where to apply PAR reduction

Apart from the question on how to do PAR reduction, an important question is what signal in the system we should have as the main criterion, and to what extent it is reasonable to focus on PAR reduction.

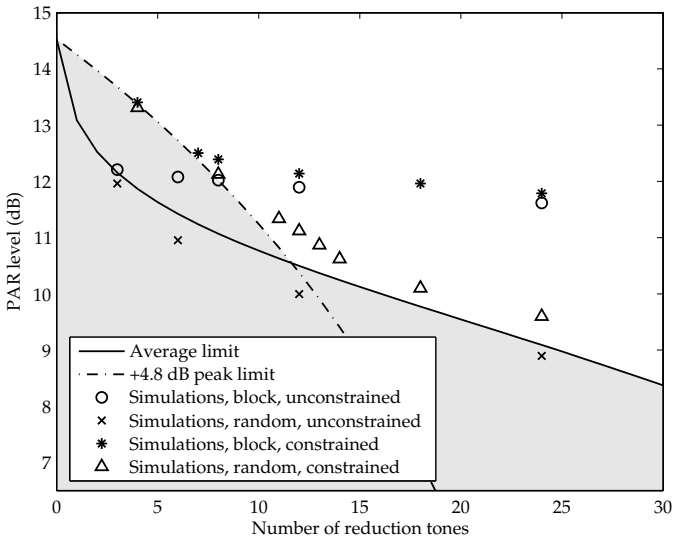

Figure 2.9: Bounds on achievable PAR as a function of number of reduction tones, for an ADSL2 system and a symbol clip probability of $2 \cdot 10^{-4}$. The solid line shows the bound based on a maximum average PSD. The dash-dotted line shows the bound based on a peak PSD. The marker symbols show simulated reduction performance, for random or block-placed tones, with or without PSD constraints.

2.2.1 Paper V: How Much PAR to Bring to the Party?

Since the tone reservation method removes possibly data-carrying tones in favor of reduction tones, a question is how much effort should be put into reducing PAR. Using too many reduction tones will eventually lead to a situation where unnecessarily high data capacity is lost.

Paper V [33] examines the special case where the peak level of the signal is the limiting factor, rather than the transmit power or PSD level. Then, applying tone reservation to reduce the signal peaks will allow for a higher average level, and thereby an increased SNR, see Figure 2.10. At the same time, excluding too many tones from the data-carrying set will remove capacity, and a certain optimum may exist. This trade-off is common in PAR reduction papers, but Paper V searches for the answer of how much PAR reduction to apply to the system in a specified system scenario, by translating from PAR levels to an easily understandable bit rate measure. Figure 2.11 (see Figure 7 in Paper V) shows the bitrate optimum for a 2 km cable.

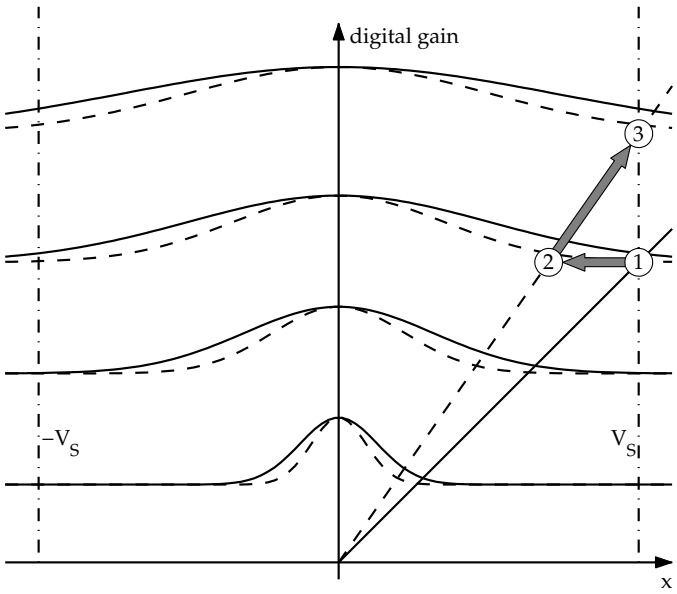

Figure 2.10: Correspondence between signal gain and amplitude distribution in a system limited by peak constraint, rather than a constraint on transmitted energy. A system without PAR reduction, represented by the straight solid line, can have the maximum gain at point 1 without violating the peak constraint. The PAR-reduced system, following the dashed straight line, could under the same peak constraint work with a higher gain, at point 3.

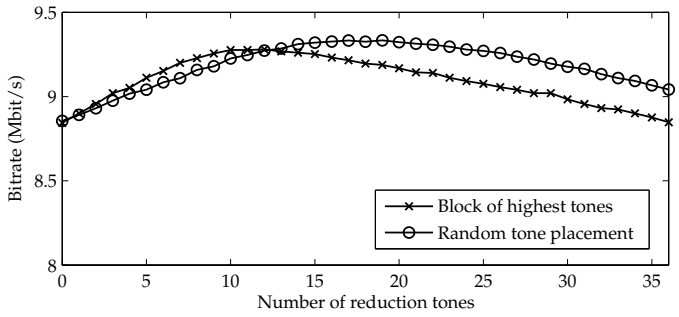

Figure 2.11: Total bitrate as a function of PAR reduction tones. 2 km copper wire loop. Note the scale on the vertical axis.

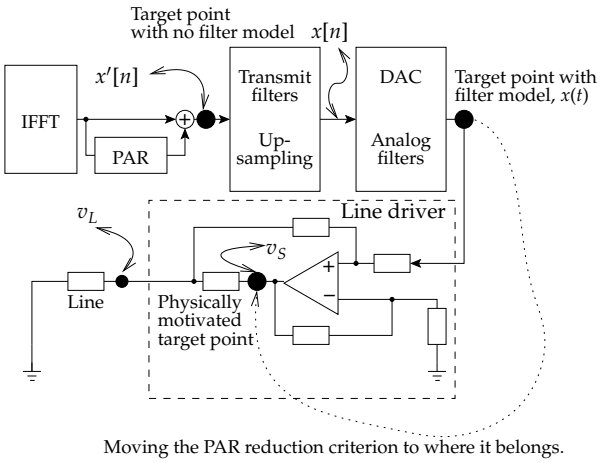

Figure 2.12: Block diagram of a DMT-based transmitter showing three different points a PAR reduction criterion can focus on. The node inside the line driver labeled v_s is the physically motivated point. The PAR at this point directly influences the power consumption of the system.

2.2.2 Paper VI: Moving the PAR Reduction Criterion into the Line Driver

Several authors note that reducing PAR on the critically sampled rate will give bad results when evaluating the continuous-time signal [31,41,60]. The solution that generally is presented is to oversample the signal by a factor of 2 to 8 before PAR reduction, in order to limit peak regrowth afterwards. This is the most straight-forward solution, also used in Paper III and Paper IV.

However, this may not necessarily be the whole truth: neither the critically sampled signal, nor the continuous-time signal at the line driver output are necessarily the correct signal. Actually, what is important is the voltage at a certain node within the line driver, node v_s in Figure 2.12. This is the point directly affected by the limits of the supply voltage. While line drivers are designed to have a linear relationship between the input and the output signals, the relationship between the input or output and the important node inside the line driver is not necessarily linear for an actively terminated line driver. Depending on the load that is attached to the system, the true function will vary. In Paper VI [64] we see that incorporating the knowledge of the correct node in the system, will make the PAR level about 0.5 dB better than without taking this into consideration. The largest difference occurs with short and thick cables, an antenna-like case where the reflections show a visible impact. The complexity will not increase much, compared to a system already using an oversampled signal.

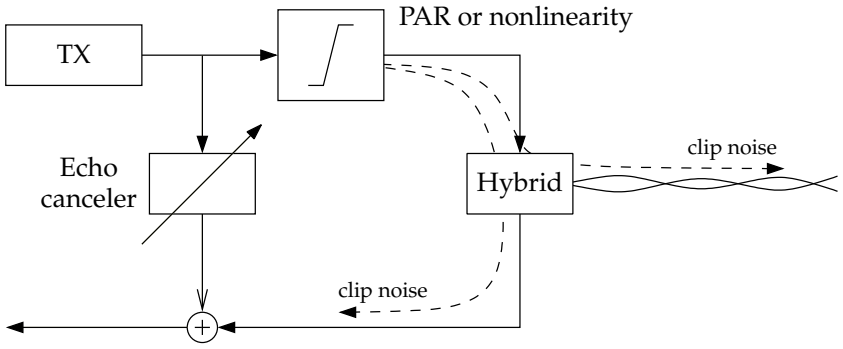

Figure 2.13: The echo from the transmitted signal propagates to the receiver through the hybrid. This can be avoided by an echo canceler, but non-linearities or PAR reduction after the echo canceler threatens receiver performance.

2.2.3 Paper VII: Implementation Notes for PAR Reduction

While the other included papers in the thesis are presented in journals or at international conferences, Paper VII is a part of an industrial implementation investigation. The algorithm proposed in Paper III is further simplified, and a rough complexity estimate is given—well below 100 MIPS, a small but not insignificant complexity. This internal report makes also a short investigation about what impact the clip noise has on the echo canceler design, see Figure 2.13, suggesting that the echo canceler could be run at the original sample rate. Furthermore, the reasoning behind the comparison of different methods from Section 1.3.3 is extended.

2.3 Other DMT topics

The two last papers deal with other topics than PAR reduction, but still focused on communication in wireline DSL systems. In most multicarrier systems, a cyclic prefix is inserted before the data symbol, in order to maintain the orthogonality between the different subcarriers and make channel equalization easier.

2.3.1 Paper VIII: OFDM Frame Synchronization for Dispersive Channels

The correlation introduced by the cyclic prefix in the transmit signal can be used for performing time and frequency synchronization. By examining

the correlation of the received symbol at a time lag of N samples, the start of the cyclic prefix can be examined with a *maximum likelihood* (ML) estimator [14]. In wireline DMT systems, the channel is typically dispersive, and stationary for significantly longer time than for wireless systems. Then, the ML estimator can be extended to include this knowledge, to produce an ML estimate also in the dispersive environment [15]. However, this estimator will be very complex, and may in practice only serve as a bound for other estimators. Paper VIII [18] rearranges the likelihood functions, to come up with an estimator structure with a linear prefilter followed by a correlating filterbank. This significantly less complex estimator structure produces comparable results to the complex original estimator.

2.3.2 Paper IX: The Cyclic Prefix of OFDM/DMT – An Analysis

The cyclic prefix is inserted in the systems in order to maintain the orthogonality between the subcarriers. This leads to a typical cyclic prefix length of the same length as the channel impulse response.

Paper IX [69] examines the ICI and ISI caused by a too short cyclic prefix, and concludes that they have the same power spectral density, concentrated to the low frequencies. The conclusion is that because of the spectral concentration, the cyclic prefix can in practice be shorter than the impulse response length without degrading system performance.

Bibliography

[1] IEEE, *Wireless LAN Medium Access Control (MAC) and Physical Layer (PHY) specifications; High-speed Physical Layer in the 5 GHz Band*. Standard 802.11a, June 2003.

[2] "Broadband radio access networks (BRAN); HIPERLAN type 2; system overview," 2000, ETSI TR 191 683.

[3] "Radio broadcasting systems; digital audio broadcasting (DAB) to mobile, portable and fixed receivers," May 2001, ETSI EN 300 401, V1.3.3.

[4] "Digital video broadcasting (DVB); framing structure, channel coding and modulation for digital terrestrial television," 2001, ETSI EN 300 744.

[5] T. Starr, J. M. Cioffi, and P. J. Silverman, *Understanding Digital Subscriber Line Technology*. Upper Saddle River, NJ, USA: Prentice Hall, 1999.

[6] J. A. C. Bingham, "Multicarrier modulation for data transmission: An idea whose time has come," *IEEE Communications Magazine*, vol. 28, pp. 5–14, May 1990.

[7] J. M. Cioffi, "A multicarrier primer," Nov. 1991, ANSI Document, T1E1.4 no. 91-157.

[8] J.-J. van de Beek, P. O. Börjesson, P. Ödling, and S. K. Wilson, "Orthogonal frequency-division multiplexing (OFDM)," invited chapter in *Review of Radio Science 1997–1999,* W. R. Stone, Ed., pp. 177–206, International Union of Radio Science (URSI), Oxford University Press, 1999.

[9] O. Edfors, M. Sandell, J.-J. van de Beek, D. Landström, and F. Sjöberg, "An introduction to orthogonal frequency-division multiplexing," Luleå University of Technology, Tech. Rep. TULEA 1996:16, Sept. 1996.

[10] C. E. Shannon, "Communication in the presence of noise," *Proc. IRE*, vol. 37, pp. 10–21, Jan. 1949.

[11] R. G. Gallager, *Information Theory and Reliable Communication*. John Wiley & Sons, 1968.

[12] P. Chow, J. Cioffi, and J. Bingham, "A practical discrete multitone transceiver loading algorithm for data transmission over spectrally shaped channels," *IEEE Transactions on Communications*, vol. 43, no. 234, pp. 773–775, Feb./Mar./Apr. 1995.

[13] ITU-T, *Asymmetric digital subscriber line (ADSL) transceivers*. Recommendation G.992.1, June 1999.

[14] J.-J. van de Beek, M. Sandell, and P. O. Börjesson, "ML estimation of time and frequency offset in OFDM systems," *IEEE Transactions on Signal Processing*, vol. 45, no. 4, July 1997.

[15] J.-J. van de Beek, P. O. Börjesson, M.-L. Boucheret, D. Landström, J. M. Arenas, P. Ödling, and S. K. Wilson, "Three non-pilot based time- and frequency estimators for OFDM," *Signal Processing*, vol. 80, no. 7, pp. 1321–1334, July 2000.

[16] D. Landström, S. K. Wilson, J.-J. van de Beek, P. Ödling, and P. O. Börjesson, "Symbol time offset estimation in coherent OFDM systems," *IEEE Transactions on Communications*, vol. 50, no. 4, pp. 545–549, Apr. 2002.

[17] D. Landström, N. Petersson, P. Ödling, and P. O. Börjesson, "Synchronization of multicarrier systems on the twisted copper pair channel," in *Proc. Radiovetenskap och Kommunikation*, Stockholm, Sweden, June 2002.

[18] ——, "OFDM frame synchronization for dispersive channels," in *Proc. International Symposium on Signal Processing and its Applications*, Kuala Lumpur, Malaysia, Aug. 2001.

[19] H. Nyquist, "Certain topics in telegraph transmission theory," *Transactions of the A. I. E. E.*, pp. 617–644, Feb. 1928.

[20] J. Kaufman, *Så funkar det (What Makes It Go?)*. Bonnier Carlsen / Western Publishing Company, 1971.

[21] P. Billingsley, *Probability and Measure*, 3rd ed. New York, NY, USA: John Wiley and Sons, 1995.

[22] D. Wulich, N. Dinur, and A. Glinowiecki, "Level clipped high-order OFDM," *IEEE Transactions on Communications*, vol. 48, no. 6, pp. 928–930, June 2000.

[23] S. Wei, D. L. Goeckel, and P. E. Kelly, "A modern extreme value theory approach to calculating the distribution of the peak-to-average power ratio in OFDM systems," in *Proc. IEEE International Conference on Communications*, vol. 3, New York, NY, USA, Apr.–May 2002, pp. 1686–1690.

[24] J. S. Chow, J. A. C. Bingham, and M. S. Flowers, "Mitigating clipping noise in multi-carrier systems," in *Proc. IEEE International Conference on Communications*, vol. 2, Montreal, Canada, 1997, pp. 715–719.

[25] H. Ochiai and H. Imai, "Performance analysis of deliberately clipped OFDM signals," *IEEE Transactions on Communications*, vol. 50, no. 1, pp. 89–101, Jan. 2002.

[26] L. Wang and C. Tellambura, "A simplified clipping and filtering technique for PAR reduction in OFDM systems," *IEEE Signal Processing Letters*, vol. 12, no. 6, pp. 453–456, June 2005.

[27] A. Gatherer and M. Polley, "Controlling clipping probability in DMT transmission," in *Proc. Asilomar Conference on Signals, Systems and Computers*, vol. 1, Pacific Grove, CA, USA, Nov. 1997, pp. 578–584.

[28] D. Kim and G. L. Stuber, "Clipping noise mitigation for OFDM by decision-aided reconstruction," *IEEE Communications Letters*, vol. 3, no. 1, pp. 4–6, Jan. 1999.

[29] J. Kliewer and T. Karp, "Clipping error resilience for peak power-constrained DMT transmission via implicit frequency domain redundancy." in *Proc. International Symposium on Signal Processing and Its Applications*, Paris, France, July 2003.

[30] J. Tellado and J. M. Cioffi, "PAR reduction in multicarrier transmission systems," Dec. 1997, ANSI Document, T1E1.4 no. 97-367.

[31] J. Tellado-Mourelo, "Peak to average power reduction for multicarrier modulation," Ph.D. dissertation, Stanford University, Stanford, CA, USA, Sept. 1999.

[32] N. Petersson, A. Johansson, P. Ödling, and P. O. Börjesson, "Analysis of tone selection for PAR reduction," in *Proc. International Conference on Information, Communications & Signal Processing*, Singapore, Oct. 2001.

[33] P. Ödling, N. Petersson, A. Johansson, and P. O. Börjesson, "How much PAR to bring to the party?" in *Proc. Nordic Signal Processing Symposium*, Tromsø–Trondheim, Norway, Oct. 2002.

[34] ITU-T, *Asymmetric digital subscriber line (ADSL) transceivers – 2 (ADSL2)*. Recommendation G.992.3, July 2002.

[35] ——, *Asymmetric Digital Subscriber Line (ADSL) transceivers – Extended bandwidth ADSL2 (ADSL2+)*. Recommendation G.992.5, May 2003.

[36] J. Tellado and J. M. Cioffi, "Revisiting DMT's PAR," Mar. 1998, ANSI Document, T1E1.4 no. 98-083.

[37] P. O. Börjesson, H. G. Feichtinger, N. Grip, M. Isaksson, N. Kaiblinger, P. Ödling, and L.-E. Persson, "A low-complexity PAR-reduction method for DMT-VDSL," in *Proc. 5th International Symposium on Digital Signal Processing for Communication Systems*, Perth, Australia, Feb. 1999, pp. 164–199.

[38] ——, "DMT PAR-reduction by weighted cancellation waveforms," in *Proc. Radiovetenskaplig Konferens*, Karlskrona, Sweden, June 1999, pp. 303–307.

[39] B. S. Krongold and D. L. Jones, "A new method for PAR reduction in baseband DMT systems," in *Proc. Asilomar Conference on Signals, Systems, and Computers*, vol. 1, Pacific Grove, CA, USA, Nov. 2001, pp. 502–506.

[40] ——, "A new tone reservation method for complex-baseband PAR reduction in OFDM systems," in *Proc. IEEE International Conference on Acoustics, Speech, and Signal Processing*, vol. 3, Orlando, FL, USA, May 2002, pp. 2321–2324.

[41] B. S. Krongold, "New techniques for multicarrier communication systems," Ph.D. dissertation, University of Illinois at Urbana-Champaign, Urbana, IL, USA, Nov. 2001.

[42] N. Andgart, B. Krongold, P. Ödling, A. Johansson, and P. O. Börjesson, "PSD-constrained PAR reduction for DMT/OFDM," *EURASIP Journal on Applied Signal Processing*, vol. 2004, no. 10, pp. 1498–1507, Aug. 2004.

[43] D. G. Luenberger, *Linear and Nonlinear Programming*. Boston, MA, USA: Addison-Wesley, 1984.

[44] D. L. Jones, "Peak power reduction in OFDM and DMT via active channel modification," in *Proc. Asilomar Conference on Signals, Systems, and Computers*, vol. 2, Pacific Grove, CA, USA, Oct. 1999, pp. 1076–1079.

[45] B. S. Krongold and D. L. Jones, "A study of active constellation extension for PAR reduction in OFDM," in *Proc. International OFDM-Workshop*, Hamburg, Germany, Sept. 2002, pp. 107–111.

[46] D. J. G. Mestdagh and P. M. P. Spruyt, "A method to reduce the probability of clipping in DMT-based transceivers," *IEEE Transactions on Communications*, vol. 44, no. 10, pp. 1234–1238, Oct. 1996.

[47] R. W. Bäuml, R. F. H. Fischer, and J. B. Huber, "Reducing the peak-to-average power ratio of multicarrier modulation by selected mapping," *Electronics Letters*, vol. 32, no. 22, pp. 2056–2057, Oct. 1996.

[48] S. H. Müller and J. B. Huber, "A novel peak power reduction scheme for OFDM," in *Proc. IEEE International Symposium on Personal, Indoor and Mobile Radio Communications*, vol. 3, 1997, pp. 1090–1094.

[49] ——, "OFDM with reduced peak-to-average power ratio by optimum combination of partial transmit sequences," *Electronics Letters*, vol. 33, no. 5, pp. 368–369, Feb. 1997.

[50] J. Tellado and J. M. Cioffi, "PAR reduction with minimal or zero bandwidth loss and low complexity," June 1998, ANSI Document, T1E1.4 no. 98-173.

[51] M. J. E. Golay, "Complementary series," *IRE Transactions on Information Theory*, vol. 7, pp. 82–87, Apr. 1961.

[52] S. Boyd, "Multitone signals with low crest factor," *IEEE Transactions on Circuits and Systems*, vol. 33, no. 10, pp. 1018–1022, Oct. 1986.

[53] B. M. Popović, "Synthesis of power efficient multitone signals with flat amplitude spectrum," *IEEE Transactions on Communications*, vol. 39, no. 7, pp. 1031–1033, July 1991.

[54] B. Vasic and J. P. LeBlanc, "Reducing peak-to-average ratios using OFDM necklaces," in *Proc. Nordic Signal Processing Symposium*, Tromsø–Trondheim, Norway, Oct. 2002.

[55] I. V. L. Clarkson and I. B. Collings, "A new joint coding and modulation scheme for channels with clipping," *Digital Signal Processing*, vol. 12, no. 2–3, pp. 223–241, Apr./July 2002.

[56] I. B. Collings and I. V. L. Clarkson, "A low-complexity lattice-based low-PAR transmission scheme for DSL channels," *IEEE Transactions on Communications*, vol. 52, no. 5, pp. 755–764, May 2004.

[57] J. A. C. Bingham, *ADSL, VDSL, and Multicarrier Modulation*. Wiley, 2000.

[58] N. Andgart and T. Magesacher, "Fair comparison of peak to average ratio reduction schemes," in *Australian Communication Theory Workshop*, Newcastle, Australia, Feb. 2004, (Poster).

[59] N. Petersson, "Peak and power reduction in multicarrier systems," Licentiate thesis, Lund University, Lund, Sweden, Nov. 2002.

[60] W. Henkel and V. Zrno, "PAR reduction revisited: an extension to Tellado's method," in *Proc. International OFDM-Workshop*, Hamburg, Germany, Sept. 2001, pp. 31.1–31.6.

[61] G. Wunder and H. Boche, "Peak value estimation of bandlimited signals from their samples, noise enhancement, and a local characterization in the neighborhood of an extremum," *IEEE Transactions on Signal Processing*, vol. 51, no. 3, pp. 771–780, Mar. 2003.

[62] H. Ehlich and K. Zeller, "Schwankung von Polynomen zwischen Gitterpunkten," *Matematische Zeitschrift*, vol. 86, pp. 41–44, 1964.

[63] B. S. Krongold and D. L. Jones, "An active-set approach for OFDM PAR reduction via tone reservation," *IEEE Transactions on Signal Processing*, vol. 52, no. 2, pp. 495–509, Feb. 2004.

[64] K. Werner, N. Larsson, N. Andgart, T. Magesacher, T. André, T. Randahl, and P. Ödling, "Moving the PAR reduction criterion into the line driver," in *Proc. European Signal Processing Conference*, Vienna, Austria, Sept. 2004.

[65] N. Petersson, A. Johansson, P. Ödling, and P. O. Börjesson, "A performance bound on PSD-constrained PAR reduction," in *Proc. IEEE International Conference on Communications*, Anchorage, AK, USA, May 2003, pp. 3498–3502.

[66] N. Andgart, P. Ödling, A. Johansson, and P. O. Börjesson, "Designing tone reservation PAR reduction," accepted for publication in *EURASIP Journal on Applied Signal Processing*.

[67] G. Lindgren, *Lectures on Stationary Stochastic Processes*. Mathematical Statistics, Lund University, Sept. 2002.

[68] S. O. Rice, "Mathematical analysis of random noise," *Bell Systems Technical Journal*, vol. 23, pp. 282–332, 1944 and vol. 24, pp 46–156, 1945.

[69] W. Henkel, G. Tauböck, P. Ödling, P. O. Börjesson, N. Petersson, and A. Johansson, "The cyclic prefix of OFDM/DMT – an analysis," in *Proc. International Zurich Seminar on Broadband Communications*, Zurich, Switzerland, Feb. 2002.

Included papers

Paper I

Paper I

Analysis of Tone Selection for PAR Reduction

Niklas Petersson, Albin Johansson, Per Ödling, and Per Ola Börjesson

Transmission systems using multi-carrier techniques suffer from high amplitude signals, high Peak-to-Average Ratios, PAR. In this paper we focus on PAR reduction by so called tone reservation, where a subset of the tones are reserved for constructing a signal that counteracts the high peaks and thereby reduces the Peak-to-Average Ratio. We investigate how to choose the tones used for the PAR reduction.

We show that there exist certain criteria that affect the PAR reduction performance of different tone sets. We address tone selection for three different cases: minimum PAR; minimum PAR with limited transmit spectrum (PSD); and fixed PAR with minimum transmit power. We note that proper tone selection can be quite different depending on the system's constraints.

Published in *Proc. International Conference on Information, Communications & Signal Processing*, (Singapore), Oct. 2001.

1 Introduction

From an overall systems perspective, the important property of the transmitted signal is that no peaks exceed a certain amplitude level given by the design. Several proposals have been made to reduce the amplitude of DMT signals, [1–3].

We address amplitude limiting of the digital signal that is input to the D/A converter and subsequently to the line-driver. In this paper we focus on PAR reduction by so called tone reservation, which have been presented in [1, 4, 5]. A subset of the available tones is chosen for PAR reduction and thereby not available for data transmission. The PAR reduction signal, $c(n)$ in Figure 1, is created by this subset.

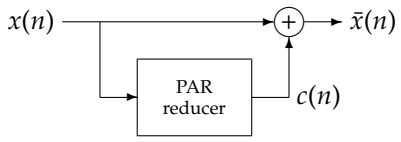

Figure 1: Addition of a PAR reduction signal, $c(n)$, that counteracts the peaks in $x(n)$.

Our intended application is a DMT baseband wireline system (e.g. ADSL, VDSL). This makes the tone-reservation approach especially attractive, since the characteristics of the channel is highly frequency dependent. At high frequencies and for long wire lengths, the attenuation is high, and capacity at these frequencies is low. Tones at these frequencies are thereby suitable to use for PAR reduction compared to tones in the lower part of the spectrum, where we would discard data capacity by removing information-carrying tones. Also tones that are not used for other reasons can be used for PAR reduction.

In this paper, we look at how to choose the tones used for the PAR reduction and extend the work found in [1]. A natural approach to PAR reduction is to try to reduce the PAR as much as possible. This will minimize the PAR in every symbol. We investigate this case in Section 3. A reasonable constraint to add in the minimization of PAR is to limit the maximum power or amplitude put on each PAR-reduction tone, which is done in Section 4. This corresponds to limiting the transmit spectrum, or power-spectral density (PSD), of the system. Actual systems have a maximum signal amplitude, which for example could be limited by the D/A converter range or maximum voltage supply for the power amplifier. The probability for $x(n)$ being larger than this limit γ should be below some acceptable number in order to have low clip distortion. In ADSL systems this clip probability is specified to 10^{-7} per sample. This leads to another possible target criterion, namely to

reduce the amplitude of the transmitted signal, $\bar{x}(n)$, down to this clip level, but no further [4,5]. In Section 5, we look at tone selection for this option.

2 Problem description

In a multi-carrier system data is modulated on several subcarriers, a number that is given by the IFFT size N in the system. An ADSL system is using $N = 512$ in the downstream direction.

The discrete time-domain signal $x(n)$ is generated by an IFFT as

$$x(n) = \frac{1}{N} \sum_{k=0}^{N-1} X(k) \exp\left(\frac{j2\pi nk}{N}\right) \tag{1}$$

where $X(k)$ are the information symbols to be transferred. Since the IFFT works as a summation of several different frequencies, the resulting signal $x(n)$ will be approximately Gaussian for large N, according to the central-limit theorem. This means that there can be some very high peaks present in the signal $x(n)$.

To counteract these signal peaks, a PAR reduction signal $c(n)$ is added,

$$\bar{x}(n) = x(n) + c(n), \tag{2}$$

c.f. Figure 1. A realization of a data signal $x(n)$ and two PAR reduction signals constructed from two different tone sets are shown in Figure 2. A contiguous block of tones gives a reduction signal $c(n)$ looking like a sinc-function, while randomly placed tones gives a noiselike reduction signal with one high sample.

2.1 Optimization criteria

Due to the real-value constraint of the time-domain signal, the upper half of the frequency window has to be the complex conjugate of the lower, i.e., $X(q)$ should satisfy the Hermitian property, $X(q) = X^*(N-q)$. The DC and Nyquist frequencies are chosen not to be included in the set of available tones, and this gives $N/2 - 1$ tones to put information on.

Denote the PAR reduction tone set with $\mathbf{I}_P$. Since the signals are real-valued, the added PAR reduction signal $c(n)$ can be written as

$$\begin{aligned} c(n) &= \frac{1}{N} \sum_{k \in \mathbf{I}_P} C(k) \exp \frac{j2\pi nk}{N} + C^*(N-k) \exp \frac{-j2\pi nk}{N} \\ &= \frac{2}{N} \sum_{k \in \mathbf{I}_P} \mathrm{Re}(C(k)) \cos \frac{2\pi nk}{N} - \mathrm{Im}(C(k)) \sin \frac{2\pi nk}{N} \\ &= \mathbf{Wg}, \end{aligned} \tag{3}$$

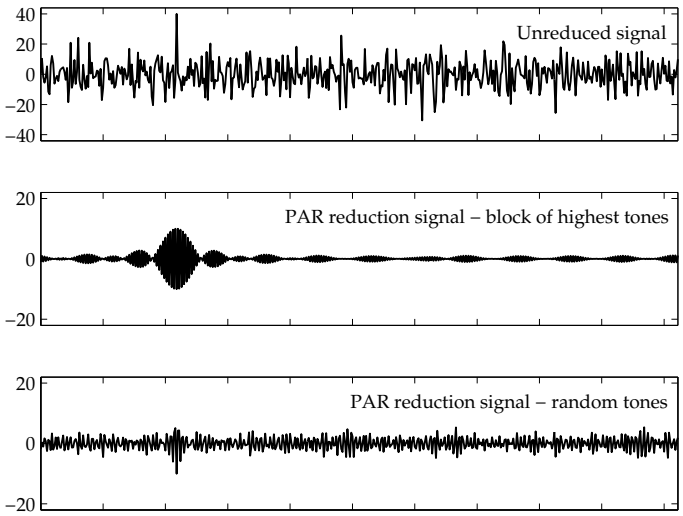

Figure 2: Realization of a data signal (upper plot) and PAR reduction signals $c(n)$ constructed from two different tone sets with $N = 512$ and 12 reduction tones. Mid plot: The PAR reduction tones are the block of tones with the highest frequencies. Lower plot: Randomly placed tones.

where $\mathbf{g} = \begin{bmatrix} \operatorname{Re} C(k) & \operatorname{Im} C(k) \end{bmatrix}$ and $\mathbf{W}$ is a transformation matrix with the cosine and sine components of the tones in $\mathbf{I}_P$. We are interested in the peak value, γ, of the output signal. Then all samples satisfy the constraint

$$|\tilde{\mathbf{x}}| = |\mathbf{x} + \mathbf{W}\mathbf{g}| \leq \gamma. \tag{4}$$

The added power could also be limited, since in reality we cannot add infinite power on the reserved tones. A power limitation is a quadratic constraint, but a linear approximation could be used instead to keep the problem solvable with basic linear or quadratic programming algorithms. What now remains is to decide the cost function. As discussed before, we could either minimize the PAR or we could keep the PAR under a fixed level and minimize for example the added power. Table 1 presents the different optimization criteria. To minimize PAR, the cost function to be minimized is simply γ. This problem formulation always has feasible solutions [6]. If we, on the other hand, want to fix the PAR level and try to minimize the energy added by $c(n)$, the cost function will be $\mathbf{g}^T\mathbf{g}$. In this case, γ has a fixed value, and it will not be possible in all cases to get the maximum peak below this level.

Table 1: Three different optimization criteria.

Section	*Optimization method*	*Minimizing*	*Constraint*
3	Minimize PAR	γ	—
4	Minimize PAR, limited PSD	γ	PSD
5	Fixed PAR, minimize power	$\mathbf{g}^T\mathbf{g}$	$\gamma \leq \gamma_{\text{clip}}$

3 Tone selection for minimizing PAR

With minimum PAR as the goal, we reduce the PAR level of every symbol as far as possible with a given set of tones. The PAR level will of course be different from symbol to symbol, and which tone selection that would be the best could also be different for every symbol. We want to find the tone selection that gives the lowest PAR when averaging over all symbols. For the tone selection, it would be intuitive to use the concept of bandwidth for guidance. If the PAR reduction signal $c(n)$ has a bandwidth similar to the data signal, it could approximate it well. Although this is true, our aim here is not to approximate the data signal, but to approximate its peaks. The bandwidth of the clipped peaks are different from the bandwidth of the signal. Thus, using reduction tones that are outside the data bandwidth could work equally well as other tones, since we just want to make an approximation of a small part of the time-domain signal.

Previous results, notably [1], suggest that it could be possible to find good and bad ways of tone selection. It is also noted that selecting randomly generated tone sets gives better results than block-placement or equally-spaced placement. There are some rules that could be used in designing the set of PAR reduction tones. For example, let us look at the case where we have equally spaced reduction tones. We can view this as a zero-padding in the frequency domain, which gives a periodic time-domain signal. Thus, constructing one peak in the reduction signal $c(n)$ will give an identical peak at some other, unwanted, place, c.f. [1]. An example of this is if all reduction tones have even numbers, in which case the time-domain signal will have a period of two.

Choosing k PAR tones in a system with N subcarriers can be done in $\binom{N/2-1}{k}$ different ways. For example, in a system with $N = 512$ subcarriers, we have in the order of 10^{29} combinations to place 20 tones. To illustrate the impact of the tone selection, and to give hints on further important criteria, a smaller system has been simulated. A system with $N = 64$ and four PAR reduction tones has been chosen. Choosing the four tones from all $N/2 - 1$ available tones gives $\binom{31}{4} = 31465$ possible tone combinations. A complete

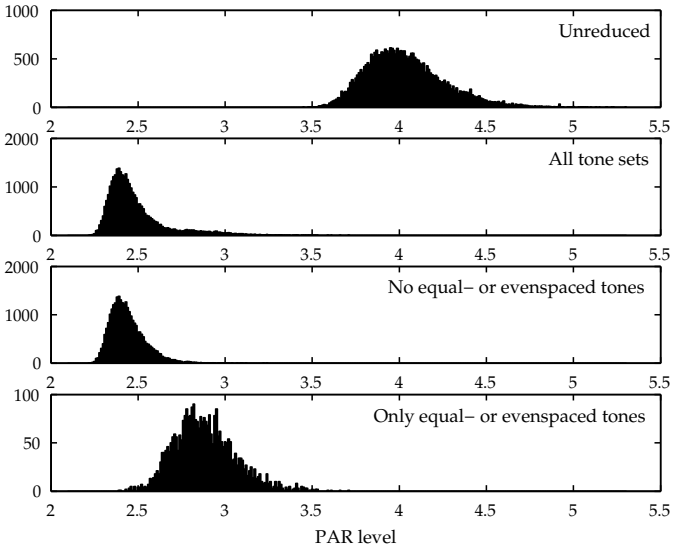

Figure 3: Maximum Peak-to-Average amplitude ratio of 500 symbols for a system with 64 subcarriers. Plots from top to bottom: 1: Unreduced signal. 2: PAR reduction using all tone sets. 3: No equal-spaced or even-spaced tones. 4: Only equal-spaced or even-spaced tones.

tone	1	2	3	4	5	6	7	8	9	10	11	12	13	14	15
block												□	□	□	□
even					□		□				□				□
equal					□			□			□			□	

Figure 4: Example of tone placements for a system with $N = 32$: Highest four tones, four even-spaced tones and four equal-spaced tones with distance 3.

simulation of all these possible tones sets has been performed, reducing the PAR of 500 data symbols for each tone set. Histograms of the maximum peaks before and after the reduction are shown in Figure 3. Results are shown for all tone sets; the case when the tone sets have equal spacing between all tones or even distances between all tones; and for the case with all but these sets. Figure 4 shows example tone-selections. According to the histograms, most of the cases with bad PAR reduction performance are concentrated to these tone sets.

We now evaluate a number of tone sets satisfying each placement

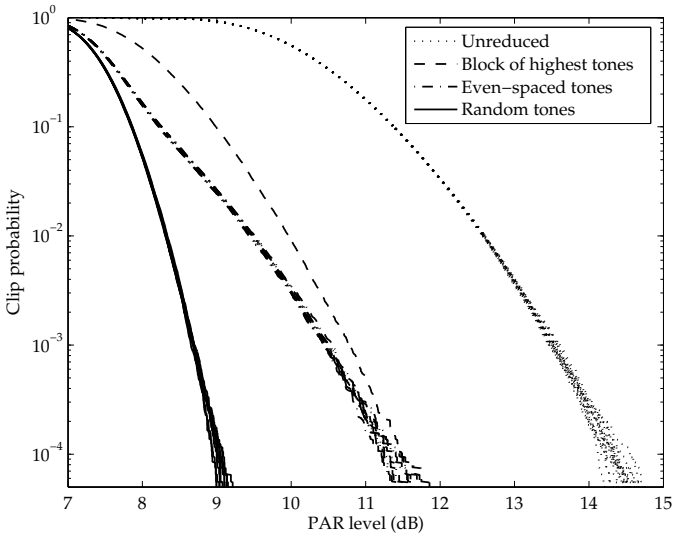

Figure 5: Symbol clip probability (one symbol equals 512 samples) for different tone placement methods. Unlimited added energy and 12 PAR reduction tones.

method for a full scale system with $N = 512$ using larger number of symbols per tone set. In Figure 5, the the probability that the signal after PAR reduction is higher than the desired limit, $\mathcal{P}(|x(n) + c(n)| > \gamma)$, is shown for different tone placement schemes. For comparison, the probabilities for the unreduced case are also shown. The tone set with only block-placed tones performs slightly worse than those with even-spaced tones, at least for high clip probabilities. At low clip probabilities, which are the most interesting, there is no significant difference between these two tone set classes. On the other hand, a random placement (with the first two classes removed from the random set) gives much lower clip probabilities. Thus, as long as certain bad tone combinations are avoided, we can expect the reduction performance to be both high and well-defined.

4 Minimizing PAR with constraining PSD mask

In the previous section, we examined what could be achieved when letting the reserved tones be used without any constraints by the optimization algorithms. A more realistic scenario is that we are not allowed to transmit unlimited power on these tones, but have to satisfy a PSD mask, constraining the power added on different tones. We now re-run the simulations

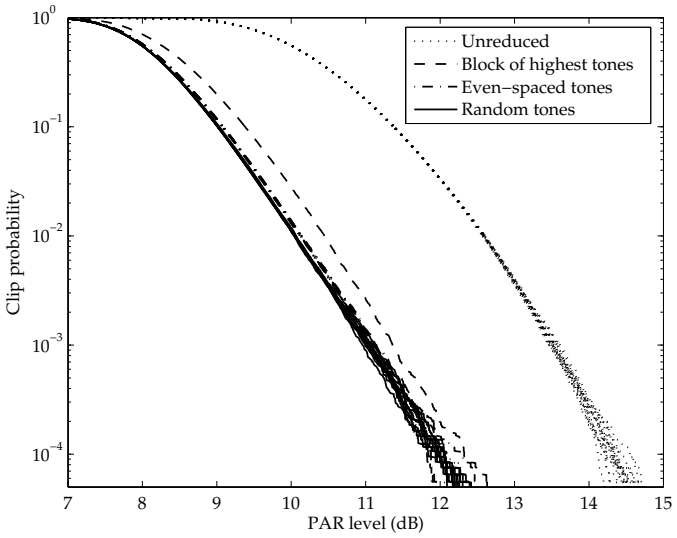

Figure 6: Symbol clip probability for different tone placement methods with 12 PAR reduction tones and constrained added energy.

using the additional constraint that the added power per tone must not exceed the average tone power on the information-carrying tones. This means that a quadratic constraint should be used, but we here use a piece-wise linear approximation, where the constraining circle in the complex plane is approximated by an octagon.

In Figure 6, the same system as in Figure 5 is used, but with the additional energy constraint. Looking at this figure, the differences between the classes of tone sets are almost gone. The only noticeable difference is that at high clip probabilities, the block-placed tone set still performs worse than the rest. Figure 7 uses 24 tones for the PAR reduction, which gives a better result, but not as good for any tone set class as the 12-tone unconstrained reduction in Figure 5.

The curves indicate that the benefit of choosing a good tone set is strongly reduced when the added power is constrained. Instead the amount of total added power becomes important, and since this is proportional to the number of PAR reduction tones, the number of tones is a more important factor than how the tones are placed. However, when the number of tones are increased further, the bad tone sets cannot benefit so much from the increased freedom. Again, we get a bigger difference between the classes of tone set.

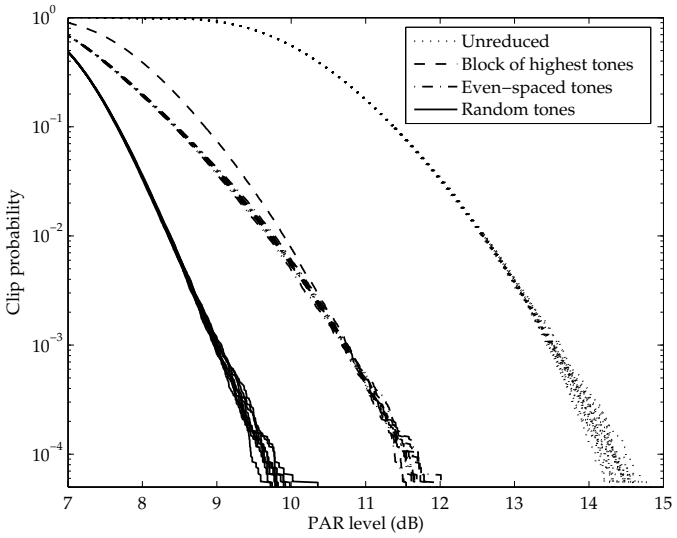

Figure 7: Symbol clip probability for different tone placement methods using 24 PAR reduction tones and constrained added energy.

5 Minimizing power with fixed PAR

In this section, we look at PAR reduction with a fixed desired PAR level as suggested in [4, 5]. Figure 8 shows an example of a clip probability curve where the desired PAR level is set to 12 dB. Thus, up to this PAR level no reduction is performed and the curve follows the unreduced curve. For signals with PAR values above this level, the curve will at best follow the curve for minimum PAR.

Figure 9 shows how the power of the added PAR reduction signal $c(n)$ depends on the sum of the parts of the data signal $x(n)$ exceeding a desired PAR limit γ. Here the reduction signal $c(n)$ has been constructed using a contiguous block of tones. In the figure it is seen that reducing one peak often creates a new peak in some other location. This is indicated with $\diamond$ and corresponds to symbols having one peak above the limit before reduction, and two peaks at the limit after the reduction. This may be due to the large sidelobes of the sinc-like base function compared to the base function for the random-placed tones, as seen in Figure 2. Figure 10 shows the same situation but using PAR reduction signals composed of sets of randomly placed tones. For the randomly placed tones, not as many new peaks are created as for the block placement case.

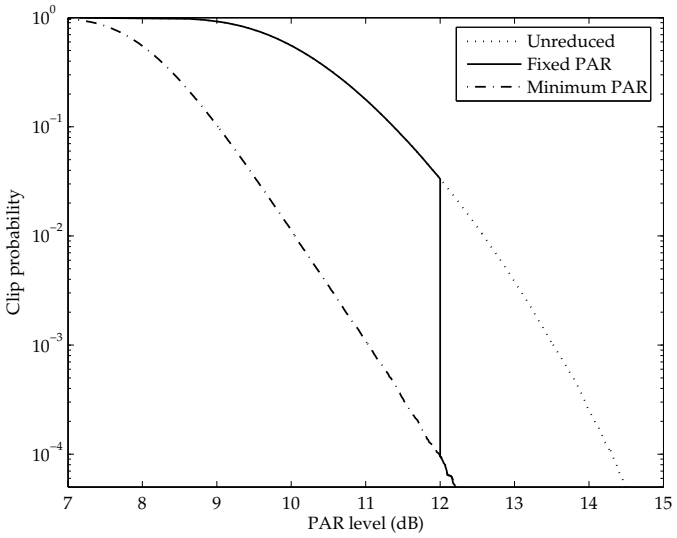

Figure 8: Example of clip probability when using a desired PAR value. 12 PAR reduction tones.

It is also seen in Figures 9 and 10 that for single peak reduction, indicated with $\circ$, the square root of the power of the added signal $c(n)$ (on the y-axis) often depends linearly on how much the peak needs to be reduced (x-axis). A line has been added in the figure to illustrate this. For two peaks, indicated with $*$, the total power needed is between the single peak case and $1/\sqrt{2}$ lower (indicated with a second line). This can be extended with more peaks, e.g. 3 peaks down to $1/\sqrt{3}$ lower (third line).

6 Summary

We have shown that depending on what constraints are used in the PAR reduction, and how much of PAR reduction that is wanted, the impact of using a good tone set varies in importance. If there are constraints on the added energy, such as not exceeding a specified PSD mask, the number of reserved tones is of primary importance, rather than the exact placement of the tones. However, when there is many tones available, also meaning a lot of added energy, the tone placement starts to be important. Then, a random placement of the tones almost surely gives good performance, and should be preferred over, for example, placements in blocks or with equal distances.

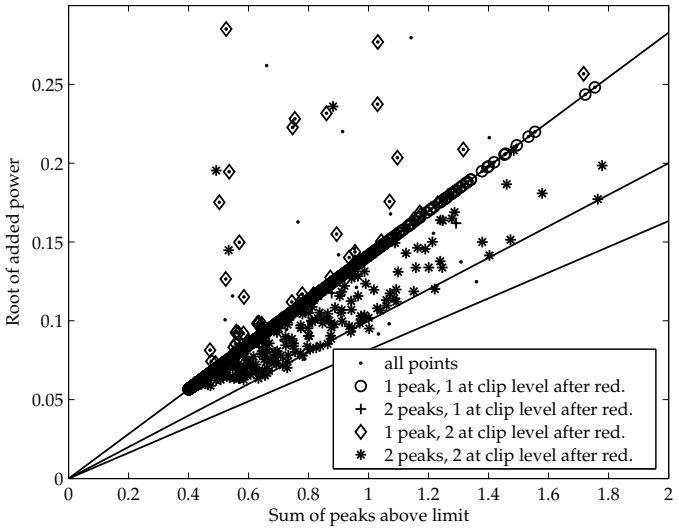

Figure 9: Dependence between the size of the added signal and the sum of signal exceeding desired PAR. The reduction tones are in a contiguous block. Single-peak ($\circ$) reduction show a linear dependence, illustrated in the figure by the added uppermost line. The outcomes of two-peak ($*$) reduction fall between the top line and the second line, $1/\sqrt{2}$ lower. The third line bounds three-peak reduction.

Bibliography

[1] J. Tellado-Mourelo, "Peak to average power reduction for multicarrier modulation," Ph.D. dissertation, Stanford University, Stanford, CA, USA, Sept. 1999.

[2] M. Friese, "Multitone signals with low crest factor," *IEEE Transactions on Communications*, vol. 45, no. 10, pp. 1338–1344, Oct. 1997.

[3] A. Gatherer and M. Polley, "Controlling clipping probability in DMT transmission," in *Proc. Asilomar Conference on Signals, Systems and Computers*, vol. 1, Pacific Grove, CA, USA, Nov. 1997, pp. 578–584.

[4] P. O. Börjesson, H. G. Feichtinger, N. Grip, M. Isaksson, N. Kaiblinger, P. Ödling, and L.-E. Persson, "A low-complexity PAR-reduction method for DMT-VDSL," in *Proc. 5th International Symposium on Digital Signal Processing for Communication Systems*, Perth, Australia, Feb. 1999, pp. 164–199.

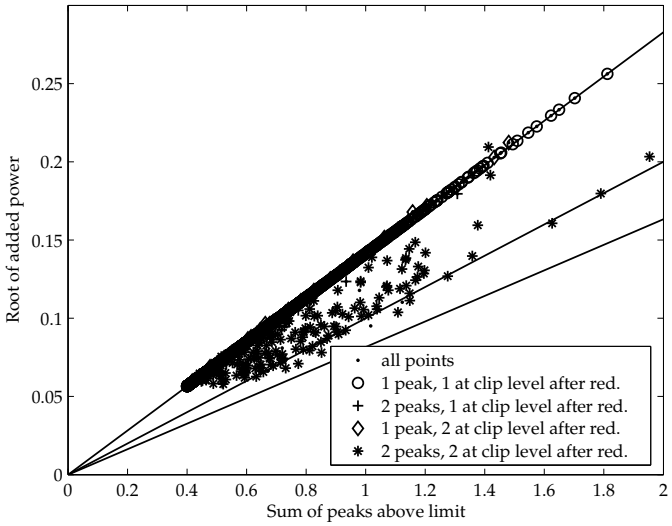

Figure 10: As in Figure 9, but with the reduction tones randomly placed.

[5] ——, "DMT PAR-reduction by weighted cancellation waveforms," in *Proc. Radiovetenskaplig Konferens*, Karlskrona, Sweden, June 1999, pp. 303–307.

[6] D. G. Luenberger, *Linear and Nonlinear Programming*. Boston, MA, USA: Addison-Wesley, 1984.

Paper II

Paper II

A Performance Bound on PSD-Constrained PAR Reduction

Niklas Petersson, Albin Johansson, Per Ödling, and Per Ola Börjesson

Communication systems using multicarrier modulation suffer from a high Peak-to-Average Ratio, PAR. In this work we use the tone reservation approach to PAR reduction, where a subset of the tones are used for PAR reduction.

We derive a bound on the achievable performance under a PSD constraint on the transmit signal. Using this bound, we show that as long as a moderate reduction performance is needed, this could be achieved with an almost arbitrary selection of the PAR reduction tones.

This bounding technique also demonstrates that, applied to an ADSL-like system, the tone reservation approach could be used for PAR reduction down to about 12 dB, considering critically sampled signals.

1 Introduction

The signal transmitted from multicarrier systems contains often spurious peaks, and has thereby a high *Peak-to-Average Ratio*, PAR. Several proposals have been made to reduce the amplitude of multicarrier signals, [1–3]. The one used here is tone reservation, which has been presented in [1, 2]. A subset of the available tones are reserved for PAR reduction, and used for creating a reduction signal that is added to the data signal in order to reduce the signal peaks, see Figure 1.

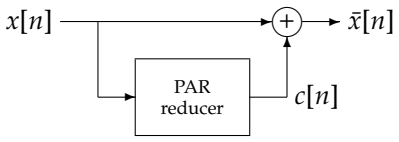

Figure 1: Addition of a PAR reduction signal, $c[n]$, that counteracts the peaks in $x[n]$. The signal $c[n]$ is a function of a small subset of tones.

We here focus on DMT baseband wireline systems, e.g. ADSL and VDSL, where the channel is a twisted pair copper wire. In Section 2, we define the data model and look at how the number of clips of an unreduced signal will depend on the chosen clip level. Depending on the set of PAR reduction tones, and what system constraints that have to be met, the reduction performance will differ. In Section 3, a bound on the achievable performance under some system constraints is derived. In Section 4, a discussion follows about how these results affect an exemplified ADSL system.

2 System model

A measure of the level of variation in a signal is the Peak-to-Average ratio, PAR. Since we want to keep the peak value as low as possible, and in the same time keep the average power high, thereby maintaining a high SNR, we look at the ratio of these two numbers.

To reduce the PAR level, a subset of the available tones is reserved for PAR reduction and thereby not available for data transmission. The PAR reduction signal, $c[n]$ in Figure 1, is created with this subset. The reduction signal is then added to the data signal, leading to a signal with lower peaks, $\bar{x}[n] = x[n] + c[n]$. Based on the data signal $x[n]$, the reduction signal $c[n]$ can be constructed using for example linear programming algorithms [1, 4], or with a low-complex placement of a single reduction peak [5, 6].

2.1 Definition of PAR

Here we have worked with the critically sampled time-discrete PAR. On a data signal $x[n]$, this is often defined [1] as

$$\mathrm{PAR}\{x[n]\} = \frac{\max |x[n]|^2}{E\,|x[n]|^2}. \tag{1}$$

To avoid the generation of new peaks or peak re-growth after the D/A converter, the expressions can be written to work on oversampled signals. However, here we proceed without this oversampling. According to the definition of PAR above, the expression for the PAR of the reduced signal $\bar{x}[n]$ should include the reduction signal in the denominator. However, if this were the case, a decrease in PAR level could be caused by a increase in the total power, without any reduction of the peak power. Thus, we define the PAR after reduction as

$$\mathrm{PAR} = \frac{\max |x[n] + c[n]|^2}{E\,|x[n]|^2}. \tag{2}$$

This is *not* a true Peak-to-Average ratio of a signal, since it is a function of the signal both before and after reduction. The definition describes how much average signal power it is possible to use under a certain peak power constraint [7].

2.2 Signal model

An ADSL system [8], which we consider in particular, uses symbol length of $N = 512$ samples (and 32 samples as cyclic prefix) in the downstream direction. The information bits are scrambled, coded and modulated onto several subcarriers in a multi-carrier system. Each subcarrier can be regarded as having a random amplitude, since this is data dependent. The summation of this large number of random sequences, will give a resulting sequence that is approximately Gaussian, due to the Central Limit Theorem. This means that the signal can have very high amplitude peaks.

We have modeled the signal as white Gaussian with variance σ^2, although all frequencies not always are used in the data signal. The probability that a single sample exceeds a given level $\gamma\sigma$, the *sample clip probability*, is

$$p_1 = P(|x[n]| > \gamma\sigma) = 2Q(\gamma). \tag{3}$$

Since all samples are independent, the number of clips in one symbol follows the binomial distribution. In particular, the probability that a symbol

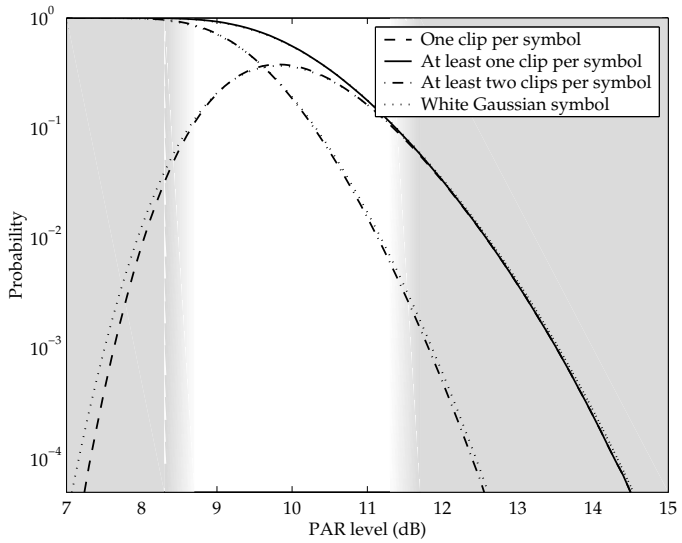

Figure 2: Probabilities of different number of clips. In the shaded area to the left, below about 8.5 dB PAR level, there will almost always be at least one clip. In the rightmost shaded area, over 11.5 dB, there will most often be maximum one clip in the signal. (The curve for one clip and the curve for at least one clip follow the same path.) Simulations made with symbol size $N = 512$ and 223 data tones used. As comparison, the theoretical values for a white Gaussian symbol are also shown as dotted lines.

has at least one sample exceeding this level, the *symbol clip probability*, can be expressed as

$$p_N = 1 - \binom{N}{0} p_1^0 (1 - p_1)^{N-0} = 1 - (1 - p_1)^N. \tag{4}$$

Figure 2 shows the symbol clip probability as a function of the clip level γ in dB, as well as the theoretical calculation, based on the binomial distribution.

3 Bound on reduction performance

In order to increase the bitrate of the system, a trade-off can be made between reserving tones for PAR reduction and keeping valuable data tones.

If there are frequencies in the spectrum where the channel SNR is too low to allow reliable data communication, these could be used for PAR reduction without discarding data capacity. In particular, the highest frequencies have bad characteristics for long wire lengths. Therefore, it is often attractive to use a number of the highest tones for PAR reduction.

From Tellado's fundamental work [1] follows that a choice of contiguous or equally-spaced tones performs worse than just selecting a tone set by random. Previous simulation results, [9], show that when putting a constraint on the maximum allowed energy per tone, the principal behavior of the PAR reduction changes abruptly. According to [9], constrained energy on the tones means that for a small number of tones, the placement of the reduction tones is not important. We will now show that the behavior demonstrated by simulations in [9] holds in general, by deriving an analytical bound on PAR reduction performance.

3.1 Bound on achievable PAR reduction for constrained tone power

Having a small number of PAR reduction tones, with a PSD constraint limiting the power on each tone, a bound can be derived on the achievable PAR level. The largest reduction signal $c[n]$ that is possible to create is when all reduction tones has the same phase at a given sample. If the difference between any data sample and the desired PAR level is bigger than this, it will be impossible to reduce that sample down to the desired PAR level.

Assume the symbol to be a white Gaussian signal with variance σ^2, a model that according to Figure 2 quite closely describes our data symbol. Then the symbol clip probability after reduction can be expressed as

$$\begin{aligned} p_N = P(\text{clip}) &= P(\max(|x[n] + c[n]|) > \gamma\sigma) \\ &= 1 - P(\text{all } |x[n] + c[n]| \leq \gamma\sigma). \end{aligned} \tag{5}$$

Let $A(i)$ denote the maximum amplitude on reduction tone i. We now assume that an arbitrary reduction signal $c[n]$ can be created, with the only limitation being that it nowhere can have a value that is higher than the sum of the amplitudes of the PAR reduction tones,

$$|c[n]| \leq A_{\max} = \sum_{i=1}^{U} A(i), \tag{6}$$

see Figure 3, with U denoting the number of tones reserved for PAR reduction. This means that we can reduce all samples in $x[n]$ where $|x[n]| \leq \gamma\sigma + A_{\max}$ down to the clip level $\gamma\sigma$. Since this model gives more degrees of freedom than a PSD constraint on each tone, and we make optimal use of

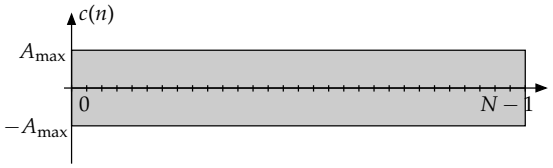

Figure 3: Limits for reduction signal in bound for PSD-constrained tone placement.

this freedom, we will then get a lower bound on the achievable PAR level for the constrained PSD case. The clip probability can be bounded as

$$\begin{aligned} p_N &= 1 - P(\text{all } |x[n] + c[n]| \leq \gamma\sigma) \\ &\geq 1 - P(\text{all } |x[n]| \leq \gamma\sigma + A_{\max}) \\ &= 1 - \left(1 - 2Q\left(\gamma + \frac{1}{\sigma}\sum_{i=1}^{U} A(i)\right)\right)^N, \end{aligned} \tag{7}$$

where we have used the assumption that the different $x[n]$ are uncorrelated. Solving this for γ, we get the lower bound on the achievable PAR level (γ^2) as a function of the desired clip probability:

$$\gamma \geq Q^{-1}\left(\frac{1 - (1 - p_N)^{1/N}}{2}\right) - \frac{1}{\sigma}\sum_{i=1}^{U} A(i). \tag{8}$$

This is the analytical lower bound, which in the next section will be numerically compared to the simulation results.

The bound is derived for critically sampled signals. Since the peak value of a continuous-time signal is as least as high as the peak value of the sampled signal, the bound also specifies a lower bound on the achievable peak level of the continuous-time signal. Then, however, the bound cannot be expected to be as tight.

3.2 Numerical evaluation with constrained power

The bound for PSD-constrained reduction in (8) is a result dependent on the maximum tone amplitudes $A(i)$. In order to compare this with the simulations, we can include the implemented constraints, where the maximum tone amplitude $A(i)$ is proportional to σ, the standard deviation of the transmitted signal:

$$A(i) = \sigma \cdot \frac{\sqrt{2}}{\sqrt{U_0 - U}} \cdot \frac{1}{\cos\frac{\pi}{s}}. \tag{9}$$

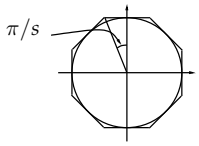

Figure 4: Constraints implemented in the linear programming algorithm. The circle represents the ideal power constraint, but the octagon is implemented as a linear approximation. This corresponds to $s = 8$ in (9).

The expression is independent of i, i.e., a constant-valued PSD constraint is used. When minimizing the PAR level using a limited energy per tone, the algorithms often choose to use the maximum allowed energy on most tones and the average added energy will be approximately the same as the maximum allowed energy. The constraint implemented therefore constrains the maximum energy per reduction tone to the average energy per data tone.[1]

The $\sqrt{2}/\sqrt{U_0 - U}$ part of (9) divides the total energy with the number of used data tones. U_0 is the number of available transmitting tones, so $U_0 - U$ will be the number of used data tones. The cosine expression at the end comes from the linear approximation of the power constraint, see Figure 4.

The bound can now be evaluated numerically using (8) and (9). Figure 5 shows how the PSD constraint affects the reduction performance for a system with 12 reduction tones. Two different tone placements are used, both randomly selected tones as well as the block of highest DFT tones. For 12 randomly selected tones, the bound becomes a tight limit below a clip probability of 10^{-3}. The difference to the block of highest tones is small when the PSD constraint is introduced. Figure 6 shows what reduction performance can be achieved as a function of number of PAR tones, evaluated for a symbol clip probability of 10^{-3}. Since the bound relates to the average performance, some individual simulations can cross this level. Figure 6 indicates that for up to about 10 PAR reduction tones, both the random placement and the block placement closely follow the bound. This indicates, that up to this number of tones, the performance is insensitive to the placement of the data reduction tones. What matters in this region is instead the total available amplitude, i.e. the number of reserved reduction tones.

[1] PSD masks, as often defined in standards, imply a constraint on the average power per tone [8].

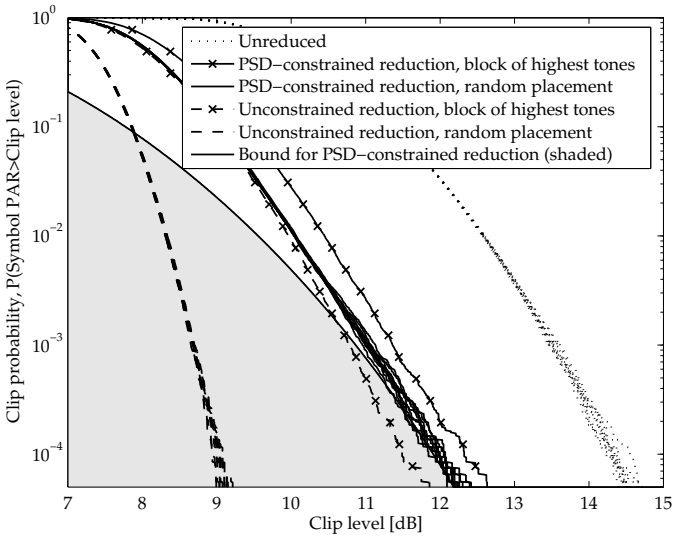

Figure 5: Symbol clip probability (one symbol equals 512 samples) for tone sets with 12 randomly selected reduction tones. The bound for constrained power is shown as a solid line. For the random placements, 10 different placement realizations are shown.

4 Implication on a system level

The ADSL standard [8] restricts the signal clips to 0.00001% of the time, corresponding to a sample clip probability of $p_1 = 10^{-7}$. According to (3), for a Gaussian signal this corresponds to a PAR level of 14.5 dB. From Figure 2, this is far away in the region where we very seldom have more than one clip. On a symbol basis, the clip probability would then most often be

$$p_N = Np_1 = 5.12 \cdot 10^{-5}. \tag{10}$$

Figure 5 shows that the bound is tighter with decreasing clip probabilities. Thus, we can expect that the bound, when varying the number of reduction tones as in Figure 6, would work at least as well as before. Figure 7 shows the same situation as Figure 6, but with this lower symbol clip probability, corresponding to the ADSL case. As seen, the curves are now not as smooth, since more of the time-consuming full linear optimizations are needed to simulate this low clip probability.

The two simulation curves and the bound curve follow the same path until well after 10 PAR reduction tones. The point where the tone placement starts to make a difference is seen to be at a PAR level about 12 dB.

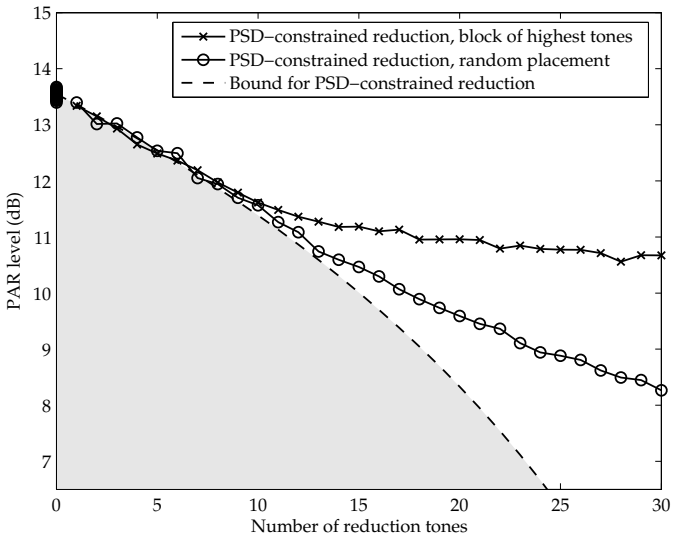

Figure 6: PAR level as a function of number of PAR reduction tones. The results are shown for a symbol clip probability of 10^{-3}. Up to 10 reduction tones, the difference between the placement methods is negligible, and the performance closely follows the bound.

In section 2.2, it was seen that starting at approximately this clip level, a clipped symbol had almost always only one clipped sample. We can interpret this result as if you have a signal that is unlikely to create more than one sample over the desired maximum limit, any tone set will do the job.

Considering the ADSL system environments, the characteristics of the cable are often worse for high frequencies. With long cable lengths, there can in many cases be impossible to have any data on the highest tones. Using these for PAR reduction would give the possibility of lower PAR values without wasting any data capacity. For PAR reduction down to about 12 dB, the chosen tone set does not really matter, and then the tone set discarding the least data could be used. For really long loops, a large part of the spectrum has too bad frequency characteristics, and there are many contiguous tones free to use. Here the reduction performance follows the upper line for block-placed tones, now performing worse than the random placement. Although the number of reduction tones increases, the performance does not increase as fast.

In general, if many tones are available and can be chosen freely, the placement of the tones starts to gain importance. Then more PAR reduction performance can be gained by creating a better tone set by spreading out the tones. In fact, the standard [8] admits that certain, otherwise data-

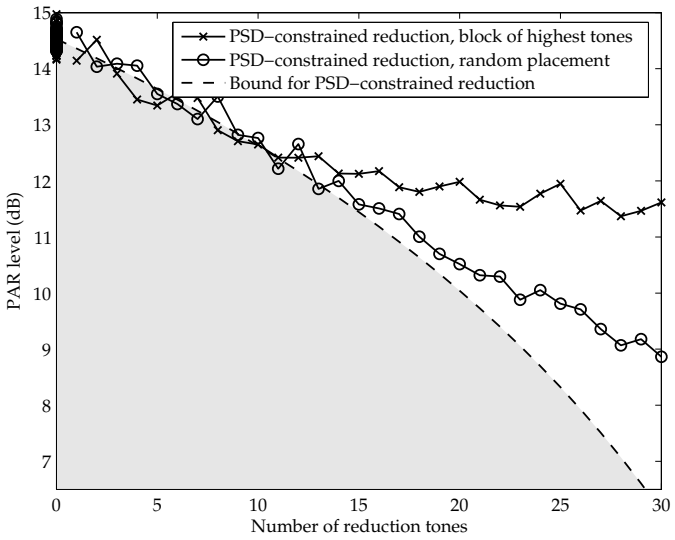

Figure 7: PAR level as a function of number of PAR reduction tones. Similar to Figure 6, but the results are shown for a symbol clip probability of $p_N = Np_1 = 5.12 \cdot 10^{-5}$, corresponding to an ADSL system.

carrying, tones are reserved for PAR reduction. Then, the reduction performance would follow the lower line for random placement, but this will at the same time discard data capacity.

The constraints on the allowed amplitude per tone in (9) can seem to be a bit hard, since the maximum added power per tone is limited to the average tone data power. Since not all data symbols need reduction at all, the reduction signal for the symbols that really need reduction could in some cases be allowed to break the PSD constraint. Such implementational issues can in the model be represented by a larger $A_{\max}$.

5 Summary

Looking at certain PAR levels intervals, the existence of signal clips can be categorized: for levels below 8.5 dB, the signal needs reduction in almost every symbol. Approaching 12 dB and above, there is very seldom more than one peak in an unreduced signal. When the signal has an exceeding sample, it is almost always the only one.

This latter region coincides with the region where any tone set can be used for PAR reduction, without losing reduction performance. When op-

erating under a PSD constraint, the reduction performance is quite limited, and according to the bound derived, up to a PAR level of about 12 dB, the importance of tone set choice is inferior to the number of reserved tones.

From the system-design point of view, when the tone set is of minor importance for the reduction performance, the tones with the lowest—possibly zero—bitload could be chosen. Thereby, considering critically sampled signals, the tone reservation approach could be used without sacrificing considerable bandwidth, for PAR reduction down to about 12 dB.

Bibliography

[1] J. Tellado-Mourelo, "Peak to average power reduction for multicarrier modulation," Ph.D. dissertation, Stanford University, Stanford, CA, USA, Sept. 1999.

[2] A. Gatherer and M. Polley, "Controlling clipping probability in DMT transmission," in *Proc. Asilomar Conference on Signals, Systems and Computers*, vol. 1, Pacific Grove, CA, USA, Nov. 1997, pp. 578–584.

[3] M. Friese, "Multitone signals with low crest factor," *IEEE Transactions on Communications*, vol. 45, no. 10, pp. 1338–1344, Oct. 1997.

[4] B. S. Krongold and D. L. Jones, "A new method for PAR reduction in baseband DMT systems," in *Proc. Asilomar Conference on Signals, Systems, and Computers*, vol. 1, Pacific Grove, CA, USA, Nov. 2001, pp. 502–506.

[5] P. O. Börjesson, H. G. Feichtinger, N. Grip, M. Isaksson, N. Kaiblinger, P. Ödling, and L.-E. Persson, "A low-complexity PAR-reduction method for DMT-VDSL," in *Proc. 5th International Symposium on Digital Signal Processing for Communication Systems*, Perth, Australia, Feb. 1999, pp. 164–199.

[6] ——, "DMT PAR-reduction by weighted cancellation waveforms," in *Proc. Radiovetenskaplig Konferens*, Karlskrona, Sweden, June 1999, pp. 303–307.

[7] N. Petersson, "Peak and power reduction in multicarrier systems," Licentiate thesis, Lund University, Lund, Sweden, Nov. 2002.

[8] ITU-T, *Asymmetric digital subscriber line (ADSL) transceivers*. Recommendation G.992.1, June 1999.

[9] N. Petersson, A. Johansson, P. Ödling, and P. O. Börjesson, "Analysis of tone selection for PAR reduction," in *Proc. International Conference on Information, Communications & Signal Processing*, Singapore, Oct. 2001.

Paper III

Paper III

PSD-Constrained PAR Reduction for DMT/OFDM

Niklas Andgart, Brian Krongold, Per Ödling,
Albin Johansson, and Per Ola Börjesson

Common to all DMT/OFDM systems is a large peak-to-average ratio (PAR), which can lead to low power efficiency and nonlinear distortion. Tone reservation uses unused or reserved tones to design a peak-canceling signal to lower the PAR of a transmit block. In DMT ADSL systems, the power allocated to these tones may be limited due to crosstalk issues with many users in one twisted pair bundle. This PSD limitation not only limits PAR reduction ability, but also makes the optimization problem more challenging to solve. Extending the recently proposed active set tone reservation method, we develop an efficient algorithm with performance close to the optimal solution.

Published in *EURASIP Journal on Applied Signal Processing*, vol. 2004, no. 10, pp. 1498–1507, Aug. 2004, published by Hindawi Publishing Corporation. This work was supported by Ericsson AB and by the Australian Research Council.

1 Introduction

Communication systems using multicarrier modulation have recently become widely used both in wireless (DVB-T, DAB, IEEE 802.11a) and wireline (ADSL, VDSL) environments [1–3]. Multicarrier systems have distinct advantages over single-carrier systems, but suffer from a serious drawback: the approximately Gaussian-distributed output samples cause a high peak-to-average ratio (PAR) that results in low power efficiency and possible nonlinear distortion.

In order to alleviate this PAR problem, many researchers have made efforts to reduce large signal peaks through a variety of PAR reduction methods [4–10]. A technique known as *tone reservation* was initially developed in [4, 5] and is well suited for discrete multitone modulation (DMT) ADSL systems over twisted pair copper wiring. A common phenomenon of this environment is a distance-dependent rolloff of the channel transfer function power with increasing frequency, resulting in upper frequency subchannels having very low SNRs and being incapable of reliably transmitting data. An additive peak-canceling signal can be constructed from these dataless tones, as in [4, 5], to help reduce the PAR problem. Further developed tone reservation algorithms have been presented in [11–18].

In ADSL and other practical systems, the peak-reduction signal may be power limited on each of the reserved tones due to crosstalk constraints with many users being serviced in one twisted pair bundle. This is, for instance, manifested in the recent ADSL2 standard [19] as a $-10\,\mathrm{dB}$ PSD limit on the reserved tones compared to the data-carrying tones. This PSD constraint on the tones can change the theoretical ability of tone reservation to reduce the PAR [20, 21] as well as the complexity versus performance tradeoff for practical algorithms.

In this paper, we analyze the PSD-constrained tone reservation problem and its complexity versus performance tradeoff. We extend the recently proposed active set tone reservation approach [16] to handle PSD constraints. Results are analyzed and compared to performance bounds, and computational complexity and algorithm alteration are detailed. In Section 2, we define the system and data model, give a description of the active set PAR reduction algorithm, and introduce PSD-constrained tone reservation. Extension of the active set approach to the PSD-constrained case is presented and analyzed in Section 3, followed by simulation results presented in Section 4.

2 DMT and tone reservation

A DMT system uses a symbol length of N samples, which is typically 512 samples in the ADSL downstream direction. Although these samples uniquely define a signal block, when considering the PAR of the analog signal, *peak regrowth* [16–18] between the sampling points upon digital-to-analog (D/A) conversion has to be considered. Oversampling of the digital signal is a viable approach.

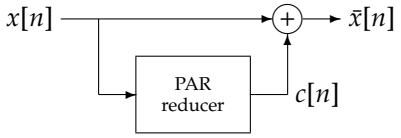

Figure 1: Addition of a PAR reduction signal, $c[n]$, that counteracts the peaks in $x[n]$. The signal $c[n]$, comprised of a small subset of tones, is a function of the data signal $x[n]$.

Figure 1 schematically describes the reduction approach. A reduction signal $c[n]$ is added to the original data signal $x[n]$, and is constructed of dataless tones that either cannot transmit data reliably (due to low SNRs) or are explicitly reserved by the system for PAR reduction. For example, in the ADSL2 standard, the mechanism for this is to exclude the reserved tones from the *supported set* of data tones during startup. The goal for the PAR reduction algorithm is to make the resulting signal, $\bar{x}[n] = x[n] + c[n]$, have a smaller amplitude span than $x[n]$. If the reduction signal is constructed of tones with low SNRs, the reduction signal $c[n]$ may be attenuated before arriving at the receiver. This makes tone reservation using low SNR tones mainly applicable to reducing the transmitter side PAR.

The PAR is defined as

$$\mathrm{PAR}\{\bar{\mathbf{x}}\} = \frac{\max_n |x[n] + c[n]|^2}{E\left[|x[n]|^2\right]}, \tag{1}$$

where the average power in the denominator is that of the data-bearing

signal before PAR reduction is applied.[1] We define

$$\begin{aligned}\bar{x}[n] &= x[n] + c[n] \\ &= \frac{1}{\sqrt{N}} \sum_{k=0}^{N-1} (X_k + C_k)\, e^{j2\pi kn/N},\end{aligned} \tag{2}$$

where X_k represents the data symbols and C_k the FFT domain PAR reduction signal. On a given DMT tone, one of them has to be zero to maintain distortionless data transmission:

$$X_k + C_k = \begin{cases} X_k, & k \in \mathcal{U}^c, \\ C_k, & k \in \mathcal{U}, \end{cases} \tag{3}$$

where $\mathcal{U}^c$ represents the set of data-bearing subchannels and $\mathcal{U}$ represents the set of available subchannels for PAR reduction.

Let $\mathbf{x}_L$ denote the data signal of one symbol block and $\mathbf{c}_L$ denote the additive peak-reduction signal generated from the tone set $\mathcal{U}$, both oversampled to L times the nominal sample rate. We focus on the specific case of a real baseband DMT system, where the data and reduction signals can be expressed as weighted sums of real-valued sinusoids and cosinusoids. In matrix form, we can write $\mathbf{c}_L = \check{\mathbf{Q}}_L \check{\mathbf{C}}$, where $\check{\mathbf{Q}}_L$ is a $NL \times 2U$ matrix of sinusoidal and cosinusoidal column vectors with frequencies specified by the U reserved tones $t_1, \ldots, t_U$,

$$\check{\mathbf{Q}}_{L(i,j)} = \begin{cases} \cos \dfrac{2\pi(i-1)t_{(j+1)/2}}{NL}, & i \text{ odd}, \\ \sin \dfrac{2\pi(i-1)t_{j/2}}{NL}, & i \text{ even}, \end{cases} \tag{4}$$

and $\check{\mathbf{C}}$ is a length $2U$ vector with the weights of these (co)sinusoids,

$$\check{\mathbf{C}}_{(i)} = \begin{cases} \dfrac{2}{\sqrt{N}} \operatorname{Re}\{C_{t_{(i+1)/2}}\}, & i \text{ odd}, \\ -\dfrac{2}{\sqrt{N}} \operatorname{Im}\{C_{t_{i/2}}\}, & i \text{ even}. \end{cases} \tag{5}$$

For this real-valued case, minimizing the peak magnitude of the resulting signal, equivalent to minimizing its peak power, can be formulated as the

[1] Although it is mainly referred to as the PAR problem, the real issue is the peak power at the high power amplifier (HPA), in DSL systems commonly called the line driver. Reducing the PAR by inflating the average power does not help. The average power is simply a way of normalizing peak power results, and this normalization factor should remain constant for comparison purposes.

linear program [5]

$$\begin{array}{ll} \text{minimize} & \gamma \\ \text{subject to} & \left\{ \begin{array}{r} \mathbf{x}_L + \check{\mathbf{Q}}_L \check{\mathbf{C}} \leq \gamma, \\ -\mathbf{x}_L - \check{\mathbf{Q}}_L \check{\mathbf{C}} \leq \gamma. \end{array} \right. \end{array} \tag{6}$$

2.1 Tone selection

It is desired that reduction signal $\mathbf{c}_L$ cancels out the peaks in the data signal $\mathbf{x}_L$ as best as possible. Total cancellation, $\mathbf{c}_L = -\mathbf{x}_L$, is naturally impossible, and an alternative, yet still unrealistic, goal is to drive the signal towards a PAR of 0 dB (i.e., the peak power and average power are equal). This tight control of the signal requires a large portion of the frequency band. In general, more reserved tones lead to a lower PAR, and therefore, a tradeoff exists between data throughput and PAR [22]. A choice must be made as to which tones will be used for PAR reduction rather than data transmission. If the system is able to freely choose, the distribution of these tones over the system bandwidth has a significant impact on PAR reduction ability. In general, with no power constraints on the reduction tones, an uneven, spread-out placement (e.g., generated by a random selection of tones) allows for very good PAR reduction [5, 23]. A significant performance loss, however, results by placing the reduction tones as a contiguous block or uniformly distributed over the entire bandwidth.

In wireline DMT systems, it is preferred to use those tones which cannot send data reliably due to insufficient SNRs, thereby maintaining the same throughput level. Generally, these tones are in the uppermost frequencies, and tend to resemble a contiguous block of tones, which is not a good tone set in terms of performance. An alternative is to reduce the system throughput by sacrificing some tones for peak reduction and achieving an uneven, spread-out placement. We will consider these two extreme cases of tone placement. In practice, a combination of these may turn out to be the most attractive choice.

After determining the set of reserved tones, the reduction signal $\mathbf{c}_L$ is created from a nominal peak-reduction kernel $\mathbf{p}$ [5], formed by projecting an impulse at $n = 0$ onto the set of tones $\mathcal{U}$. This corresponds to the least squares approximation of the impulse with equal weight on each reduction tone. Other forms of $\mathbf{p}$ generated by different criteria, such as minimizing the size of their sidelobes, have been suggested in [5].

2.2 Active set tone reservation

The linear program in (6) can be solved with a simplex method, but is expensive with a complexity of $O(N^2L^2)$ operations. Computationally efficient

$O(NL)$ approaches based upon projection-onto convex sets (POCS) and gradient projection were developed in [4] and [5], respectively, but suffer from slow convergence. A recent $O(NL)$ approach [13, 16] was developed based on active set methods [24] and exhibits rapid convergence towards a minimax PAR solution. Whereas a finite number of iterations will achieve the optimal PAR level γ^* for the given tone set, a very good suboptimal solution can be achieved in two or three iterations, making this an attractive practical solution.

As in the gradient project and POCS approaches, the active-set approach reduces the PAR through the use of the kernel $\mathbf{p}$. Circularly shifted versions of this kernel, $\mathbf{p}_{\langle\cdot\rangle}$, also lie in the signal space generated from $\mathcal{U}$, allowing easy reduction of a peak at an arbitrary sample location.

Beginning with the sample of largest magnitude γ_0 at location n_0, the peak is reduced by subtracting a scaled version of $\mathbf{p}_{\langle n_0\rangle}$ until a second peak at some location n_1 is *balanced* with it at some magnitude $\gamma_1 < \gamma_0$. These two peaks are then reduced equally through a linear combination of $\mathbf{p}_{\langle n_0\rangle}$ and $\mathbf{p}_{\langle n_1\rangle}$ until a third peak is balanced. These three peaks are reduced equally until a fourth is balanced, and so forth. When a sample is at the peak magnitude, it signifies an active inequality constraint (i.e., strictly equal) in (6), and the active-set approach is therefore building a set of active constraints. Mathematically, the iteration updates can be written as

$$\bar{\mathbf{x}}^{(i)} = \bar{\mathbf{x}}^{(i-1)} - \mu^{(i)}\hat{\mathbf{p}}^{(i)}, \tag{7}$$

where $\bar{\mathbf{x}}^{(i)}$ represents the signal after the ith iteration, $\hat{\mathbf{p}}^{(i)}$ is the descent direction in the ith iteration, and $\mu^{(i)}$ represents the descent step size.

At the start of the ith iteration, there will be i peaks which are balanced at locations $n_0, n_1, \ldots, n_{i-1}$. To keep these peaks balanced, the next iteration descent must satisfy

$$\hat{p}^{(i)}_{n_k} = \operatorname{sign}\left(\bar{x}^{(i)}_{n_k}\right) = S_{n_k}, \quad k = 0, 1, \ldots, i-1, \tag{8}$$

with the assumption that we scale $\hat{\mathbf{p}}^{(i)}$ to have unit magnitude in locations corresponding to the active set of peaks. No matter what value of $\mu^{(i)}$ is chosen, the magnitudes of the peaks at $n_0, n_1, \ldots, n_{i-1}$ will remain equal. The $\hat{p}_{n_i}$ values can be calculated as

$$\hat{\mathbf{p}}^{(i)} = \sum_{k=0}^{i-1} \alpha_k^{(i)}\, \mathbf{p}_{\langle n_k\rangle}, \tag{9}$$

where the $\alpha_k^{(i)}$ are computed by solving the $i \times i$ system of equations

$$\begin{bmatrix} 1 & p_{n_0-n_1} & \cdots & p_{n_0-n_{i-1}} \\ p_{n_1-n_0} & 1 & \cdots & p_{n_1-n_{i-1}} \\ \vdots & \vdots & \ddots & \vdots \\ p_{n_{i-1}-n_0} & p_{n_{i-1}-n_1} & \cdots & 1 \end{bmatrix} \begin{bmatrix} \alpha_0^{(i)} \\ \alpha_1^{(i)} \\ \vdots \\ \alpha_{i-1}^{(i)} \end{bmatrix} = \begin{bmatrix} S_{n_0} \\ S_{n_1} \\ \vdots \\ S_{n_{i-1}} \end{bmatrix}. \tag{10}$$

This requires an $i \times i$ matrix inverse, but in practical implementations, i will typically be at most 3, and the inverse cost is then insignificant relative to the the total iteration complexity. Furthermore, efficient inverse techniques [25] can be applied as in addition to being symmetric (due to the symmetry of $\mathbf{p}$), the matrix in a given iteration is contained in the matrix for the next iteration.

The step size $\mu^{(i)}$ required to balance the next active peak is determined by testing samples as follows[2] (see [15,16] for more details),

$$\mu^{(i)} = \min_{q \notin \mathcal{A}} \left(\frac{\gamma^{(i-1)} - \left| \bar{x}_q^{(i-1)} \right|}{1 - \text{sign}\left(\bar{x}_q^{(i-1)} \right) \hat{p}_q^{(i)}} \geq 0 \right), \tag{11}$$

where $\mathcal{A}$ represents the set of samples in the active set. Strategies exist [15,16] to reduce the sample testing complexity as the structure of $\bar{\mathbf{x}}^{(i)}$ and $\hat{\mathbf{p}}^{(i)}$ can be exploited to eliminate many potential samples from consideration. For practical implementation, the division operation can be replaced by a multiplication with the output of a prestored inverse lookup table to approximate $1/\left(1 - \text{sign}\left(\bar{x}_q^{(i-1)}\right) \hat{p}_q^{(i)}\right)$. Exact values are not needed for comparison purposes, and therefore, a dense lookup table is not required.

2.3 PSD-constrained tone reservation

Solving (6) for the optimum PAR value will in many cases cause the power on the reduction tones to grow immensely as the very last bits of reduction performance require large reduction signals. A standardized system generally has to follow certain PSD constraints on data tones. Similar rules are applicable for reduction tones as well, especially in wireline systems where crosstalk exists and the effect on other users should be kept to a minimum. Thus, a system may have to abide by instantaneous and/or average power constraints on the reserved tones.

What the PSD constraint should be is a system design issue based upon factors such as crosstalk and power consumption or, in practice, often determined by a standard. In the new ADSL2 ITU-T Recommendation [19, figure

[2] The $\min(\cdot \geq 0)$ notation means to take the minimum over the non-negative elements.

8-19/G.992.3], *passband* tones are under strict control and can be grouped into different categories: one group of tones is for data transmission and another group consists of monitored tones for receiver functions (e.g., channel estimation). Both of these groups belong to the *medley set*. Tones that are not in the medley set have a PSD restriction 10 dB below the nominal PSD level and these are the tones that can be used for PAR reduction.

Since the PSD is a measurement averaged over time, the power on the tones may be allowed to vary from symbol to symbol, and the instantaneous power of a symbol may therefore exceed the PSD constraint. As an example, consider a target PAR value of 12 dB and the uppermost probability curves for unreduced signals shown in Figures 4 to 9. It follows that approximately 8% of the symbols require PAR reduction, and due to averaging, a revised PSD constraint on the reserved tones can be determined. If PAR reduction is employed for only 8% of the symbols, we can allow an average reserved-tone power $10\log(1/0.08) \approx 11$ dB above its overall -10 dB PSD constraint. This results in a revised PSD constraint on the reserved tones $-10\,\text{dB} + 11\,\text{dB} = +1\,\text{dB}$ above the nominal PSD mask for the ADSL2 system.

When processing one symbol at a time, however, a peak-power constraint per tone for each symbol is much easier to deal with than an averaged PSD constraint. Using this power constraint can cause the averaged PSD figure to be somewhat less than this peak constraint. Nevertheless, for a given peak-power constraint per tone, a corresponding averaged PSD level can be determined experimentally for a specific system, and the constraints can then be interchanged. In the rest of this paper, we consider the peak power limitation, or *instantaneous* PSD constraint, on each tone rather than a PSD as a result of averaging.

Incorporating the power constraint on each tone, the PSD restriction becomes part of (6) in the form of a quadratic constraint:

$$\begin{aligned} &\text{minimize} \quad \gamma \\ &\text{subject to} \quad \begin{cases} \mathbf{x}_L + \check{\mathbf{Q}}_L \check{\mathbf{C}} \leq \gamma, \\ -\mathbf{x}_L - \check{\mathbf{Q}}_L \check{\mathbf{C}} \leq \gamma, \\ \check{\mathbf{C}}^2_{(2l-1)} + \check{\mathbf{C}}^2_{(2l)} \leq A^2_{l,\max}, \end{cases} \end{aligned} \tag{12}$$

where $A_{l,\max}$ is the limitation in amplitude on tone t_l. Due to the introduction of quadratic constraints, the problem is no longer a linear program, but instead a *Quadratically Constrained Quadratic Program* (QCQP).

3 PSD-constrained active set approach

3.1 Modifications for PSD constraints

If the active set algorithm is to be used in the PSD-constrained case, it must be modified. Letting $\check{C}_l$ denote the lth element of $\check{\mathbf{C}}$ (including both cosine and sine parts), the total weight on tone t_l after iteration i can be described as

$$\check{C}_l^{(i)} = \check{C}_l^{(i-1)} + \Delta\check{C}_l^{(i)}, \tag{13}$$

where the increments $\Delta\check{C}_l^{(i)}$ in each iteration include the effect from reducing one additional peak. Using the stepsize $\mu^{(i)}$ and weighting $\alpha_k^{(i)}$ from (9), the increments $\Delta\check{C}_l^{(i)}$ can be expressed in cosine and sine components.

$$\begin{aligned}\Delta\check{C}_l^{(i)} &= \left[\begin{array}{cc} \Delta\check{C}_{l,\cos}^{(i)} & \Delta\check{C}_{l,\sin}^{(i)} \end{array}\right] \\ &= K\mu^{(i)} \sum_{k=0}^{i-1} \alpha_k^{(i)} \left[\begin{array}{cc} \cos\left(\dfrac{2\pi t_l n_k}{NL}\right) & \sin\left(\dfrac{2\pi t_l n_k}{NL}\right) \end{array}\right],\end{aligned} \tag{14}$$

where K is a known constant that results from normalizing $\mathbf{p}$ so that $p_0 = 1$. We can think of three main outcomes when performing an active set iteration at an instance where none of the PSD constraints have been met or exceeded:

(*i*) *A new peak is balanced and no PSD constraints are met.* This is the same case as with no PSD constraint. The algorithm can continue with its next step.

(*ii*) *All tones meet/exceed the PSD constraints at the same time.* This happens when reducing one peak and reaching the PSD constraint before a second active peak is encountered.

(*iii*) *Some tones meet/exceed the PSD constraint.* This can happen when two or more peaks are already balanced. Then different tones will likely have different magnitudes, see Figure 2.

For case (*i*), the algorithm will be identical to what is described in Section 2.2. For case (*ii*), the algorithm merely takes the step $\mu_{\max}$ that fills all subchannels to the PSD constraint, and the optimal solution has been reached.

The interesting question is what to do in case (*iii*), as some of the tones have filled up or gone past their PSD constraints, while others are still available for further reduction. The μ descent can easily be scaled back to where

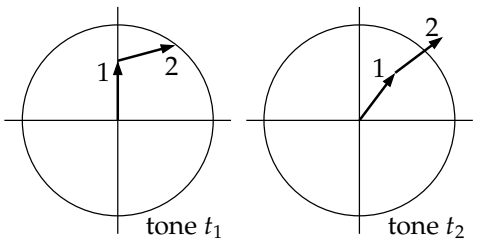

Figure 2: Addition of the tone weights for reduction of two different peaks can cause the PSD constraint to be reached on certain tones before others.

the first tone reaches the PSD constraint, that tone can be frozen, and the remaining tones can be used for PAR reduction for subsequent iterations. This process can be repeated until all tones reach the PSD constraint. We note that an iteration now refers to the operations performed to reach either a new active peak or a new tone that meets the PSD constraint.

3.2 Cost-versus-performance issues

It can be expected that once any tone reaches the PSD constraint, many or all of the remaining tones are not far from reaching it as well. At this point, the problem is that convergence speed (i.e., additional PAR reduction per iteration) is severely reduced as a new iteration must be performed to the point where either a new tone reaches the PSD constraint or a new active peak is encountered.

After each new tone reaches the PSD constraint and is shut off, the set $\mathcal{U}$ changes and a new nominal peak-reduction kernel $\mathbf{p}$ needs to be recomputed. Rather than compute the projection of an impulse onto the remaining tones, the contribution of the removed tone can just be subtracted (using NL operations) from the latest $\mathbf{p}$.

3.3 Low complexity algorithm

The cost-versus-performance tradeoff dictates that it may not be worth iterating beyond the point where the first tone reaches the PSD constraint, and therefore not utilizing the available remaining power in the other tones. This low complexity approach saves a lot of computation and results in only a small performance loss from the optimal solution as simulations show in the next section. The complexity of this extended algorithm is the same as the unconstrained active set approach with an additional extra cost of

keeping track of the signal power in each tone. This cost is insignificant compared to the rest of the algorithm since $U \ll NL$.

During each iteration, a new $\hat{\mathbf{p}}^{(i)}$ is created according to (9), and in parallel to that, the new signal in each tone is calculated, based on the additional contributions according to (14). Before applying (7) and potentially wasting operations, $2U$ multiplies and U adds are used to check the tones powers against the PSD constraint. If any of the tones exceed the PSD constraint, $\mu^{(i)}$ must be scaled back to find the point where the PSD constraint is met with one or more tones. The quadratic equation

$$\left| C_l^{(i-1)} + \beta_l \mu^{(i)} \Delta C_l^{(i)} \right|^2 = A_{l,\max}^2 \tag{15}$$

is solved for β_l for the tone(s) exceeding the PSD constraint, and the minimum β_l value is chosen to scale $\mu^{(i)}$. This modified stepsize is then used in (7) to compute the final PAR-reduced signal.

3.4 Performance bounds

It is important to gauge how much performance is lost when using this low complexity algorithm that halts PAR reduction once any tone reaches the PSD constraint. Three lower bounds on achievable PAR level are now presented.

Bound on minimum PAR

The resulting PAR level after the low complexity algorithm can be compared to the optimal solution of (12). This equation represents a QCQP, and still is a convex problem. Linear approximations of the quadratic constraint (see Figure 3) can be employed to transform the problem back to linear programming form [21], in order to solve the problem with linear programming algorithms. Thereby, a performance bound[3] can be computed through simulations. It should be noted that this bound on the optimal solution is extremely tight when used with polygons of 16 sides and larger.

$A_{\max}$ bound

The constraint on maximum power per tone (equivalent to a constraint on the maximum magnitude) results in limiting the magnitude of the peak-reduction signal to $A_{\max}$, where

$$A_{\max} = \sum_{l=1}^{U} A_{l,\max}. \tag{16}$$

[3]The polygonal approximation completely bounds the circle, thus, the resulting performance will be at least as good as the quadratically constrained optimal solution.

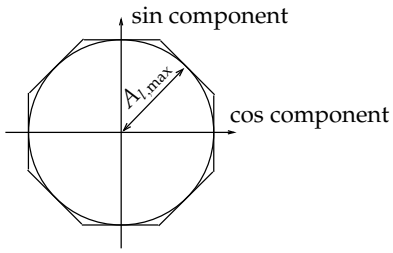

Figure 3: Linear approximation of the quadratic magnitude constraints. An octagon is shown here, but a polygon with a larger number of sides can be used for a better approximation.

We assume that an arbitrary peak-reduction signal can be created, with the only limitation being that its amplitude is between $-A_{\max}$ and $A_{\max}$. As a result, starting with a symbol with peak level $\max|x_L[n]|$, the peak level can at best be reduced down to $\max|x_L[n]| - A_{\max}$. Since this model admits additional degrees of freedom compared to the true reduction signal, it serves as a lower bound on the achievable PAR level. Given a peak value for a symbol block, this can be expressed as

$$\max|\bar{\mathbf{x}}_L| = \max|\mathbf{x}_L + \mathbf{c}_L| \geq \max|\mathbf{x}_L| - A_{\max}. \tag{17}$$

This $A_{\max}$ bound shows that when the PSD constraint is quite restrictive and only a small number of tones are reserved, PAR reduction performance is severely limited, even with an arbitrary choice of reduction tones [20,21]. In this case, a choice of tones discarding the minimum amount of data capacity may be the most favorable.

2-Bound

The $A_{\max}$ bound from (17) corresponds to the achieved peak level when all tones are filled in order to reduce the largest peak in $\mathbf{x}_L$. A similar bound can be computed after the active set approach has already performed its first iteration. The two balanced peaks can be reduced (without any regard for the other samples, and thus making a bound) until all tones meet the PSD constraint. This bound, which we refer to as the *2-bound*, is simple to simulate because α_0 and α_1 must be of equal magnitude due to the symmetry of $\mathbf{p}$.

4 Simulations

A DMT system with symbol length $N = 512$ is simulated with tones 33–255 used for either data transmission or PAR reduction (these system pa-

rameters are the same for downlink ADSL transmission). Each of the data-carrying tones uses a 1024-point QAM constellation. Before active set processing, the signals have been oversampled by the factor $L = 4$ to limit analog peak-regrowth effects upon digital-to-analog conversion. It has been observed that operating on the digital $L = 1$ signal does not provide any worthwhile PAR reduction performance at the analog signal [15]. Oversampling to $L = 4$ makes the computational cost increase by a factor of 4, although $L = 2$ could be employed for a performance decrease which varies based upon the number of tones, their locations, and PSD constraints.

As described in Section 2.3, the averaged PSD constraint for the reduction tones could be set to about 1 dB above the nominal PSD mask for the given example. We now use this figure as a guideline for the instantaneous PSD mask in the following simulations. To illustrate the effects when varying the maximum reduction power per tone, the simulations will first use a restrictive constraint set at the nominal PSD mask, and then use a looser mask, where the magnitude is increased by 50% (+3.5 dB).

We view the forthcoming PAR results on a per-symbol basis using the simulated probability that at least one sample in a symbol block exceeds a certain PAR level. This corresponds to taking the maximum value over one symbol in (1), thereby reflecting the probability that a symbol is transmitted with distortion. This clip probability also is commonly used in the literature. A viable alternative would be to evaluate the clip probability of each individual sample, which reflects the percentage of time the transmitted signal is clipped.

4.1 Block placed tones

Restrictive PSD constraint

Figure 4 shows simulations with the upper block of 12 tones (number 244–255) used for PAR reduction and subjected to an instantaneous PSD constraint equal to the nominal PSD level for the data tones. The curves show the reduction performance using the extended active set algorithm, stopping as soon as any PSD constraint is reached. Shown on the vertical axis is the probability that the time domain symbol block $\bar{\mathbf{x}}_L$ would be clipped if subjected to a clip level γ_c on the x-axis, that is,

$$\text{Prob}\big(\text{PAR}\,\{\bar{\mathbf{x}}_L\} > \gamma_c\big). \tag{18}$$

Starting at the rightmost line, corresponding to the clip probability of an unreduced symbol, curves representing iterations one through four are shown.

The two leftmost curves show the lower bounds from Section 3.4 ($A_{\max}$ bound and 2-bound), which the simulations cannot cross. The third lowest

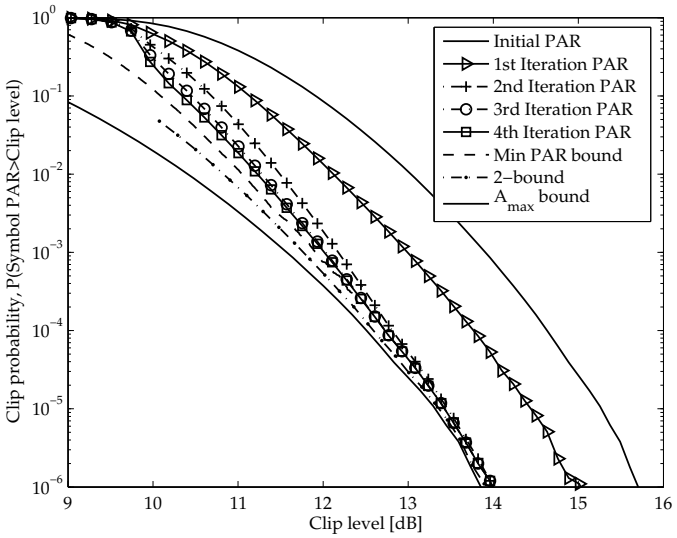

Figure 4: Symbol clip probability for 12 PAR reduction tones, chosen as a contiguous block of the highest tones. Up to four active set iterations are applied, but the algorithm stops once any tone hits the PSD constraint. The three leftmost curves represent optimal solution bounds.

curve, dashed and ending at a clip probability of $3 \cdot 10^{-4}$ is the PAR achieved by finding the minimum value of (6) with linearized quadratic constraints (a 32-sided polygon, cf. Figure 3) and using the same upper block of 12 tones. This curve will also serve as a bound for the suboptimal algorithm, but due to its much larger complexity, this curve has not been simulated for the lower clip probabilities.

Looking at the performance of the low complexity algorithm, we see that for the higher clip probabilities, there is a performance gain of about 0.15 dB going beyond two iterations, and an additional 0.1 dB compared to the minimum PAR bound (dashed line). At the lower clip probabilities, we see that the curves converge towards the $A_{\max}$ bound from (17).

Here we see a situation where a restrictive PSD constraint and a small number of reduction tones set a limit on the achievable PAR level. The reduction performance is limited by the $A_{\max}$ bound, and not necessarily by the block placement reduction performance. The low complexity algorithm provides near-optimal performance at a very low cost for this system.

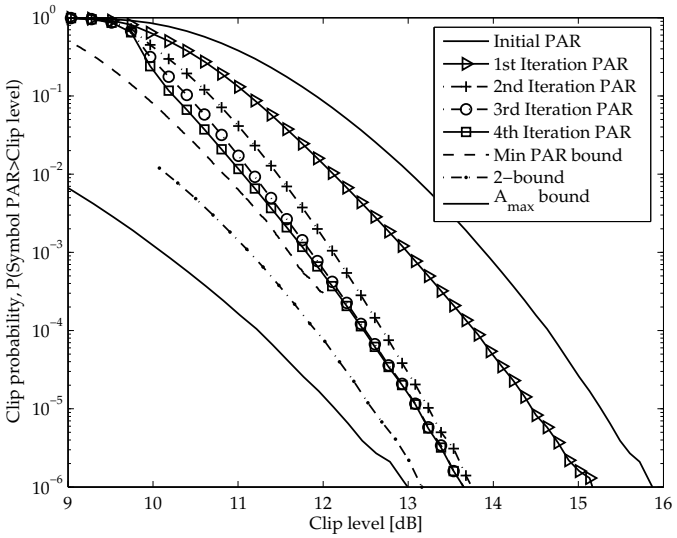

Figure 5: Symbol clip probability for PAR reduction with the 12 highest tones. The PSD constraint allows 50% higher magnitude per tone than in Figure 4. The reduction performance shows only a small gain compared to Figure 4, showing that this placement cannot take much advantage of the loosened PSD constraint.

Loosening the PSD constraint

In Figure 5, the PSD constraint is increased by 50% in magnitude for each tone. Comparing the figures, we see that the lower bound decreases due to an increase of the maximum reduction signal. However, the simulated reduction performance, including the optimal solution, increases by only about 0.3 dB. The block placement simply cannot take advantage of the increased reduction power, and is the real limiting factor in this case. Looking at the performance of the low complexity algorithm, we see that its loss compared to the minimum PAR bound is about 0.2 dB.

Increasing the number of tones

Figure 6 shows results for when the upper block of 24 tones are used for PAR reduction along with the same PSD constraint as in Figure 4. Looking at the figure, we see that the gain from 12 to 24 tones is only about 0.4 dB, which is small considering that the maximum reduction magnitude has been doubled (the $A_{\max}$ bound is significantly lower). In this situation, however, we see that after 4 active set iterations, we are about 0.2 dB from the minimum

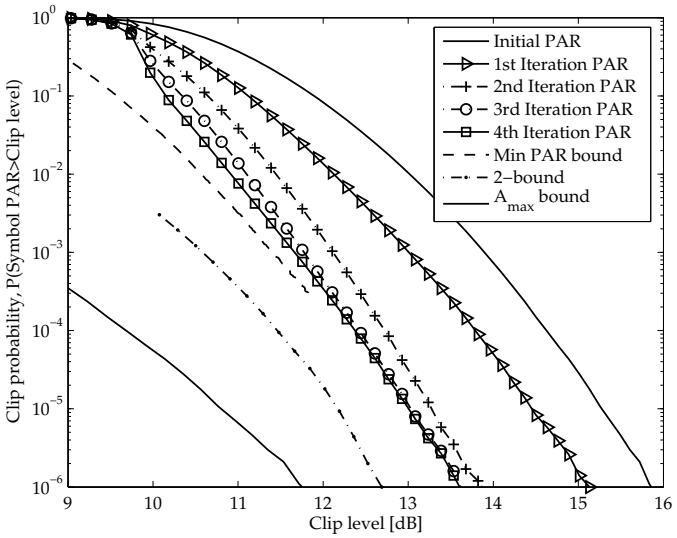

Figure 6: Symbol clip probability for PAR reduction with the 24 highest tones with the same PSD constraint used in Figure 4. The simulations indicate only a small reduction gain compared to Figure 4, showing that adding extra tones to the reserved block does not help PAR reduction much.

PAR bound at higher probabilities, thus telling us that further iterations are likely not worth the significant cost to achieve it.

4.2 Randomly chosen tones

We have seen that even when constraints (PSD limit or number of tones) are loosened, a bad toneset selection can still be a limiting factor. Now a more "spread-out" toneset is evaluated, where the reserved tones are randomly selected in the interval between 33 and 255 inclusive.

Restrictive PSD constraint

Figure 7 shows similar simulations as Figure 4, using the restrictive instantaneous PSD constraint, equal to the average power mask for the data tones. Looking at the figure, the iterations quickly converge to within 0.1 dB of the $A_{\max}$ bound, and the performance is only slightly better than for block placed tones. Here the $A_{\max}$ bound effectively sets the limitation on system performance [20, 21].

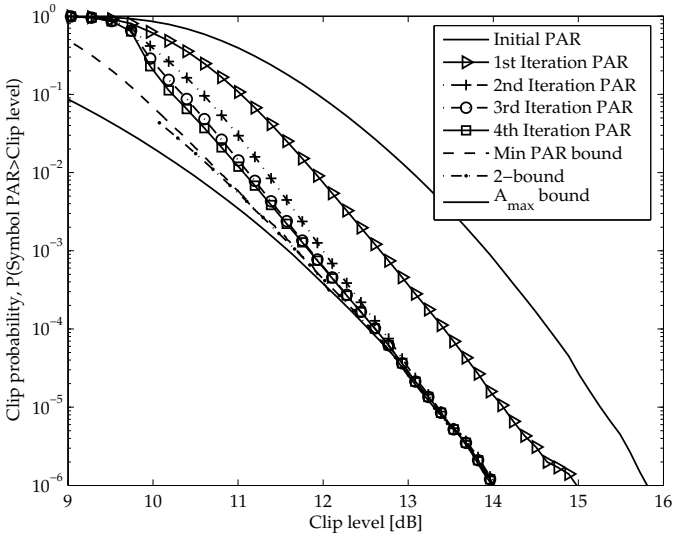

Figure 7: Symbol clip probability for 12 randomly chosen PAR reduction tones. The three lowest curves show bounds on the achievable performance as in previous simulations.

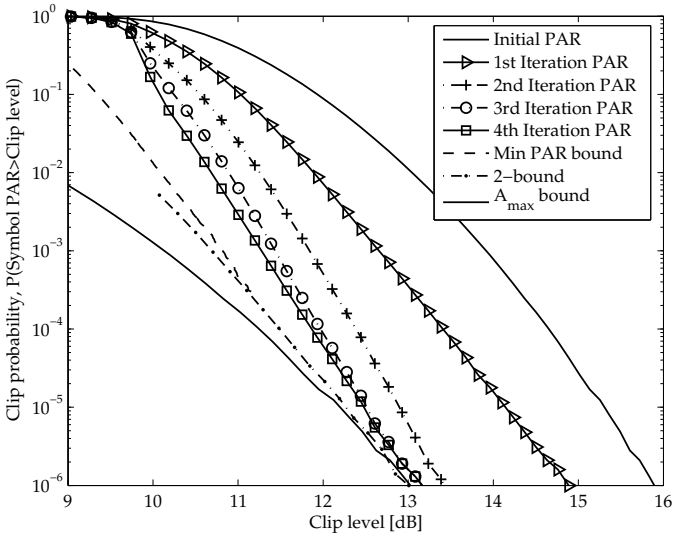

Figure 8: Symbol clip probability for PAR reduction with 12 random tones. The PSD constraint allows 50% higher magnitude per tone than in Figure 7.

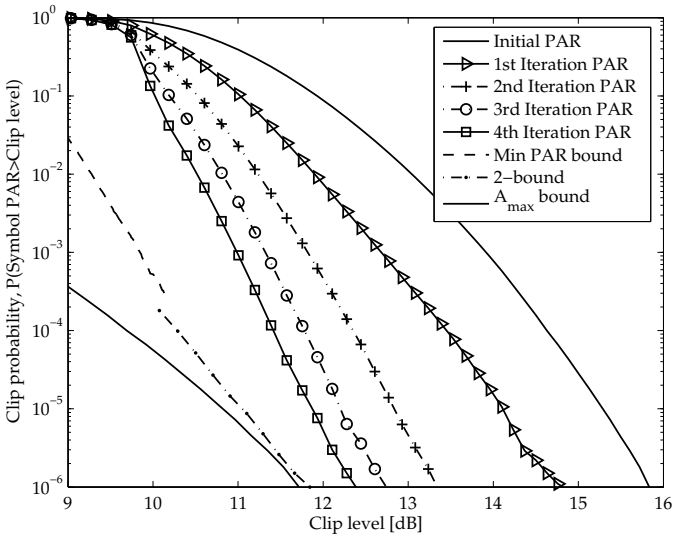

Figure 9: Symbol clip probability for PAR reduction with 24 random tones with the same PSD constraint used in Figure 7.

Loosening the PSD constraint

Figure 8 shows the performance when the PSD constraint is set to allow for a tone magnitude 50% higher than before. The reduction performance has increased thanks to more allowed power. At the lower clip probabilities, the gains are close to 1 dB compared to Figure 7, and the active set results are very close to the performance bounds. At higher clip probabilities, the gains are close to 0.5 dB, but are a noticeable distance from the very tight minimum-PAR bound. This is only a minor issue, since in these regions, the PAR level after 3 or 4 iterations is already rather low.

Increasing the number of tones

Finally, Figure 9 shows simulations using 24 randomly chosen tones, with the restrictive PSD constraint. Due to the superior reduction ability for this placement type, the resulting PAR level is clearly lower than in the previous simulation. The allowed $A_{\max}$ is 100% higher here than with half the number of tones, and we see that a larger number of active set iterations may be needed to achieve PAR levels very close to the optimal solution. However, when considering lower clip probabilities, the 4th active set iteration is not very far from the 2-bound.

5 Conclusions

Introducing PSD constraints into tone reservation affects the achievable PAR reduction and significantly alters the complexity-versus-performance tradeoff for practical algorithms. The results in this paper show the impact that PSD constraints have on tone reservation performance, and it is clear that the effect when using randomly chosen tone sets is more severe than for contiguous tone sets.

A low complexity suboptimal solution has been presented, and results show that its performance is close to optimal solution bounds. Since small performance increases incur a major computation cost (greater than the low complexity algorithm itself), we assert that our proposed approach gives a very good tradeoff of complexity and PAR reduction.

To evaluate whether the oversampling of $L = 4$ is sufficient, the signals were oversampled by an additional factor of 4 after reduction. The peak regrowth has been observed to be less than $0.2\,\mathrm{dB}$. Further studies could also include the effect on peak regrowth after the filter chain present in the transmitter [16–18].

An important special case results when a non-uniform PSD constraint is given, that is, more power is allowed on some reserved tones than others. In this case, certain tones may reach their PSD constraint much sooner than the rest, and sizeable performance gains beyond this stoppage point may still exist. An intelligent approach may be to modify the formation of $\mathbf{p}$ by weighting the impulse projection onto the tones according to the non uniformity of the PSD mask. In this way, the more restricted tones do not reach their PSD constraint with greater ease than the others.

Although the real baseband DMT case is the main focus of this paper, the principles can also be applied to the complex baseband case (for wireless OFDM systems), as an active set approach for this case has already been developed in [14,16]. The problem with tone reservation in wireless systems is that it may not be desirable to sacrifice data tones in a fading channel. However, it is possible that in a fixed wireless scenario (with a slowly varying channel), channel state feedback could be employed and certain subchannels with low SNRs could be used for tone reservation.

Bibliography

[1] J. A. C. Bingham, "Multicarrier modulation for data transmission: An idea whose time has come," *IEEE Communications Magazine*, vol. 28, pp. 5–14, May 1990.

[2] T. Starr, J. M. Cioffi, and P. J. Silverman, *Understanding Digital Subscriber Line Technology*. Upper Saddle River, NJ, USA: Prentice Hall, 1999.

[3] ITU-T, *Asymmetric digital subscriber line (ADSL) transceivers*. Recommendation G.992.1, June 1999.

[4] A. Gatherer and M. Polley, "Controlling clipping probability in DMT transmission," in *Proc. Asilomar Conference on Signals, Systems and Computers*, vol. 1, Pacific Grove, CA, USA, Nov. 1997, pp. 578–584.

[5] J. Tellado-Mourelo, "Peak to average power reduction for multicarrier modulation," Ph.D. dissertation, Stanford University, Stanford, CA, USA, Sept. 1999.

[6] M. Friese, "Multitone signals with low crest factor," *IEEE Transactions on Communications*, vol. 45, no. 10, pp. 1338–1344, Oct. 1997.

[7] D. L. Jones, "Peak power reduction in OFDM and DMT via active channel modification," in *Proc. Asilomar Conference on Signals, Systems, and Computers*, vol. 2, Pacific Grove, CA, USA, Oct. 1999, pp. 1076–1079.

[8] D. J. G. Mestdagh and P. M. P. Spruyt, "A method to reduce the probability of clipping in DMT-based transceivers," *IEEE Transactions on Communications*, vol. 44, no. 10, pp. 1234–1238, Oct. 1996.

[9] B. M. Popović, "Synthesis of power efficient multitone signals with flat amplitude spectrum," *IEEE Transactions on Communications*, vol. 39, no. 7, pp. 1031–1033, July 1991.

[10] R. W. Bäuml, R. F. H. Fischer, and J. B. Huber, "Reducing the peak-to-average power ratio of multicarrier modulation by selected mapping," *Electronics Letters*, vol. 32, no. 22, pp. 2056–2057, Oct. 1996.

[11] P. O. Börjesson, H. G. Feichtinger, N. Grip, M. Isaksson, N. Kaiblinger, P. Ödling, and L.-E. Persson, "A low-complexity PAR-reduction method for DMT-VDSL," in *Proc. 5th International Symposium on Digital Signal Processing for Communication Systems*, Perth, Australia, Feb. 1999, pp. 164–199.

[12] ——, "DMT PAR-reduction by weighted cancellation waveforms," in *Proc. Radiovetenskaplig Konferens*, Karlskrona, Sweden, June 1999, pp. 303–307.

[13] B. S. Krongold and D. L. Jones, "A new method for PAR reduction in baseband DMT systems," in *Proc. Asilomar Conference on Signals, Systems, and Computers*, vol. 1, Pacific Grove, CA, USA, Nov. 2001, pp. 502–506.

[14] ——, "A new tone reservation method for complex-baseband PAR reduction in OFDM systems," in *Proc. IEEE International Conference on Acoustics, Speech, and Signal Processing*, vol. 3, Orlando, FL, USA, May 2002, pp. 2321–2324.

[15] B. S. Krongold, "New techniques for multicarrier communication systems," Ph.D. dissertation, University of Illinois at Urbana-Champaign, Urbana, IL, USA, Nov. 2001.

[16] B. S. Krongold and D. L. Jones, "An active-set approach for OFDM PAR reduction via tone reservation," *IEEE Transactions on Signal Processing*, vol. 52, no. 2, pp. 495–509, Feb. 2004.

[17] W. Henkel and V. Zrno, "PAR reduction revisited: an extension to Tellado's method," in *Proc. International OFDM-Workshop*, Hamburg, Germany, Sept. 2001, pp. 31.1–31.6.

[18] J. Tellado and J. M. Cioffi, *Further Results on Peak-to-Average Ratio Reduction*. ANSI Document, T1E1.4 no. 98-252, Aug. 1998.

[19] ITU-T, *Asymmetric digital subscriber line (ADSL) transceivers – 2 (ADSL2)*. Recommendation G.992.3, July 2002.

[20] N. Petersson, A. Johansson, P. Ödling, and P. O. Börjesson, "A performance bound on PSD-constrained PAR reduction," in *Proc. IEEE International Conference on Communications*, Anchorage, AK, USA, May 2003, pp. 3498–3502.

[21] N. Petersson, "Peak and power reduction in multicarrier systems," Licentiate thesis, Lund University, Lund, Sweden, Nov. 2002.

[22] P. Ödling, N. Petersson, A. Johansson, and P. O. Börjesson, "How much PAR to bring to the party?" in *Proc. Nordic Signal Processing Symposium*, Tromsø–Trondheim, Norway, Oct. 2002.

[23] N. Petersson, A. Johansson, P. Ödling, and P. O. Börjesson, "Analysis of tone selection for PAR reduction," in *Proc. International Conference on Information, Communications & Signal Processing*, Singapore, Oct. 2001.

[24] D. G. Luenberger, *Linear and Nonlinear Programming*. Boston, MA, USA: Addison-Wesley, 1984.

[25] G. H. Golub and C. F. van Loan, *Matrix Computations*, 2nd ed. Baltimore, MD: John Hopkins University Press, 1989.

Paper IV

Paper IV

Designing Tone Reservation PAR Reduction

Niklas Andgart, Per Ödling, Albin Johansson, and Per Ola Börjesson

Tone reservation peak-to-average (PAR) reduction is an established area when it comes to bringing down signal peaks in multicarrier (DMT or OFDM) systems. When designing such a system, some questions often arise about PAR-reduction. Is it worth the effort? How much can it give? How much does it give depending on the parameter choices? With this paper, we attempt to answer these questions without resolving to extensive simulations for every system and every parameter choice. From a specification of the allowed spectrum, for instance prescribed by a standard, including a PSD-mask and a number of tones, we analytically predict achievable PAR-levels, and thus implicitly suggest parameter choices. We use the ADSL2 and ADSL2+ systems as design examples.

Accepted for publication in *EURASIP Journal on Applied Signal Processing*, published by Hindawi Publishing Corporation. This work was supported by Ericsson AB; the Eureka projects MIDAS A110 and BANITS; and by the MUSE project of the European Union's 6th framework programme.

1 Introduction

With *discrete multitone modulation* (DMT) as the dominating modulation scheme in *digital subscriber line* (DSL) systems, there is a problem with high signal amplitudes. This is caused by several independent sequences adding up to a signal that approximately will adhere to a Gaussian distribution and is commonly referred to as a high *peak to average ratio* (PAR). Several methods have been presented to alleviate this problem [1–7].

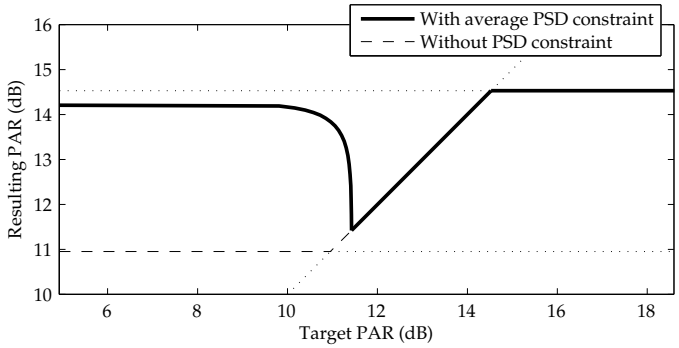

Figure 1: Relationship between target PAR and the resulting PAR level for reduction with 6 tones, with and without constraints on average reduction PSD. The narrow optimum and its lack of tolerance for design errors illustrates the non-intuitive behaviour of PAR reduction under PSD constraints. It also emphasizes the need of design methods such as those given in this paper.

We focus on the tone reservation method, which has been presented in [1, 2], with further improvements in [8–12]. Following the constraints set up by the standards, the achievable performance is limited, and can be determined by mathematical analysis in combination with some sound engineering assumptions. Construction of a system where the designer is unaware of the limitations will likely lead to a severe violation of the *power spectral density* (PSD) mask, or to a worse performance than what could be expected. This is illustrated in Figure 1, where the target PAR level is of significant importance. Aiming at a too low PAR level will lead to a violation of the PSD, or to a much worse result if the PSD is somehow enforced. In this paper we explain this relationship and develop means to predict what can be done when applying tone reservation PAR reduction to a practical DMT system. The aim is to produce results that are valid without having to run extensive simulations for each individual case. Hence, we will look at a number of bounds and engineering approximations that will tell us what

can be done in the complete system.

When a system designer is contemplating whether it is worthwhile to include PAR reduction in a system or not, it normally requires a lot of work to develop a simulation chain in order to evaluate the potential gain. With the results presented here, the "worthwhile or not" question can easily be answered in an afternoon by a skilled engineer. A simulation chain would then only be developed when needed, *i.e.*, for the precise determination of PAR-reduction parameter values. A practicing engineer, who only at a later stage would like to enjoy the theory, could for now skip reading Sections 2 and 3, and move directly to Section 4.

Earlier work has discussed the existence and effect of a PSD bound for tone reservation [13] and algorithms suitable for implementing it [12]. This paper aims at explaining in which situations this PSD constraint is an issue. It also intends to show what levels on PSD constraints and expected PAR reduction performance that can be used in a system design.

The paper starts out with discussing practical standardised systems and what would be proper engineering assumptions. In Section 2, the system and its requirements are defined and a set of theoretical results necessary for the analysis is given. Thereafter, Section 3 analyses what impact this has on reduction performance. The results from this section is summarised in Section 4, where practical instructions for using them are given in a "how-to" style. Section 5 applies the results to an ADSL2 system and also extends the analysis to include ADSL2+ systems.

2 A system in practice

The Gaussian distribution of the transmit signal [14] implies a possibility of very high peak amplitudes. This may lead to that the signal is clipped or, if the amplitude span of the line driver is increased, high power dissipation. This is especially the case with the commonly used class AB line drivers, where the power dissipation in the line driver is directly dependent on the supply voltage. Notably, the line driver, or power amplifier, is responsible for the major part[1] of the total power consumption in many communication systems, *e.g.*, DSL systems [15].

2.1 PAR reduction in standardised systems

As a first example system, we will look at an ADSL2 system using an FFT size of 512 in the downstream direction. Since the lowest part of the frequency band, covering the first 32 tones, is used for analogue telephony

[1] Anything between 50–80% could be considered normal, where the numbers have been increasing over time as the digital system-parts have become more and more efficient.

and upstream transmission, only tones 33–255 are available for downstream data transmission. These parameters are the same as for the well-established ADSL1 system [16], with the ADSL2 standard [17] more closely defining the requirements on subcarriers that could be used for PAR reduction. We quote the most relevant text in Appendix A. The ADSL2 standard is also a base for the ADSL2+ standard [18], which follows similar specifications. The main difference is the double downstream bandwidth (tones 33–511), and that ADSL2+ systems thereby operate with an FFT size of 1024 in the downstream direction.

In the ADSL2 standard, the PSD mask on the reduction tones is set to $-10\,\mathrm{dB}$ relative to the PSD for the data tones [17], see also Appendix A. A question now is how the PSD should be properly measured. Since the PSD commonly is averaged over time, the instantaneous PSD may be allowed to vary between symbols, with certain symbols exceeding the average PSD constraint. We will consider two extreme cases of averaging time, as well as a reasonable intermediate point.

One extreme would be to average over long time. Thereby, we could sometimes allow high instantaneous PSD levels, if we most of the time use little or no power. This interpretation of the definition restricts only the average level, without imposing any restrictions on individual symbols. This can generate occasional large reduction signals, with the average still being below the limit. There are reasons to why this may be undesirable, for instance, large amplitudes on the reduction tones could generate intermodulation interference to neighbouring, data-carrying subcarriers by exciting nonlinearities in the line driver. Other users or other systems in the same cable bundle can also be affected through crosstalk. Although this interpretation of the PSD limitation is standard compliant, it is neither neighbour friendly, nor necessarily according to the spirit of the standard.

The other extreme is when the PSD of each particular symbol has to conform with the $-10\,\mathrm{dB}$ limitation. This results in a very strict peak PSD constraint and a quite low PAR reduction performance.

A compromise between these two cases, with a limit on average PSD as well as a looser limit on maximum instantaneous PSD, would give a standard-compliant system that is not overly inefficient but still friendly to neighbouring users. The value of the peak PSD limit can be obtained from the acceptable amount of disturbance that can be put on other users.

2.2 Tone reservation

The goal with all PAR reduction methods is to generate a transmit signal that has a low amplitude swing. Different approaches to PAR reduction exist, but only a few are viable alternatives to include in standardised DSL systems. The schemes possible to use are those that are transparent to the

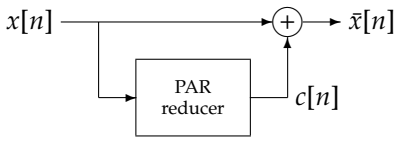

Figure 2: A PAR reduction signal, $c[n]$, is added to the data signal $x[n]$ to counteract the peaks in $x[n]$. The signal $c[n]$ is a function of the data signal $x[n]$, and is constructed from a small subset of tones.

receiver side, meaning that the receiver does not have to know about the existence of PAR reduction, nor which method is being used.

One of these viable methods is the tone reservation method [1, 2], which adds a reduction signal $c[n]$ to the data signal $x[n]$, see Figure 2. The goal is to make the resulting signal $\bar{x}[n] = x[n] + c[n]$ have a lower amplitude span than before. The PAR is defined as

$$\mathrm{PAR}\{\bar{\mathbf{x}}\} = \frac{\max_n |x[n] + c[n]|^2}{\sigma^2}, \tag{1}$$

where the peak power is compared to the average power *before* the PAR reduction is applied, $\sigma^2 = E[|x[n]|^2]$.

The reduction signal $c[n]$ is constructed of a set of reserved subcarriers, which are not used for data transmission. These may be tones that cannot transmit data reliably, or tones that are explicitly reserved for PAR reduction. Naturally, the reduction performance will increase as the number of reserved tones is increased. At the same time, excluding too many tones from the set of data-carrying tones will reduce the data capacity of the system unnecessarily [19]. Thus, it is of interest to, already at an early stage in a system design, have some knowledge about the reduction capabilities for a certain number of tones in order to balance this trade-off.

In matrix form, we define the signal model as

$$\bar{\mathbf{x}}_L = \mathbf{x}_L + \mathbf{c}_L = \mathbf{x}_L + \check{\mathbf{Q}}_L \check{\mathbf{C}}. \tag{2}$$

We let the length-NL vector $\mathbf{x}_L$ denote the data signal of one symbol block and $\mathbf{c}_L$ the reduction signal of the same length. The FFT size is denoted by N and the number L represents the oversampling factor, which we introduce in order to have a better control of the continuous-time PAR. The construction of $\mathbf{c}_L$ from the reserved tones is written as $\mathbf{c}_L = \check{\mathbf{Q}}_L \check{\mathbf{C}}$, where $\check{\mathbf{Q}}_L$ is a $NL \times 2U$ matrix of sine and cosine basis vectors with frequencies specified by the U reserved tones $t_1, \ldots, t_U$ [12].

2.3 Optimisation criteria

Having defined the reduction model in (2) above, we now formulate what the reduction algorithm should aim at. The most common approach in PAR reduction is basically to reduce the signal as much as possible. In the real-valued, baseband environment of a DSL system, this can be formulated as a linear programme [2]:

$$\begin{array}{ll} \underset{\check{\mathbf{C}}}{\text{minimise}} & \gamma \\ \text{subject to} & |\mathbf{x}_L + \check{\mathbf{Q}}_L \check{\mathbf{C}}| \leq \gamma\sigma. \end{array} \tag{3}$$

The inequality compares each vector element to the right-hand side scalar $\gamma\sigma$, which is the level of the highest signal peaks.

When assigning a certain target PAR level to the system, the algorithm can be told not to put any efforts in reducing the peak level further down than this level. Since what is important in practice is to avoid signal clipping through overloading the line driver or clipping in the D/A converter, there is no reason to reduce the PAR of already acceptable symbols. Additionally, reducing the peak level further may cause the power on the reduction tones to increase to undesired levels. We can then define the optimisation criterion as minimising the added reduction power given a certain target crest factor γ_{target}, or target PAR level γ^2_{target} [15]:

$$\begin{array}{ll} \underset{\check{\mathbf{C}}}{\text{minimise}} & \check{\mathbf{C}}^T\check{\mathbf{C}} \\ \text{subject to} & |\mathbf{x}_L + \check{\mathbf{Q}}_L \check{\mathbf{C}}| \leq \gamma_{\text{target}}\sigma. \end{array} \tag{4}$$

This quadratic programme does not always have feasible solutions since it cannot be guaranteed that the target PAR level γ^2_{target} is achievable. Thus, we choose to minimise the PAR level if the target PAR is not reached.

To take the maximum allowed PSD level into consideration, a set of quadratic constraints can be added to (3) and (4):

$$\check{\mathbf{C}}^2_{l,\sin} + \check{\mathbf{C}}^2_{l,\cos} \leq A^2_{l,\max}, \tag{5}$$

where $A_{l,\max}$ denotes the maximum magnitude for reduction tone t_l, with $l \in \{1 \ldots U\}$, and $\check{\mathbf{C}}_{l,\sin}$ and $\check{\mathbf{C}}_{l,\cos}$ denote the sine and cosine weights on a certain reduction tone. This introduction of a set of quadratic constraints will result in (3) and (4) no longer being linear or quadratic programmes. However, they will still be quadratically constrained problems, which still are convex and thereby reasonably easy to solve.

What will be studied now is the combination of the problem formulations in (3) and (4):

(*i*) First, try to solve (4) with the additional constraints in (5) to obtain the target PAR with as little added power as possible.

(*ii*) If this fails, solve (3) and (5) to minimise the PAR level.

A suitable algorithm for practical implementation is the active-set algorithm [9, 12, 20]. Solving for the minimum PAR, this algorithm will converge to a solution close to the optimal solution already after a few iterations, and the PSD constraints can easily be incorporated [12].

2.4 Expression for PAR for an unreduced signal

In order to analyse what is achievable with the PAR reduction algorithm, the distribution of the PAR for an unreduced signal has to be derived. We here focus on the symbol clip probability, defined as the probability that the maximum sample value in a full DMT frame is above a certain level. This reflects the probability that a symbol is distorted during transmission. Our choice of definition is commonly used in the literature, although it would also be possible to view the clip probability on a per-sample basis.

Assuming that the signal after the IFFT is Gaussian IID, $x[n] \in N(0, \sigma^2)$, the sample clip probability at level $\gamma\sigma$ is

$$\mathcal{P}_1(\gamma) = \text{Prob}(|x[n]| > \gamma\sigma) = 2Q(\gamma), \tag{6}$$

where the $Q(\cdot)$ function denotes the tail probability for a Gaussian random variable,

$$Q(x) = \frac{1}{\sqrt{2\pi}} \int_x^\infty e^{-x^2/2}\, dx. \tag{7}$$

The symbol clip probability for the symbol of N IID samples is straightforward to calculate [2]:

$$\begin{aligned} \mathcal{P}_N(\gamma) &= 1 - \text{Prob}(\text{all } |x[n]| < \gamma\sigma) = 1 - (1 - \mathcal{P}_1(\gamma))^N \\ &= 1 - (1 - 2Q(\gamma))^N. \end{aligned} \tag{8}$$

For an oversampled signal, the sample clip probability is identical to the critically sampled case. The derivation of the symbol clip probability is not as easy to obtain, due to that the signal no longer is IID. However, assuming that the signal is continuous-time band-limited Gaussian noise gives us a possibility of deriving the clip probability using Rice's formula. The derivation is given in Appendix B, and the resulting expression is

$$\mathcal{P}_S(\gamma) = \text{Prob}(\text{clip at } \gamma\sigma) = 1 - \exp\left(-\frac{N}{\sqrt{3}} e^{-\gamma^2/2}\right). \tag{9}$$

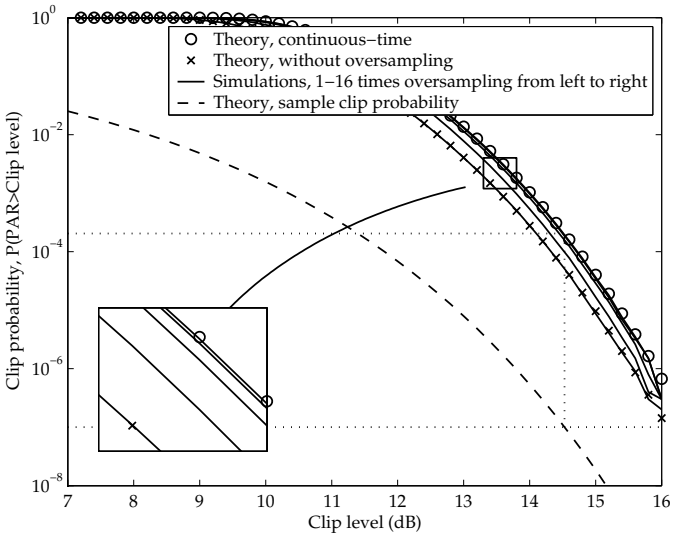

Figure 3: Symbol clip probability for an unreduced signal of length $N = 512$, evaluated at different levels of oversampling. The cross-marks show the theoretical values for a white Gaussian signal without oversampling and the circles show the calculated values for a lowpass continuous-time white signal using Rice's formula. The solid lines show, from left to right, the simulated clip probability for a signal without oversampling, and with 2, 4, 8, and 16 times oversampling, respectively. After four to eight times oversampling, the calculated results for the continuous-time signal describes the data signal closely. The dashed line shows the sample clip probability, which is the same for continuous-time signals as for signals without oversampling. The dotted lines show the translation between sample and symbol clip probabilities. Starting at the sample clip probability 10^{-7}, we see that this corresponds to a clip level of $\gamma_{\text{unred}} = 14.5\,\text{dB}$, which for the continuous-time signal corresponds to the symbol clip probability $p_{\text{symclip}} = 2 \cdot 10^{-4}$.

Figure 3 shows the sample and symbol clip probabilities for different levels of oversampling, from $L = 1$ to $L = 16$, for a system with a symbol length of $N = 512$. As seen from the figure, with increasing oversampling, the expression from (9) gives an excellent match.

In Figure 4 we plot some qualitative results of when PAR reduction is needed. The solid line is the same as the theoretical values marked with circles in Figure 3, showing the probability of at least one clip in a symbol from (9). Using (36) in Appendix B, we plot two more lines showing the

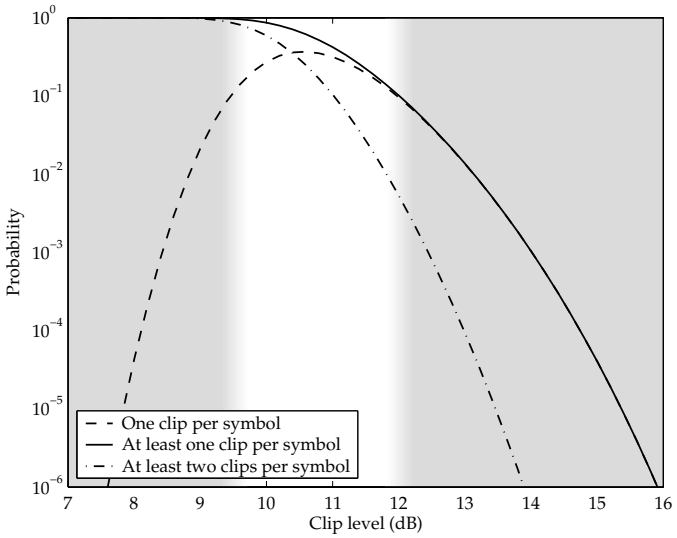

Figure 4: Probabilities of different number of clips, for a symbol length of $N = 512$. In the shaded area to the left, we will almost always have one or many clips. In the rightmost shaded area, there will most often be one or zero clips.

probabilities of at least two clips, and exactly one clip, respectively. We see that in the leftmost shaded region, the reduction algorithm will have to be active for almost every symbol. In the rightmost region, there will very seldom be more than one peak exceeding a given level. We will use these results to judge when the bounds developed in Section 3 are reasonably tight.

Moving on, while we focus on the symbol clip probability, the ADSL standard [16] is based on unreduced signals and sets the limit on clip probability on a per-sample basis. The signal is restricted to be clipped no more than the fraction 10^{-7} of the time. Translating this to a symbol clip probability is not straight-forward, since there can be one or many clips in a clipped symbol. However, considering an unreduced signal, we can use the expression for the sample clip probability in (6) to get the acceptable clip level:

$$\gamma_{\text{unred}} = Q^{-1}(10^{-7}/2) = 5.33 \;\; (14.5\,\text{dB}). \tag{10}$$

Then, we can use (9) with this clip level to get a value of the symbol clip probability:

$$p_{\text{symclip}} = 1 - \exp\left(-\frac{N}{\sqrt{3}} e^{-5.33^2/2}\right), \tag{11}$$

approximately $2 \cdot 10^{-4}$ for $N = 512$. This translation is also shown with the dotted lines in Figure 3. This γ_{unred} value is used as a reference in Figures 6, 7, 8, 11 and 12, and the p_{symclip} is shown as the baseline reference in Figure 9.

3 Performance prediction with bounds

Our aim is to see, or rather predict, what PAR level we can achieve with the tone reservation approach and PSD restrictions. We present a material allowing to do this analytically, without having to resort to extensive system simulations, which are often quite complicated when it comes to PAR reduction. Based on the optimisation criteria and distribution of the unreduced signal from the previous section, bounds for the achievable PAR level given a certain system using a certain number of tones will be derived. For easy practical use of these bounds, the outcome of this section will be summarised in Section 4.

3.1 Limitations imposed by a maximum average PSD

We will now analyse what can be done under the $-10\,\text{dB}$ per tone PSD limitation on the reduction signal compared to the data signal. Most of the symbols do not have very high signal peaks, and thus do not need a large reduction signal to pass under the clip level. We will assign a target PAR level to the algorithm, and not put any efforts in reducing the signal further down. We will also define a maximum magnitude per reduction tone. It can be expected that having a high target PAR level, only a few symbols will need reduction and the maximum tone magnitude can be set high, still having an average PSD below the limit. On the other hand, lowering the target PAR will demand reduction of more symbols, and the maximum reduction magnitude has to be kept lower, to not violate the average PSD constraint. This lower reduction magnitude will, in turn, make it difficult to achieve the target PAR. We will predict the best balance of target PAR level γ^2_{target} (how often reduction is used) and allowed reduction magnitude A (to stay below the PSD limit).

Allowed magnitude

We start by predicting the average power needed to reduce the signal down to the target PAR level γ^2_{target}. Then we can assign a maximum tone magnitude to avoid a too high average power. For an individual symbol, we use the following lower bound on reduction tone magnitude:

Assume that the signal has a maximum peak with magnitude $x_{\max}$. To reduce the signal down to a PAR of γ^2_{target} requires at least a total reduction

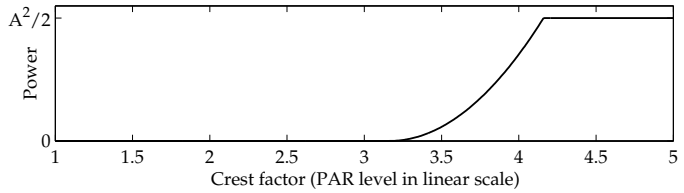

Figure 5: Illustration of (12), showing minimum instantaneous power on a reduction tone as a function of peak magnitude, with a target PAR level of 10 dB, $\gamma_{\text{target}} = 3.16$. The axes are shown in linear scale. Aiming at the target PAR level of 10 dB, the reduction algorithm will not be active below this value. Above $\gamma_{\text{target}} + UA/\sigma = 4.16$ (12.4 dB), the algorithm will output the maximum power $A^2/2$.

tone magnitude of $x_{\max} - \gamma_{\text{target}}\sigma$.
Proof: Only looking at the highest peak of the signal, we see that letting all reduction tones be in phase at this sample, with a total magnitude of $x_{\max} - \gamma_{\text{target}}\sigma$ in the counter-phase direction, will reduce the signal down to $\gamma_{\text{target}}\sigma$, with PAR γ^2_{target}. All other scenarios, such as taking into consideration other samples in the original signal, and the possibility of generating new peaks, would need a larger reduction signal. □

For an individual symbol with peak magnitude $x_{\max}$, we then need at least the total magnitude $x_{\max} - \gamma_{\text{target}}\sigma$, spread over the U tones. With the same PSD constraints on all tones, we would like to have the maximum tone magnitude as low as possible, which means having the same magnitude $(x_{\max} - \gamma_{\text{target}}\sigma)/U$ on all reduction tones. This could also be seen as a lower bound, or perhaps rather a best case, for a PSD-friendly average reduction power spread over the tones. Depending on the peak magnitude $x_{\max}$, the instantaneous reduction power on a certain tone will at least be

$$g(x_{\max}) = \begin{cases} 0 & x_{\max} \leq \gamma_{\text{target}}\sigma \\ \frac{1}{2}\left(\frac{x_{\max} - \gamma_{\text{target}}\sigma}{U}\right)^2 & \gamma_{\text{target}}\sigma < x_{\max} \leq \gamma_{\text{target}}\sigma + UA \\ A^2/2 & x_{\max} > \gamma_{\text{target}}\sigma + UA, \end{cases} \tag{12}$$

where A denotes the maximum allowed reduction magnitude per tone, see also Figure 5. Following step (*ii*) of the optimisation criterion given in Section 2.3, for peak levels above $\gamma_{\text{target}}\sigma + UA$, the algorithm can only output this large reduction signal, and the target PAR will thereby not be achieved.

To evaluate the minimum average PSD for a tone, we calculate the expected value of (12). For this, we need the density function $f(\gamma)$ for the

normalised peak magnitude $x_{\max}/\sigma$, based on the clip probability from (9):

$$\begin{aligned} f(\gamma) &= \frac{\partial F(\gamma)}{\partial \gamma} = \frac{\partial (1 - \mathcal{P}_S(\gamma))}{\partial \gamma} \\ &= \frac{\partial}{\partial \gamma} \exp\left(-\frac{N}{\sqrt{3}} e^{-\gamma^2/2}\right) \\ &= \frac{N\gamma}{\sqrt{3}} \exp\left(-\frac{N}{\sqrt{3}} e^{-\gamma^2/2}\right) e^{-\gamma^2/2}. \end{aligned} \tag{13}$$

Then we can calculate a lower bound on the average reduction power on each tone as the expected value of the minimum instantaneous power:

$$\begin{aligned} \text{Power}_{\text{red}} &\geq \int_0^\infty g(\gamma\sigma) f(\gamma)\, d\gamma \\ &= \int_{\gamma_{\text{target}}}^{\gamma_{\text{target}} + UA/\sigma} 1/2 \left(\frac{\gamma\sigma - \gamma_{\text{target}}\sigma}{U}\right)^2 f(\gamma)\, d\gamma + \int_{\gamma_{\text{target}} + UA/\sigma}^{\infty} A^2/2\, f(\gamma)\, d\gamma \\ &= \frac{1}{2U^2} \int_{\gamma_{\text{target}}}^{\gamma_{\text{target}} + UA/\sigma} \left(\gamma\sigma - \gamma_{\text{target}}\sigma\right)^2 f(\gamma)\, d\gamma + \frac{A^2}{2} \mathcal{P}_S\left(\gamma_{\text{target}} + \frac{UA}{\sigma}\right). \end{aligned} \tag{14}$$

In addition, to conform to the PSD limitation of a reduction tone PSD of 10 dB below the data-tone PSD, we can calculate the allowed average power $\text{Power}_{\text{red}}$ on a reduction tone as

$$\text{Power}_{\text{red}} \leq 10^{-10/10} \text{Power}_{\text{data}} = 10^{-1} \frac{\sigma^2}{U_0 - U}, \tag{15}$$

where U_0 is the number of tones originally available for data transmission before introducing tone reservation. The average power on the data tones, $\text{Power}_{\text{data}}$, is obtained by dividing the total signal power σ^2 with the number of tones used for data transmission. We assume that the power on the data tones fills the PSD mask completely. It is now possible to use the two $\text{Power}_{\text{red}}$ expressions in (14) and (15) to to solve for the maximum value of A. The thick solid lines, starting in the bottom left and bending upwards, in Figure 6 show the resulting values of the maximum magnitude A as a function of a certain target PAR level. The four lines correspond, from right to left, to systems with 3, 6, 12 and 24 tones, respectively. Choosing a target PAR level, we can read out the highest value we could set the maximum tone magnitude A to in order not to exceed the PSD limit on average. Thus, the allowed area is to the right, or below, the thick solid lines.

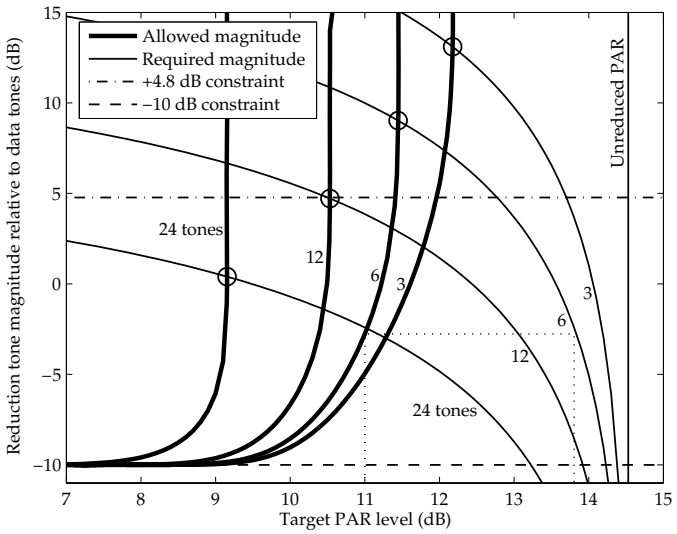

Figure 6: The thick solid lines starting from the bottom left corner and bending upwards show the maximum reduction tone magnitude without exceeding the average PSD level, when aiming at the target PAR level shown on the horizontal axis. The thin solid lines starting from the bottom right show what reduction tone magnitude is needed to possibly achieve the target PAR level on the horizontal axis. The two horizontal lines at $+4.8\,\mathrm{dB}$ and $-10\,\mathrm{dB}$ show the limitations when having a maximum peak PSD, as described in Section 3.2.

For very low target PAR levels in the system, almost all symbols will need to be reduced. In order to not exceed the constraint on the average PSD, we have to put a strict constraint on the maximum tone amplitude, A. For low target PAR levels, it can be seen that the thick solid lines for the peak constraint A converge to the average constraint at $-10\,\mathrm{dB}$.

On the other hand, if we aim at a not too low PAR, fewer symbols will need reduction, cf. Figure 4. Then the reduction signal can be allowed to be much stronger on occasional symbols without violating the average PSD limit. In Figure 6, the curves are bending strongly upwards at certain PAR levels. Choosing a target PAR level a bit above this value will allow a strong reduction signal, and thus a high probability of attaining the target.

Required magnitude

The curves developed in Section 3.1 and shown in Figure 6 tell us how much power we can put on the reduction tones without exceeding the PSD mask on average. However, the thick lines in Figure 6 give only a bound on an allowable region for combinations of the target PAR level γ^2_{target} and maximum reduction tone magnitude. They say nothing about what is achievable, *i.e.*, they do not guarantee that the target PAR level can, or will be, reached. Here we can reuse the lower bound on reduction tone magnitude from Section 3.1. Based on this bound and the distribution of the unreduced signal peak from (9), we can calculate what reduction tone magnitude at least is needed for a certain level of reduction at a certain clip probability:

$$A \geq \frac{(\gamma_{\text{unred}} - \gamma_{\text{target}})\sigma}{U}, \tag{16}$$

where γ_{unred} is the crest factor for the unreduced signal at the clip probability $p_{\text{symclip}} = 2 \cdot 10^{-4}$, as described in Section 2.4.

The thin solid lines starting from the bottom right in Figure 6 show this tone magnitude as a function of target PAR level, for 3, 6, 12, and 24 tones. The rightmost vertical line shows the PAR of the unreduced signal, γ^2_{unred}, which is about 14.5 dB at the clip probability $2 \cdot 10^{-4}$. To be able to reduce the signal level down to the target PAR on the horizontal axis, we need at least the amount of tone magnitude specified by the thin solid lines.

For each number of tones we then have two different lower bounds. The limit on average PSD gives a maximum allowed tone magnitude, and (16) gives a value of the minimum needed magnitude. Both bounds give a lower limit on PAR level and the allowable area is to the right of both curves. If it would be attainable, the best point would be given by the intersection of the bounds, for each number or tones marked with a circle in the figure.

The solid lines in Figure 6 show the allowed and required magnitude based on derivations only assuming one peak. Here Figure 4 comes to our aid. There we can see that the one-peak-only assumption almost always holds above 12 dB. To evaluate the derivations, simulation results are shown in Figure 7 with thin dashed lines next to the bounds. Looking at the thick curves for allowed tone magnitude, we see that for a low number of tones, the simulations closely follow the bound. For a higher number of tones, we cannot allow ourselves as high magnitude as the bound suggests. The reason is that with a high number of tones, we can work at low PAR levels, which means that we may have several peaks, c.f. the leftmost grey area in Figure 4. Then the reduction algorithm has to spend power on reducing many peaks, and not one single peak, which is the situation the bound describes. Also, for the thin bound lines we see that the bounds are tighter at higher PAR levels. Reduction to low levels will generate signals

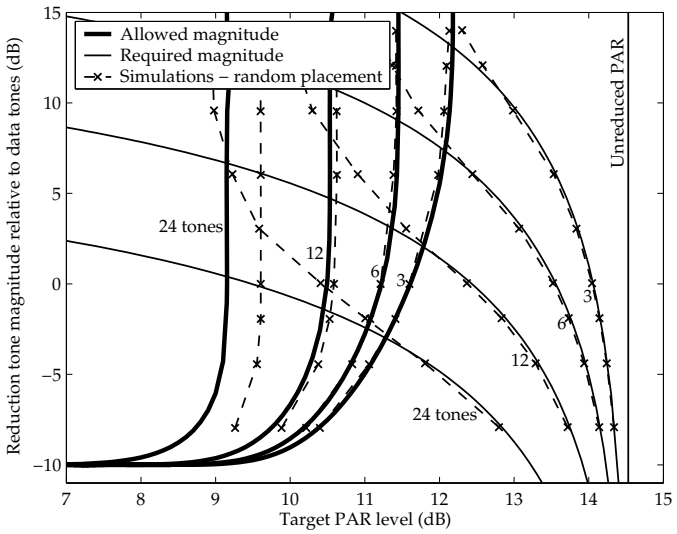

Figure 7: The bounds from Figure 6, shown together with simulations with a random placement of tones. Since the bounds only calculate with a single signal peak, the simulations results move somewhat upwards and to the right.

with many peaks, again deviating from the basic case the bound is based on. Considering the simulations, the intersection points move upwards, to a higher magnitude per tone, rather than rightwards, to a higher PAR. The bound gives a good indication about the PAR, while it may show a too low required tone magnitude. The bounds will be further evaluated with simulations in Section 5.

Influence of target PSD

The balancing of target PAR level and allowed maximum amplitude is difficult. As an example, consider a system with six reduction tones. From Figure 6 we see that the optimal point is 11.4 dB. Let us assume that the designer chooses a target PAR level of 11.0 dB, which is below this point. Following the dotted line at 11.0 dB in Figure 6 up to the thick line corresponding to the allowed magnitude, we see that the maximum allowed reduction tone magnitude is -2.8 dB compared to the data tones. If the algorithm really aims at the 11.0 dB level, the PSD mask will be violated. Otherwise, the reduction tone magnitude has to be limited to -2.8 dB. Following the dotted line along this level to the thin 6-tone curve to the right

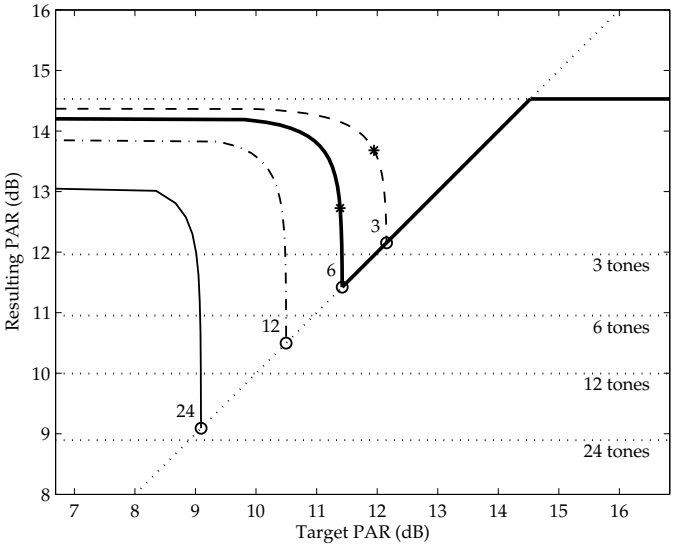

Figure 8: Relationship between target PAR and the effective resulting PAR level (given that the average PSD level is enforced), for reduction with 3, 6, 12, and 24 tones. The curve for 6 tones is highlighted. The dotted horizontal lines show the simulated value for reduction without PSD constraints, for the same number of tones. The asterisks show the combined -10 dB average PSD bound and $+4.8$ dB peak PSD bound based on FEXT calculations as described in Section 3.2. The 12 and 24 tone cases are not constrained by the $+4.8$ dB peak PSD bound.

shows us that we at maximum can reach a resulting PAR of 13.8 dB, or a crest factor of 4.90.

This relationship between target and resulting PAR while conforming to the PSD mask is shown in Figure 8. As described in the previous example, we can get the maximum A value based on a certain target PAR. Then we can use (16) to get the bound on resulting PAR,

$$\gamma \geq \gamma_{\text{unred}} - UA/\sigma, \tag{17}$$

shown on the vertical axis for a clip probability of $2 \cdot 10^{-4}$. From the figure we see that there is a sharp optimum for each choice of number of tones. Aiming a little bit lower than this optimum, the resulting PAR level is severely increased (or in practice, the average PSD would be violated). The upper horizontal line shows the PAR when having no reduction at all, and the four lower lines show simulation results of what could be achieved

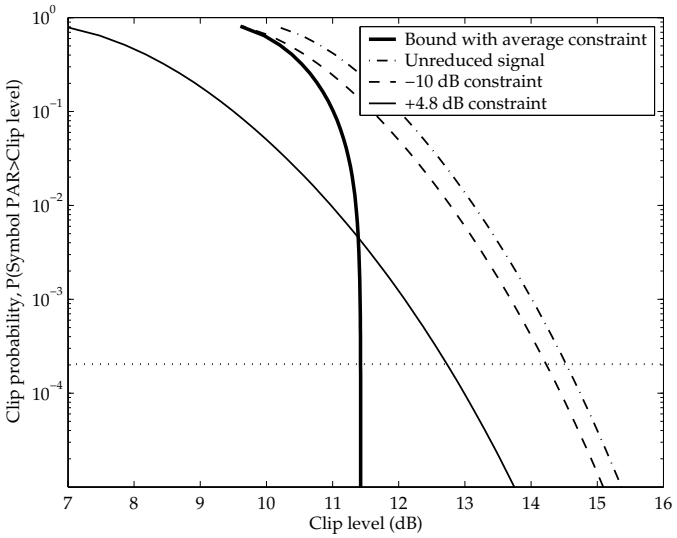

Figure 9: Clip probability curve for reduction with 6 tones. The thick line shows the bound for reduction under the average constraint for any parameter choice. The rightmost dash-dotted curve shows the PAR for an unreduced signal according to (9), and the dashed curve shows the bound when using no averaging. The thin solid line shows the bound when using the $+4.8\,\mathrm{dB}$ constraint based on the FEXT calculations in Section 3.2.

when not having any PSD constraints. The optimum points discussed above have higher PAR than these levels, which shows that the system performance is primarily limited by the constraint in PSD levels. Having no PSD constraints gives results dependent on the number and placement of the reduction tones.

Evaluating the bound in Figure 8 for different clip probabilities will give new values of the optimum points. These optimum points can then be plotted in a clip probability curve, commonly shown in PAR reduction papers; see the thick line in Figure 9.

Worth to notice in Figure 9 is that we get a minimum obtainable PAR that is almost independent on what clip probability you look at. Also, since the curve represents the best solution given different clip probabilities, a fixed design cannot get arbitrarily close to this bound at all values. We can only expect a system with a certain parameter choice to get close to the bound at the very specific target PAR level the system is designed for.

Combination of allowed and required magnitude

We are now ready to define this optimum point in terms of achievable PAR level for a system with certain number of tones. First we combine the two $\text{Power}_{\text{red}}$ expressions in (14) and (15) to get the relationship between A and U. To get a set of best design choices of U and γ_{target} (although maybe not reachable), we let the maximum allowed magnitude A be equal to the minimum needed required value from (16). After eliminating the dependence on σ^2, the resulting expression is

$$10^{-1}\frac{1}{U_0-U} \geq \frac{1}{2U^2}\int_{\gamma_{\text{target}}}^{\gamma_{\text{unred}}}\left(\gamma-\gamma_{\text{target}}\right)^2 f(\gamma)\,d\gamma + \frac{1}{2U^2}\left(\gamma_{\text{unred}}-\gamma_{\text{target}}\right)^2 \underbrace{\int_{\gamma_{\text{unred}}}^{\infty} f(\gamma)\,d\gamma}_{=\,p_{\text{symclip}}\text{ from (11)}}\ , \tag{18}$$

where we note that the second integral is the tail probability p_{symclip} at level γ_{unred}. Let us interpret this equation. To the left, we have the allowed power on a tone, from the limit on the average PSD. To the right, we have a sum of two terms. The first is the power per tone needed to reduce from the peak level down to the target level. This corresponds to the first item in the optimisation formulation, "reduce down to the target PAR level using as little added power as possible". The second expression corresponds to the cases when the allowed instantaneous power is insufficient for reducing the peak down to the target PAR level. For these cases, we reduce with the maximum available instantaneous tone magnitude A, which from (16) is equal to $\sigma(\gamma_{\text{unred}}-\gamma_{\text{target}})/U$. This corresponds to the second item in the optimisation formulation, "minimise the PAR level if the target is unreachable". Compared to the first integral, the second term is very small, since it includes the small probability p_{symclip} of a signal larger than γ_{unred}. Note that (18) easily can be solved with regards to U and γ_{target}. The relationship between U and the target PAR level is shown in Figures 11 and 12 in the upcoming section.

3.2 Limitations imposed by a maximum peak PSD

The derivations so far concerned only a limit on average PSD level. In Section 2.1 was discussed that a maximum instantaneous level may be needed as well, which will affect the reachable PAR level according to (17). This is the case considered in [12, 13], which we elaborate on here to give more detailed guidelines of where to put the constraint. We will consider the most

restrictive case first, when the peak value is constrained at $-10\,\mathrm{dB}$ and we do not use any averaging at all, and then extend to a scenario based on crosstalk calculations.

Constraint without averaging

For the case when no averaging is done between different symbols, all symbols need to comply with the $-10\,\mathrm{dB}$ limitation and we cannot take advantage of the fact that most of the symbols need no or a very small amount of reduction. Thus, no power can be saved for the cases when it is needed to reduce a strong peak.

Two horizontal dashed lines are shown in Figure 6. The lower one is placed at $-10\,\mathrm{dB}$ and corresponds to this limitation. In addition to being on the right-hand side of the bounds discussed before, we now also have to be below this horizontal line. As can be seen from the figure, this severely affects the reduction performance. For example, using only 6 PAR reduction tones, only about $0.3\,\mathrm{dB}$ reduction can be achieved. In this case, the PAR reduction will most likely not be worth the effort.

In Figure 8, the curves move right and down with increasing target PAR level. Not using any averaging corresponds to having so low target PAR that all symbols need reduction. What may be possible to achieve here is thus shown by the values to the left in the figure. Having this strict limitation on the reduction signal makes the PAR reduction only usable if there is a high number of tones available for PAR reduction, for instance when there are many tones unavailable to carry data due to low SNR.

Constraint based on FEXT calculations

The two previous extreme cases show very different reduction results, due to the difference in maximum allowed magnitude. It can be expected that there should be a maximum instantaneous tone power somewhere in between, determined to not cause harmful interference to other users. If we consider the *far-end crosstalk* (FEXT), we can come up with a reasonable point to put the PSD constraint at.

Consider a situation where our modem in question is responsible for one quarter of the FEXT to a certain neighbouring modem, a fairly pessimistic case. As our reduction tones are at $-10\,\mathrm{dB}$ of our data tones, it means that the neighbouring modem in question on the reduction tones are expecting a FEXT level of three quarters of the normal level. ADSL is designed to use a SNR margin of 6 dB. If that user has a SNR margin of 6 dB, how much can we then increase our disturbance, without more than half of this SNR margin being lost? Adding 3 dB to the FEXT level means adding (during an instant only) as much FEXT as the user already has from all the other users, *i.e.*,

Symbol	*Description*	*Typical value*
N	FFT size	ADSL1: 512 ADSL2: 1024
γ_{unred}	Crest factor (PAR in linear scale) for the unreduced signal	5.33 (14.5dB)
U_0	Number of data tones available before PAR	ADSL1: 223 ADSL2: 479
dB_{avg}	Average PSD constraint in dB	-10
dB_{peak}	Peak PSD constraint in dB	$+4.8$

Table 1: System parameters for calculation of reduction bounds

Symbol	*Description*
U	Number of reduction tones
γ_{target}	Target crest factor

Table 2: Design parameters for calculation of reduction bounds

matching the three quarters of the nominal FEXT level. This is three times the one quarter we have on the data carrying tones, which means a peak level of $+4.8\,\text{dB}$ on our reduction tones as compared to our data carrying tones.

This level is shown as the upper horizontal dash-dotted line in Figure 6. We also need to be below this line, but compared to the previous, much more restrictive, case, the system now has more reduction capabilities. The 24-tone system is not affected at all by this peak constraint, and the 12-tone system has just enough magnitude to avoid being affected. However, the systems with 3 and 6 tones are still limited by the constraint, which is also shown with the asterisks in Figure 8.

4 Numerical recipe

To summarize the previous section, we will now give a description of how to, based on a certain system environment, generate an estimate of PAR reduction performance under PSD constraints. A description and typical values of the system parameters are given in Table 1, and the design parameters we want to obtain values on are given in Table 2.

To get a lower bound on the achievable PAR under an average PSD constraint dB_{avg}, typically $-10\,\text{dB}$, use for example MATLAB's quad function to

evaluate the following function, directly following from (18).

$$\frac{U^2}{U_0 - U} 2 \cdot 10^{\mathrm{dB}_{\mathrm{avg}}/10} \geq$$
$$\geq \int_{\gamma_{\mathrm{target}}}^{\gamma_{\mathrm{unred}}} \left(\gamma - \gamma_{\mathrm{target}}\right)^2 f(\gamma)\, d\gamma + \mathcal{P}_S(\gamma_{\mathrm{unred}}) \left(\gamma_{\mathrm{unred}} - \gamma_{\mathrm{target}}\right)^2, \tag{19}$$

where

$$f(\gamma) = \frac{N\gamma}{\sqrt{3}} \exp\left(-\frac{N}{\sqrt{3}} e^{-\gamma^2/2}\right) e^{-\gamma^2/2} \tag{20}$$

and

$$\mathcal{P}_S(\gamma) = 1 - \exp\left(-\frac{N}{\sqrt{3}} e^{-\gamma^2/2}\right). \tag{21}$$

This equation can be plotted for U (number of reduction tones) as a function of γ_{target} (target PAR level), showing the minimum number of reduction tones needed to achieve a certain PAR level. An example of this bound is plotted as the solid line in Figure 10.

A lower bound on achievable PAR under a peak PSD constraint $\mathrm{dB}_{\mathrm{peak}}$, typically $+4.8\,\mathrm{dB}$, is from (17) given by

$$\gamma \geq \gamma_{\mathrm{unred}} - 10^{\mathrm{dB}_{\mathrm{peak}}/20} \frac{U\sqrt{2}}{\sqrt{U_0 - U}}, \tag{22}$$

Such a bound has been plotted with the dash-dotted line in Figure 10. Together with the previous bound, is defines an unreachable region marked with grey. When designing a system using randomly chosen tones, choosing a point 1 dB outside this area should be sufficient as a tentative design choice. The 1 dB margin will be motivated in the following section.

5 Effects on system performance

Using the method in Section 4, we now combine the bounds from Section 3 to evaluate what effect these will have on system performance, first for an ADSL2 system, then also for an ADSL2+ system.

5.1 ADSL2 system with combined peak and average constraints

Looking at the bounds for different number of tones at a certain clip probability, we obtain a plot of the achievable PAR as a function of the number

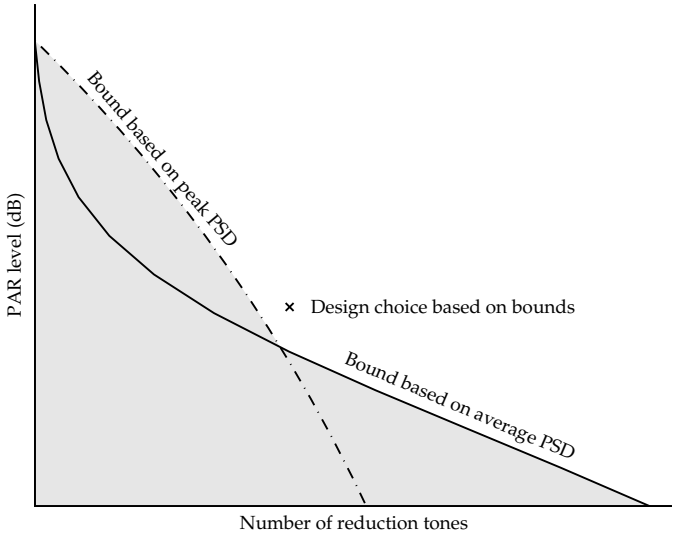

Figure 10: Schematic figure of two bounds on achievable PAR reduction, shown as a function of number of reduction tones. The two bounds based on maximum average and maximum peak PSD define an unreachable region. For system design, a target point with a certain safety margin is desired.

of reduction tones, see Figure 11. These curves show what performance could at best be achieved when having a certain number of reduction tones evaluated at a certain probability.

The solid line shows the bound for reduction under the $-10\,\mathrm{dB}$ average PSD limit from (18) in Section 3.1. As seen, the bound decreases very fast in the beginning, to then decrease slower at a higher number of reduction tones. With only a few tones, we can effectively reduce the highest peaks in the signal. These high peaks occur very seldom, so significant reduction can be achieved without increasing the average PSD much. Using more tones, we can start working with lower peaks in the signal as well. This means that we need to reduce the signal much more often, and we cannot take advantage as much of averaging.

The two other lines show the peak PSD constraints from Section 3.2, using equation (17). The upper dashed line shows the restrictive $-10\,\mathrm{dB}$ PSD constraint based on no averaging. Since this constraint admits only a very small reduction signal, we would have to use a very large number of tones to get any significant PAR reduction. More interesting is the $+4.8\,\mathrm{dB}$ constraint imposed by the FEXT calculations, shown by the dash-dotted line.

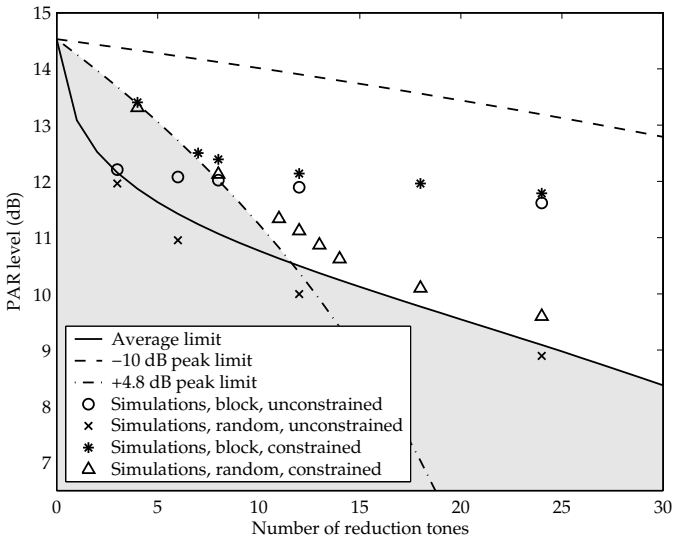

Figure 11: Bounds on achievable PAR as a function of number of reduction tones, for an ADSL2 system with $N = 512$, and a symbol clip probability of $2 \cdot 10^{-4}$. The solid line shows the bound based on a maximum average PSD. The dash-dotted line shows the bound based on a peak PSD set by FEXT calculations, and the upper dashed line is the very restrictive case when no averaging is used at all. The marker symbols show simulated reduction performance, for random or block-placed tones, with or without PSD constraints.

The larger allowed signal for this case will give a significantly better performance. We can see that the bound crosses the bound based on average PSD after 11 reduction tones. The good performance for only a few tones indicated by that bound demanded a very large reduction signal. Having a constraint on this as well, we see that the combined bound, with both the solid and dash-dotted lines, will show a better yield per tone in the beginning up to 11 tones. After this point, the average PSD will be the limiting factor, and the performance will increase slower.

The lines only represent bounds on achievable performance based on PSD limitations. The performance will also depend on what tones are chosen as reduction tones. Without PSD-constraints, tones spread out over the frequency band in an unstructured manner will give better results than regularly or block-placed tones [2, 15, 21]. However, spreading out tones over the whole frequency band is not too attractive in wireline systems as the SNR for the lower part of the spectrum generally is much better than for the

highest tones. We will consider two extreme cases: tones randomly placed over the frequency band and tones allocated as a contiguous block of the highest tones. In practice, a combination of these extreme cases may be a good choice.

Simulation results for reduction with and without PSD constraints are also shown in Figure 11. The simulations are done with 8 times oversampling, and a 32-sided linear approximation [12] of the quadratic power constraint in (5). For the simulations without PSD constraints, we see that the performance for the block-placed tones increases very slowly with the number of reduction tones, compared to the random placement. Most of the reduction performance is achieved after only a few reduction tones. Nevertheless, when the PSD is constrained, the peak-PSD bound sets the limit on performance up to about 8 tones. This suggests that the tone placement is of minor importance for this low number of tones.

Since the bound for the peak constraints decreases faster than the bound for the average constraint, we are interested in the point where the two bounds meet. From the figure this can be seen to be between 11 and 12 tones. Simulations performed with randomly scattered tones are shown with the triangles. The bounds give us a good hint about what the resulting performance will be. However, with a high number of tones, we do not end up as close to the bounds as we do with a low number of tones. The difference is around one half dB. This could be seen already in Figure 6. There, the simulations did not allow as much reduction magnitude as the bound suggested, due to the bound only calculating with one peak.

The simulated PAR for the number of tones where the bounds cross was around 11.3 dB. Translating to linear scale, we have a crest factor of about 3.7. It is interesting to know what this means in volts on the line if this is to be used, *e.g.*, to design the supply voltage to the line driver. If we have a transmit power of $P = 20\,\text{dBm}$ (100 mW), and a load of $R = 100\,\Omega$, the RMS value of the transmit signal is $U = \sqrt{PR} = \sqrt{0.1\,\text{W} \cdot 100\,\Omega} = 3.16\,\text{V}$. This means that we instead of $3.16\,\text{V} \cdot 5.33 \approx 17\,\text{V}$ now have a peak of $3.16\,\text{V} \cdot 3.7 \approx 12\,\text{V}$. (In practice, this calculation is more complicated, involving higher loads, step-up transformers, etc.)

The reduction in signal span and supply voltage gives a good indication on power consumption in the line driver. However, the exact relationship between the supply voltage and power consumption is not straightforward, since it depends on how capacitive the load is [22]. The rules of thumb for power consumption given by designers of line drivers vary between linear and quadratic functions of the supply voltage. Reduction from 17 V to 12 V would then mean a power reduction between 30% and 50%.

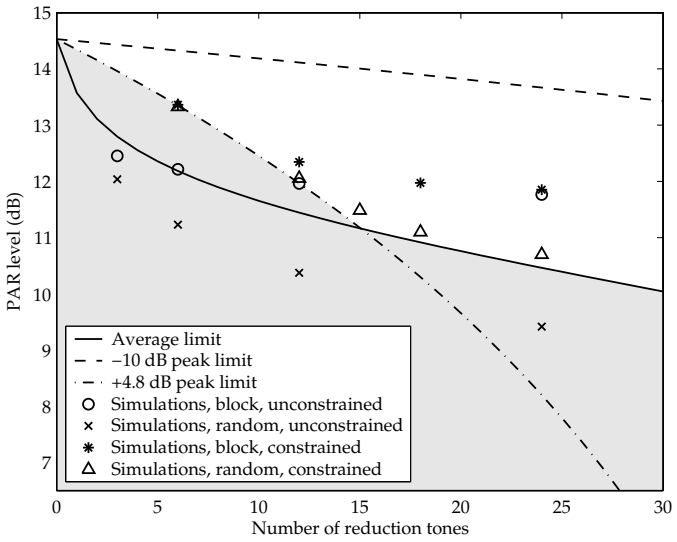

Figure 12: Bounds on achievable PAR as a function of number of reduction tones. This figure is like Figure 11, but shows an ADSL2+ system with $N = 1024$, and a symbol clip probability of $4 \cdot 10^{-4}$.

5.2 Extension to ADSL2+

The derivations so far have described a system with an FFT length of 512 in the downstream direction, such as ADSL2. ADSL2+, the extension of ADSL2, uses more downstream bandwidth, which means that the downstream FFT length here instead is 1024, and all tones in the newly added top half of the spectrum are used for downstream transmission.

We have seen that the limits on achievable PAR reduction performance are strongly dependent on the number of PAR reduction tones. Increasing the system FFT size to 1024 moves the intersection point between the two bounds up to about 15 tones, as shown in Figure 12. The simulation results are here closer to the bound than in the ADSL2 case, much dependent on that the bound here is almost 1 dB from what the simulations show could be achieved without any PSD constraints. We see that also in this case, we can expect a faster PAR decrease down to about 11 dB. Below that level, a higher number of tones is needed for the same gain.

If we compare Figures 11 and 12, we see that the bounds have moved to the right for the ADSL2+ case with the double number of subcarriers. The success in PAR reduction depends on how large reduction signal we can create, in comparison to the size of the data signal. Thus, what is impor-

tant for good reduction under a PSD constraint is often the *relative* number of reduction tones. On the contrary, the reduction performance of the non-constrained reduction is more dependent on the *absolute* number of reduction tones, since what effects the reduction performance here, is the how well we can create an impulse in counter-phase to the signal peak.

6 Conclusions

Applying tone reservation to DSL systems can reduce the system PAR, with algorithms possible to implement in current standards. For implementation, low-cost active-set based algorithms may be a good choice [12]. However, designing the algorithms, care must be taken not to exceed the PSD levels set up by the standards. Introducing PSD constraints will significantly alter the achievable performance of the reduction systems.

Using the requirements specified in the ITU standards and extending this with engineering assumptions, we have derived bounds on achievable performance. These bounds are applicable to most DMT systems, such as ADSL2 and ADSL2+. Simulations searching for the optimal solution confirm that the bounds give a good indication of realistic system performance.

We have demonstrated how these bounds can be used to predict system performance for varying parameter choices, and we have exemplified how they can be used to tailor PAR reduction to different systems. Thus, the bounds can be used to quickly determine if tone reservation PAR reduction is a worthwhile technology to be included in a system. Using the bounds, this can be done in an afternoon. After a positive indication, the system design could then proceed with the large task to create a simulation chain in order to fine-tune the settings for the PAR reduction algorithm.

A PSD constraints formulated in the standards

The ADSL1 standard [16] defines the PSD constraints as:

"For the subcarriers with ($b_i = 0$ and $g_i = 0$), the ATU-C transmitter should and is recommended to transmit no power on those subcarriers. The ATU-R receiver cannot assume any particular PSD levels on those subcarriers. The transmit PSD levels of those subcarriers with $g_i = 0$ shall be at least 10 dB below the sync symbol reference transmit PSD level if the subcarrier is below the lowest used subcarrier (lowest i with $b_i > 0$) and shall be below the sync symbol reference transmit PSD level if the subcarrier is above the lowest used subcarrier."

In ITU standards, the word *shall* defines a mandatory requirement,

should a recommendation, and *may* an option. The ADSL1 standard thus recommends to not use these subcarriers for PAR reduction, but allows the same PSD as for the data tones, except for a -10 dB limitation on the tones below the lowest data subcarrier.

In the newer ADSL2 standard [17], the formulation is:

*"For the subcarriers not in the MEDLEYset, the ATU shall transmit no power on the subcarrier (*i.e.*, $Z_i = 0$, see §8.8.2) if the subcarrier is below the first used subcarrier index or if the subcarrier is in the SUPPORTEDset and in the BLACKOUTset. Otherwise, the ATU may transmit at a discretionary transmit PSD level on the subcarrier (which may change from symbol to symbol), not to exceed the maximum transmit PSD level for these subcarriers. The maximum transmit PSD level for each of these subcarriers shall be defined as* 10 *dB below the reference transmit PSD level, fine tuned by RMSGI dB (see §8.5) and limited to the transmit spectral mask."*

Below the lowest data subcarrier, no PAR reduction tones are allowed. However, there is no recommendation to not use the other subcarriers as reduction tones, as long as they are at least 10 dB below the data tone PSD.

Summarizing the standards, we see that although the recommendation is to not put any power at all on the reduction tones, the ADSL1 standard allows much higher power, compared to the ADSL2 standard. Thus, the more well-defined ADSL2 formulation sets a stricter limit on reduction performance.

B Derivation of the PAR for an oversampled system

The derivation is based on the signal viewed as a Gaussian process [14]. This can also be intuitively motivated by the Central Limit Theorem when adding many subcarriers with independent data. We model the signal as Gaussian noise with constant spectral density in the frequency interval up to f_1:

$$R(f) = \begin{cases} \frac{\sigma^2}{2f_1} & \text{if } -f_1 \leq f \leq f_1 \\ 0 & \text{otherwise.} \end{cases} \tag{23}$$

Rice's formula for a Gaussian stationary process [23, 24] states that the intensity of upcrossings, *i.e.*, the expected number of upcrossings of the level $\gamma\sigma$ in an interval of length 1, is

$$\mu^+(\gamma\sigma) = E(N^+_{[0,1](x,\gamma\sigma)}) = \frac{1}{2\pi}\sqrt{\frac{\lambda_2}{\lambda_0}}e^{-\gamma\sigma^2/(2\lambda_0)}, \tag{24}$$

where λ_0 and λ_2 are functions of the covariance function $r(\tau)$,

$$\lambda_0 = r(0) \quad \text{and} \quad \lambda_2 = -r''(0). \tag{25}$$

If we consider the case when the level $\gamma\sigma$ is high enough for the crossing times to be spread out and independent, we can model the time between each crossing as exponentially distributed. Then the number of upcrossings during the interval of length 1 follows a Poisson process with intensity $\mu^+(\gamma\sigma)$. The corresponding process describing the number of downcrossings of the level $-\gamma\sigma$ will have identical intensity, due to the symmetry and zero mean of the signal. We are interested in the intensity of crossing either $\gamma\sigma$ or $-\gamma\sigma$, and this intensity could then be described by the sum of the two single-sided intensities.

The probability that we will have no crossings of the level $\gamma\sigma$ in a time interval of length T is

$$\text{Prob}(\max(|x|) < \gamma\sigma) = e^{-T2\mu^+(\gamma\sigma)}, \tag{26}$$

and the clip probability is thereby given by

$$\mathcal{P}_S(\gamma) = \text{Prob(clip at level } \gamma\sigma) = 1 - e^{-T2\mu^+(\gamma\sigma)}. \tag{27}$$

To solve this for our signal, we start with calculating the covariance function:

$$r(\tau) = \int_{-\infty}^{\infty} e^{j2\pi f\tau} R(f)\, df = \sigma^2 \frac{\sin(2\pi\tau f_1)}{2\pi\tau f_1}, \tag{28}$$

which shows the variance of the signal, $r(0) = \sigma^2$. Differentiating $r(\tau)$ gives

$$r'(\tau) = \sigma^2 \left(\frac{\cos(2\,\pi\,\tau f_1)}{\tau} - \frac{1}{2}\,\frac{\sin(2\,\pi\,\tau f_1)}{\pi\,\tau^2 f_1} \right) \tag{29}$$

and

$$\begin{aligned} &r''(\tau) = \\ &= \sigma^2 \left(-2\,\frac{\sin(2\,\pi\,\tau f_1)\pi\, f_1}{\tau} - 2\,\frac{\cos(2\,\pi\,\tau f_1)}{\tau^2} + \frac{\sin(2\,\pi\,\tau f_1)}{\pi\,\tau^3 f_1} \right). \end{aligned} \tag{30}$$

Then the intensities λ_0 and λ_2 are given by

$$\lambda_0 = r(0) = \sigma^2 \tag{31}$$

and

$$\begin{aligned}\lambda_2 &= -r''(0) = -\lim_{\tau\to 0} r''(\tau)\\ &= 4\pi^2 f_1^2\sigma^2 - \lim_{\tau\to 0}\sigma^2\left[-\frac{2}{\tau^2}\left(1-\frac{1}{2}(4\pi^2\tau^2 f_1^2)+O(\tau^4)\right)\right.\\ &\qquad\left.+\frac{1}{\pi\tau^3 f_1}\left((2\pi\tau f_1)-\frac{1}{6}(8\pi^3\tau^3 f_1^3)+O(\tau^5)\right)\right]\\ &= 4\pi^2 f_1^2\sigma^2 - \lim_{\tau\to 0}\sigma^2\left[+4\pi^2 f_1^2 - \frac{8}{6}\pi^2 f_1^2 + O(\tau^2)\right]\\ &= \frac{4}{3}\pi^2 f_1^2\sigma^2. \end{aligned} \tag{32}$$

Inserting this into (24) and (27), we get

$$\begin{aligned}\mathcal{P}_S(\gamma) &= 1-\exp\left(-T\frac{2}{2\pi}\sqrt{\frac{(2\pi f_1)^2}{3}}e^{-\gamma^2\sigma^2/(2\lambda_0)}\right)\\ &= 1-\exp\left(-2Tf_1\frac{1}{\sqrt{3}}e^{-\gamma^2/2}\right).\end{aligned} \tag{33}$$

The factor Tf_1 is dependent on the symbol length. If the sample rate is F_s, and the whole band up to the Nyquist frequency is used, then $f_1 = F_s/2$. At the same time, T corresponds to N samples, each $1/F_s$ in time. Thereby,

$$Tf_1 = \frac{N}{F_s}\frac{F_s}{2} = \frac{N}{2}. \tag{34}$$

The resulting clip probability is then

$$\mathcal{P}_S(\gamma) = \text{Prob(clip at level } \gamma\sigma) = 1-\exp\left(-\frac{N}{\sqrt{3}}e^{-\gamma^2/2}\right). \tag{35}$$

Notable with this approximation is that the clip probability for $\gamma = 0$ is not exactly one but instead $1-\exp(-N/\sqrt{3})$. As mentioned, when modelling the crossings with a Poisson process, the model is not applicable when we have a too low clip level, *i.e.*, close to 0. However, this low region is not of interest. The related problem of deriving clip probability for a complex-valued continuous-time OFDM signal was addressed in [25].

Using the Poisson process model, we can also calculate the probability for exactly a certain number of clips. In particular, the probability for one single clip during a symbol interval is

$$T2\mu^+(\gamma\sigma)\,e^{-T2\mu^+(\gamma\sigma)} = \frac{N}{\sqrt{3}}e^{-\gamma^2/2}\exp\left(-\frac{N}{\sqrt{3}}e^{-\gamma^2/2}\right). \tag{36}$$

Bibliography

[1] A. Gatherer and M. Polley, "Controlling clipping probability in DMT transmission," in *Proc. Asilomar Conference on Signals, Systems and Computers*, vol. 1, Pacific Grove, CA, USA, Nov. 1997, pp. 578–584.

[2] J. Tellado-Mourelo, "Peak to average power reduction for multicarrier modulation," Ph.D. dissertation, Stanford University, Stanford, CA, USA, Sept. 1999.

[3] M. Friese, "Multitone signals with low crest factor," *IEEE Transactions on Communications*, vol. 45, no. 10, pp. 1338–1344, Oct. 1997.

[4] D. J. G. Mestdagh and P. M. P. Spruyt, "A method to reduce the probability of clipping in DMT-based transceivers," *IEEE Transactions on Communications*, vol. 44, no. 10, pp. 1234–1238, Oct. 1996.

[5] B. M. Popović, "Synthesis of power efficient multitone signals with flat amplitude spectrum," *IEEE Transactions on Communications*, vol. 39, no. 7, pp. 1031–1033, July 1991.

[6] R. W. Bäuml, R. F. H. Fischer, and J. B. Huber, "Reducing the peak-to-average power ratio of multicarrier modulation by selected mapping," *Electronics Letters*, vol. 32, no. 22, pp. 2056–2057, Oct. 1996.

[7] D. L. Jones, "Peak power reduction in OFDM and DMT via active channel modification," in *Proc. Asilomar Conference on Signals, Systems, and Computers*, vol. 2, Pacific Grove, CA, USA, Oct. 1999, pp. 1076–1079.

[8] P. O. Börjesson, H. G. Feichtinger, N. Grip, M. Isaksson, N. Kaiblinger, P. Ödling, and L.-E. Persson, "A low-complexity PAR-reduction method for DMT-VDSL," in *Proc. 5th International Symposium on Digital Signal Processing for Communication Systems*, Perth, Australia, Feb. 1999, pp. 164–199.

[9] B. S. Krongold and D. L. Jones, "An active-set approach for OFDM PAR reduction via tone reservation," *IEEE Transactions on Signal Processing*, vol. 52, no. 2, pp. 495–509, Feb. 2004.

[10] W. Henkel and V. Zrno, "PAR reduction revisited: an extension to Tellado's method," in *Proc. International OFDM-Workshop*, Hamburg, Germany, Sept. 2001, pp. 31.1–31.6.

[11] J. Tellado and J. M. Cioffi, *Further Results on Peak-to-Average Ratio Reduction*. ANSI Document, T1E1.4 no. 98-252, Aug. 1998.

[12] N. Andgart, B. Krongold, P. Ödling, A. Johansson, and P. O. Börjesson, "PSD-constrained PAR reduction for DMT/OFDM," *EURASIP Journal on Applied Signal Processing*, vol. 2004, no. 10, pp. 1498–1507, Aug. 2004.

[13] N. Petersson, A. Johansson, P. Ödling, and P. O. Börjesson, "A performance bound on PSD-constrained PAR reduction," in *Proc. IEEE International Conference on Communications*, Anchorage, AK, USA, May 2003, pp. 3498–3502.

[14] S. Wei, D. L. Goeckel, and P. E. Kelly, "A modern extreme value theory approach to calculating the distribution of the peak-to-average power ratio in OFDM systems," in *Proc. IEEE International Conference on Communications*, vol. 3, New York, NY, USA, Apr.–May 2002, pp. 1686–1690.

[15] N. Petersson, "Peak and power reduction in multicarrier systems," Licentiate thesis, Lund University, Lund, Sweden, Nov. 2002.

[16] ITU-T, *Asymmetric digital subscriber line (ADSL) transceivers*. Recommendation G.992.1, June 1999.

[17] ——, *Asymmetric digital subscriber line (ADSL) transceivers – 2 (ADSL2)*. Recommendation G.992.3, July 2002.

[18] ——, *Asymmetric Digital Subscriber Line (ADSL) transceivers – Extended bandwidth ADSL2 (ADSL2+)*. Recommendation G.992.5, May 2003.

[19] P. Ödling, N. Petersson, A. Johansson, and P. O. Börjesson, "How much PAR to bring to the party?" in *Proc. Nordic Signal Processing Symposium*, Tromsø–Trondheim, Norway, Oct. 2002.

[20] D. G. Luenberger, *Linear and Nonlinear Programming*. Boston, MA, USA: Addison-Wesley, 1984.

[21] N. Petersson, A. Johansson, P. Ödling, and P. O. Börjesson, "Analysis of tone selection for PAR reduction," in *Proc. International Conference on Information, Communications & Signal Processing*, Singapore, Oct. 2001.

[22] N. Larsson and K. Werner, "Signal peak reduction for power amplifiers with active termination," Master's thesis, Lund Institute of Technology, Dec. 2002.

[23] G. Lindgren, *Lectures on Stationary Stochastic Processes*. Mathematical Statistics, Lund University, Sept. 2002.

[24] S. O. Rice, "Mathematical analysis of random noise," *Bell Systems Technical Journal*, vol. 23, pp. 282–332, 1944 and vol. 24, pp 46–156, 1945.

[25] H. Ochiai and H. Imai, "On the distribution of the peak-to-average power ratio in OFDM signals," *IEEE Transactions on Communications*, vol. 49, no. 2, pp. 282–289, Feb. 2001.

Paper V

Paper V

How Much PAR to Bring to the Party?

Per Ödling, Niklas Petersson, Albin Johansson, and Per Ola Börjesson

Reducing Peak-to-Average power Ratios (PAR) is an established research topic that has now begun to find its way into products. This gives rise to new questions of dimensioning. Here we address how much PAR reduction that should be applied in a practical system. We demonstrate that the amount of PAR reduction can be found with the appropriate system models. This is applied to the tone-reservation PAR reduction method in an ADSL system.

In some frequency regions, the SNR is in practice often limited by the dynamic of the transmitter's analog front-end. Other frequency regions are strongly attenuated by the channel and contribute very little to the system's capacity. Using multicarrier modulation, we address how much of the spectrum that could be used to improve the SNR in the other regions by reducing the amplitude swing of the transmit signal.

Published in *Proc. Nordic Signal Processing Symposium*, (Tromsø–Trondheim, Norway), Oct. 2002.

1 Introduction

The processing capability of digital circuits increases rapidly, also in comparison to the development of analog technology. This development makes it increasingly beneficial to use digital signal processing to alleviate the requirements on analog system components, and make life a bit easier for the designers of, *e.g.*, analog front-ends. This trend is strong in the area of signal processing today.

One of the main limiting factors in many of today's telecommunication devices is power consumption. Power consumption limits stand-by time and talk-time in cellular phones. Power consumption also limits the degree of integration in many devices. If you make them too small, they become too warm and burn up, because the power consumption is too high. And level of integration is a very important factor in determining cost. Digital signal processing can be used to reduce power consumption by handling as much as possible in the digital domain, and conditioning the signals so that power-efficient system design become possible. We will illustrate this by means of an example where the power consumption is essentially determined by a single, obvious factor.

Wireline broadband service in the form of ADSL, the Asymmetric Digital Subscriber Line standard, is catching on quickly in many countries. What the end-customer has to pay for ADSL is much determined by the cost that the telecommunications operator has, which, in turn, strongly depends on the level of integration of the central-office end (CO) modem. Space requirement, maintenance, and price of the modem per line depends on how many lines of ADSL that fit on a single line-card. The number of lines per line card is limited by the line-card's power consumption and its ability to dissipate this power. In order to dig deeper, we need to look at what components on a line-board that draws so much power.

For ADSL transceivers, the development of digital processing has led to a situation where the digital circuitry parts of the system stands for a little as about 15% of the total power dissipation. Another 15% is consumed by analog-to-digital and digital-to-analog converters. Meanwhile, the power efficiency of the analog front-end has not undergone as rapid improvement, causing the line driver be responsible for about 70% of the total power dissipation, see Figure 1. It is clear that much effort could be spent in the digital processing, if this would lower the power dissipation in the line driver.

Now we know that it is the line-driver we should focus on, but we need to know how we can reduce its power consumption. It turns out that it is essentially proportional to the square of the line-drivers supply voltage, V_S^2. Thus, this single factor essentially determines the power consumption of the whole transceiver. Pushing on, the supply voltage is chosen according to the

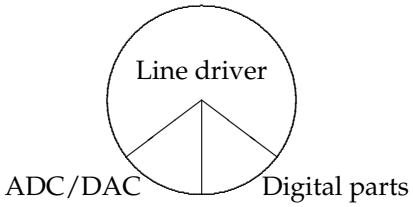

Figure 1: Power distribution in an ADSL transceiver.

desired swing of the transmit signal, that is, to accommodate the large peaks in the signal. Finally, we smell a signal processing problem that we can work with. By reducing the peak level of the transmit signal without affecting the quality of the data transmission, we will greatly reduce the power consumption. And, through the above long chain of dependencies, reduce the cost of ADSL. This research area is called peak-to-average rate reduction, PAR-reduction, or sometimes PAPR-reduction, with the word "power" giving the extra "P".

The rest of this paper discusses how to optimize the PAR-reduction scheme. The morale of the paper is that it *can* and should be optimized, and the paper gives some pointers of how. We continue with the ADSL-example and apply a particular method of PAR-reduction called *tone reservation*. The general idea is to let the transmitter overlay the data signal with another signal that will be orthogonal to the data signal in the receiver.

2 Multicarrier modulation and PAR reduction

ADSL modems are based on multicarrier transmission, in particular on the variant called DMT, Discrete Multi-Tone, modulation. DMT elegantly solves the equalization problem, allows for very efficient channel usage, and in general has many appealing properties. However, in DMT systems, the transmitted signal often have high peak values, and thereby high PAR, because the signal is a sum of many independent component signals. Indeed, for DMT systems with a high number of subcarriers, the transmit signal will even have a close to Gaussian amplitude distribution. The amplitude distribution for a Gaussian transmit signal is shown in Figure 2.

In order to control the amount of signal clipping (by the line-driver and digital to analog converter), the ADSL standard [1] specifies a clip rate of no more than 10^{-7}. In order to achieve this, the line driver supply voltage V_S has to be more than five times the standard deviation of the signal, as shown in Figure 2.

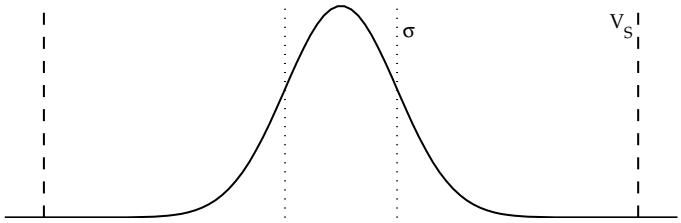

Figure 2: Power distribution for the Gaussian-like symbol. The line driver needs a power supply of more than five times the standard deviation in order to achieve low enough clip distortion.

The area of Peak-to-Average power Ratio (PAR) reduction aims at reducing the dynamic range of a transmit signal before it is fed to the D/A-converter and the analog front-end. This, for instance, reduces the requirements on the resolution of the D/A-converter and the region in which the power amplifier, or line-driver, needs to have a linear amplification. This gain can, as an example, be used to reduce to supply voltage to the line-driver and thus save power. The situation which we consider here, is when the system is limited by a peak constraint, as opposed to a limited transmit energy. The peak constraint can be a model for systems where there is a tight limitation on the power dissipation from the line driver.

Several proposals have been presented for reducing the amplitude of multicarrier signals, [2–4]. Tone reservation, which has been presented in [2, 4] and further investigated in [5–9], has lately gained much industrial interest and has started to appear in advanced communication products. With the tone reservation approach, a subset of the available tones are reserved for PAR reduction, as shown in Figure 3. These tones are used for creating a reduction signal (which is then orthogonal to the data signal) that is added to the data signal in order to reduce the peaks in the resulting signal, see Figure 4.

3 Trade-offs

In this paper we focus on how many tones one should use for PAR-reduction in the tone-reservation approach in order to maximize system performance. However, this is tightly connected with what tones that are selected. The PAR reduction performance differs between different tone sets. In the example in Figure 3, the tone set chosen is a contiguous block in one end of the spectrum. It has been noted [2, 5] that choosing a random place-

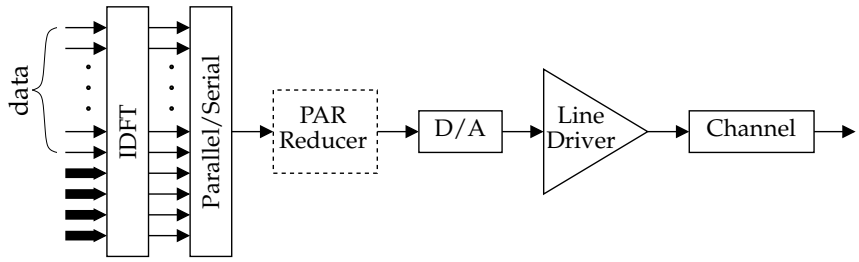

Figure 3: System model, where a subset of the subcarriers (shown with thick arrows) are reserved for PAR reduction.

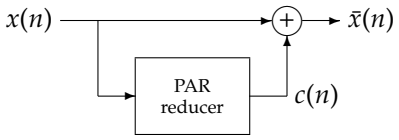

Figure 4: Addition of a PAR reduction signal, $c(n)$, that counteracts the peaks in $x(n)$.

ment in many cases gives better reduction results. This is because tone sets with a structured placement, such as choosing only a block of contiguous tones in one part of the spectrum will not efficiently approximate the data signal, which includes frequencies spread over the whole band. Using linear programming algorithms in the PAR reducer in Figure 4, a simulation example is shown in Figure 5. Here the reduction performance is shown as a function of the number of PAR reduction tones, when the signal strength on the reserved reduction tones is limited in a similar way as the data-carrying tones. Obviously, the random placement gives better results, but only when using many reduction tones. Having few tones, which would typically be the case in practice, the performance is almost independent of tone placement [6].

Reserving tones for PAR reduction will mean that they no longer are available for data transmission. Thus, the capacity of these tones, *i.e.*, the data that could have been sent on them, will no longer contribute to the total system throughput. The number of bits per carrier is determined by a bitloading procedure using the predicted received SNR on each subcarrier. The signal strength is given by the transmitted signal's PSD mask, the channel's attenuation, and the noise. The receiver's perceived noise floor is usually a mix of transmitted noise, such as quantization noise and intermodulation distortion, thermal noise, and crosstalk interference. Both the channel's attenuation and the crosstalk interference tend to increase strongly with fre-

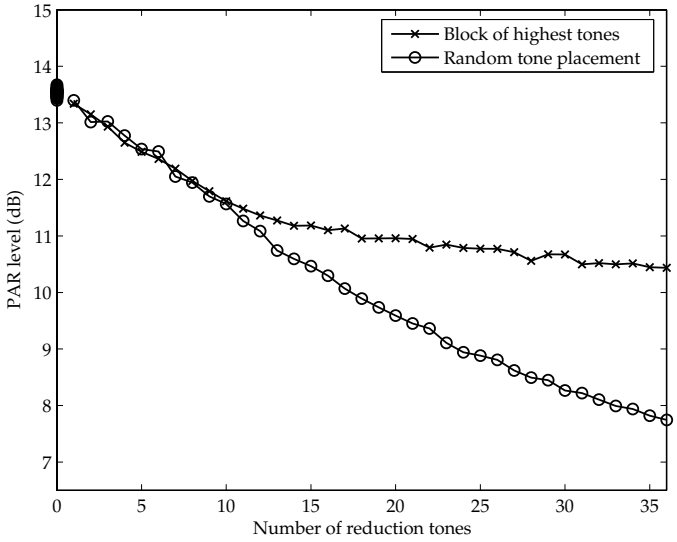

Figure 5: PAR reduction performance as a function of number of reduction tones. The figure shows simulations with constrained tone power, and is evaluated for a symbol clip probability of 10^{-3}.

quency in wireline communication systems. The tones at high frequencies thus usually carry few, if any, bits.

On the other hand, the tones at low frequencies can often carry a large number of bits, and the SNR on these tones is often limited by transmit noise. Using some tones to generate a dummy signal that reduces the PAR of the total transmitted signal can then create an increased SNR on other tones. With proper design of the PAR reduction, the increased capacity on the remaining data tones can then outweigh the loss of capacity stemming from the tones used to generate the dummy signal.

However, using more and more tones for PAR reduction, it is clear that eventually the system looses capacity for every added tone. And it is equally clear that, given a certain system, channel, etc, that an optimum exists.

In Figure 6, a schematic plot of the amplitude distribution of the signal (horizontal axis) is shown for a number of different amplifier gains (vertical axis). Having a low gain into the amplifier, the width of the Gaussian distribution from Figure 2 will be narrower. The solid curves show the distribution for a system with no PAR reduction, and the dashed curves, repre-

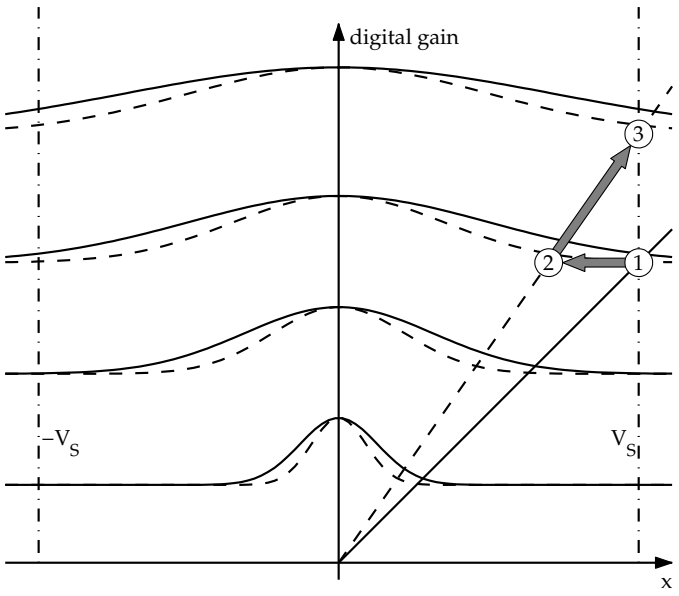

Figure 6: Correspondence between signal gain and amplitude distribution on a system limited by peak constraint, rather than a constraint on transmitted energy. A system without PAR reduction, represented by the straight solid line, can have the maximum gain at point 1 without violating the peak constraint. The PAR-reduced system, following the dashed straight line, could under the same peak constraint work with a higher gain.

senting the signal after PAR reduction, show a not as wide distribution. The straight diagonal lines show what supply voltage V_S is needed to achieve desired clip probability. Since the signal after reduction, dashed lines, has smaller tails on the distribution, the corresponding line is more upward—a larger amplifier gain can be tolerated having a certain amplitude limit.

Now, let the amplitude have a certain limit. This could as described previously be caused by demands on high integration, battery-life considerations, etc. As the digital gain before the line driver increases, the width of the distributions, including their tails, starts to grow, and at point 1 in the figure, the maximum allowed amplitude is reached. Then, using this maximum gain, the system can support a certain bitrate.

Keeping this gain, and instead considering a PAR-reduced system, will move us to the straight dashed line instead, ending up in figure point 2.

Here, the same gain is used, meaning that the SNR and thereby the bitload will be the same on each of the subcarriers. Since the PAR reduction used reserves a set of tones, the number of data-carrying subcarriers will somewhat decrease and thereby also the bitrate. However, the amplitude limit is not reached in point 2, thereby allowing an increase in amplifier gain. Then we will move from point 2 to point 3, where we once again reach the amplitude limit. Stuck at this limit, we now have a larger gain on the amplifier, meaning that the SNR has increased. Thereby it could be possible to achieve a larger total bitload in point 3 than in point 1.

4 Simulation results

To illustrate the described trade-offs, a number of simulation have been performed. These are run for an ADSL-like downlink system, with an FFT size of 512 samples. The subcarriers numbered 33–255 are used for transmitting data, while the low part of the spectrum is reserved for uplink transmission. These are the same parameters that were used in Figure 5.

Figure 7 shows a simulation for a 2 km copper wire, for PAR reduction with two different classes of tone placements, and for different number of reduction tones. Looking at the two curves, we see that the performance improves while reserving more tones for PAR reduction. After about 12 tones, the performance for the block placement starts to decrease. Compare to Figure 5, where the two placement classes are equally performing in the beginning, but where the random placement continues to improve its performance. Taking away tones from the data-carrying set will lower the bitrate. This loss will differ for different placements, which can be seen in the left part of the plot. Here the reduction performance of the two classes are equal, but the block placement discards the least number of data bits. Eventually, both curves reach their respective maximum throughput, after which the bitrate will be lowered when removing more data tones.

In Figure 8 the same simulation is shown using a longer copper wire, of 4 km. This channel does not admit the same throughput as the shorter one, but the improvement is larger when introducing the PAR reduction. (Figures 7 and 8 use the same relative vertical span, with the top of the bitrate axis being 40% higher than the bottom.) We can also see that the curve representing the placement with the highest tones never shows a decreasing performance. This is caused by the channel, which has so large attenuation on the high frequencies that no bits can be transmitted here at all. Then no data capacity at all is lost when reserving the highest numbered subcarriers. Eventually, when a very large number of subcarriers is used, the performance will degrade.

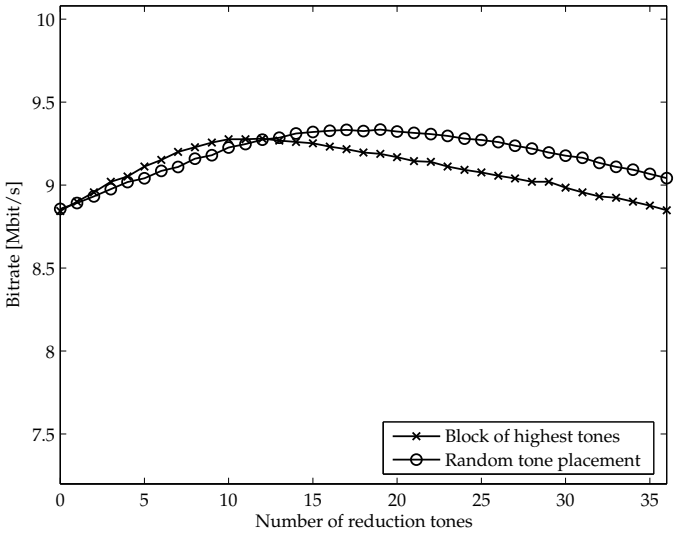

Figure 7: Total bitrate as a function of PAR reduction tones. 2 km copper wire loop. Note the scale on the vertical axis.

5 Summary

Considering the power dissipation of an ADSL system, we have seen that the point to focus on is to lower the supply voltage to the line driver. Here we have worked with the approach that this limiting factor is so crucial, that it is an important constraint on the system throughput.

Looking at the tone reservation approach to PAR reduction, the gain of implementing the algorithms can be evaluated. By varying system parameters one can construct a spectrum of cases ranging from where PAR reduction should not be applied at all (high quality analog front-end, short cable) to where a lot of tones should be used for PAR-reduction.

Bibliography

[1] ITU-T, *Asymmetric digital subscriber line (ADSL) transceivers*. Recommendation G.992.1, June 1999.

[2] J. Tellado-Mourelo, "Peak to average power reduction for multicarrier modulation," Ph.D. dissertation, Stanford University, Stanford, CA, USA, Sept. 1999.

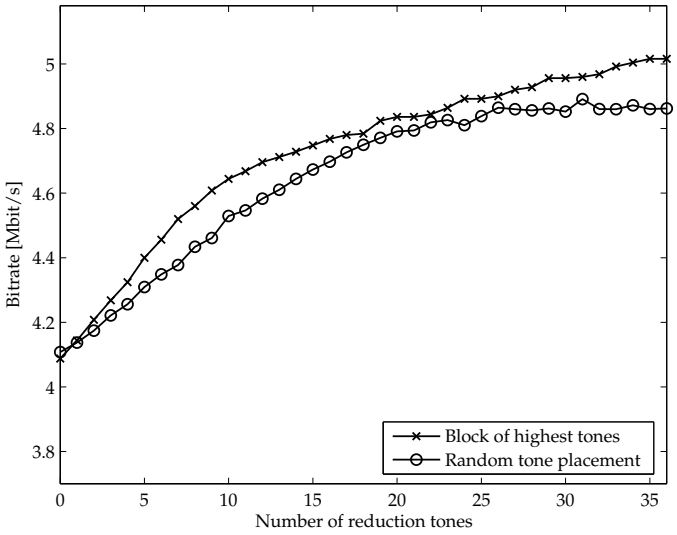

Figure 8: Total bitrate as a function of PAR reduction tones. 4 km copper wire loop. Note the scale on the vertical axis.

[3] M. Friese, "Multitone signals with low crest factor," *IEEE Transactions on Communications*, vol. 45, no. 10, pp. 1338–1344, Oct. 1997.

[4] A. Gatherer and M. Polley, "Controlling clipping probability in DMT transmission," in *Proc. Asilomar Conference on Signals, Systems and Computers*, vol. 1, Pacific Grove, CA, USA, Nov. 1997, pp. 578–584.

[5] N. Petersson, A. Johansson, P. Ödling, and P. O. Börjesson, "Analysis of tone selection for PAR reduction," in *Proc. International Conference on Information, Communications & Signal Processing*, Singapore, Oct. 2001.

[6] ——, "Reducing power consumption with selected orthogonal signals," in *Proc. Radiovetenskap och Kommunikation*, Stockholm, Sweden, June 2002.

[7] B. S. Krongold, "New techniques for multicarrier communication systems," Ph.D. dissertation, University of Illinois at Urbana-Champaign, Urbana, IL, USA, Nov. 2001.

[8] P. O. Börjesson, H. G. Feichtinger, N. Grip, M. Isaksson, N. Kaiblinger, P. Ödling, and L.-E. Persson, "A low-complexity PAR-reduction method for DMT-VDSL," in *Proc. 5th International Symposium on Digital Signal*

Processing for Communication Systems, Perth, Australia, Feb. 1999, pp. 164–199.

[9] ——, "DMT PAR-reduction by weighted cancellation waveforms," in *Proc. Radiovetenskaplig Konferens*, Karlskrona, Sweden, June 1999, pp. 303–307.

Paper VI

Paper VI

Moving the PAR Reduction Criterion into the Line Driver

Karl Werner, Niklas Larsson, Niklas Andgart, Thomas Magesacher,
Tore André, Torbjörn Randahl, and Per Ödling

Traditionally, Peak to Average Ratio (PAR) reduction in digital subscriber line (DSL) transmitters focuses on a digital-domain signal, either at the output of the baseband processing block or at the input of the digital-to-analogue converter (DAC). However, analysis of a DSL transceiver shows that the power dissipation is highly dependent on the PAR at a certain node inside the line driver. Thus, in order to be fully effective, the algorithm design should include the power amplifier dynamics. A typical, actively terminated, line driver is analysed and a model is constructed for PAR reduction purposes. The PAR reduction algorithm is then extended to take advantage of the model. Simulations show that algorithms which are designed to reduce PAR at the new, physically motivated, node obtain about 0.5 dB lower PAR evaluated at this node compared to methods that focus on the PAR of the DAC input.

Published in *Proc. European Signal Processing Conference*, (Vienna, Austria), Sept. 2004.

1 Motivation

Enormous investments have been made in the copper-based infrastructure during the last century. Discrete Multitone (DMT) technology such as ADSL enables high-speed data transmission over the existing telephone lines. Operators, in particular alternative providers, who often have to rent facilities closely located to highly populated areas for their equipment, try to pack DMT transceivers for as many customers as possible into the available space. An important limiting factor with this respect is power dissipation in the transmitter, i.e., the part of the consumed power that is not transmitted on the line.

The line driver is the circuit that provides the interface of the transceiver to the physical line. It is usually an amplifier of class AB. Typically, 70% of the power dissipation of a DMT transceiver occurs in the line driver [1]. To avoid distortion of the transmitted signal, the line driver should provide linear amplification over the amplitude span of the signal. Typical line drivers have a power dissipation that is approximately proportional (see [2]) to the span of the linear amplification region at a certain node inside the line driver. It is thus desirable to keep the signal swing at this point as small as possible.

With DMT based transmission, the sample amplitude distribution of the transmitted signal is approximately Gaussian, thus there is a probability of very high amplitude for some samples [3]. A number of methods have been suggested [3-6] for the reduction of the signal's *Peak to Average Ratio*, PAR[1]. Usually, PAR reduction methods concentrate on a signal in the digital domain, before or after the transmit filters (see Figure 1). In the following, focus of the PAR reduction is moved to a point inside the line driver, where the PAR directly influences the power dissipation. The signal at this point does not coincide with the signal input to the line driver and the analysis and algorithm design therefore require detailed knowledge of the line driver.

A model that is generally applicable to actively terminated line drivers is developed in Section 2 and used to extend an important PAR reduction algorithm in Section 3. Simulations evaluating the performance of the idea for an ADSL downstream link, as described in annex A of the corresponding standardisation document [7], are presented in Section 4.

[1]The PAR of a signal $x(\tau)$ in the interval $\mathcal{T}$ is defined as $\mathrm{PAR} = \frac{\max_{\tau\in\mathcal{T}} |x(\tau)|^2}{\sigma^2}$, where σ^2 is the average symbol energy *before* PAR reduction. Normalising by the energy after PAR reduction would cause a bias towards lower PAR values.

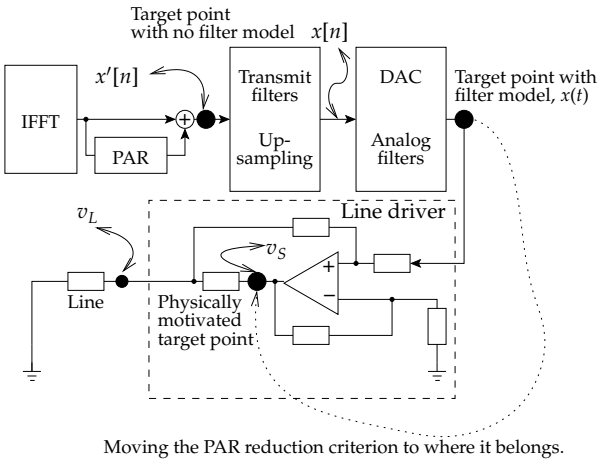

Figure 1: Block diagram of a DMT-based transmitter showing three different points a PAR reduction criterion can focus on. The node inside the line driver labeled v_S is the physically motivated point. The PAR at this point directly influences the power consumption of the system.

2 Modelling the line driver

A typical, simplified line driver structure is shown in Figure 2. Line drivers are often built around two identical amplifiers such as the one in Figure 2, where one of them acts in counter phase. Each amplifier thus provides half the required voltage and half the output resistance. Since the two amplifiers are identical, PAR reduction considerations only need to focus on one of them. Apart from producing the required voltage amplification and current driving capabilities, the line driver should also minimise the receive signal energy loss. This implies that the output impedance should match the impedance of the load, over the frequency band of interest. In traditional design, this is achieved by connecting a resistor, here referred to as R_S, with the same impedance as the load in series with the line driver and the line. This corresponds to $R_1 = \infty$ in Figure 2. Such a design has the drawback of high power dissipation; half of the power of the line driver is wasted in R_S.

In modern designs the output resistance is actively synthesised, and R_S can be made smaller without sacrificing the quality of the received signal. The line driver treated in the following uses this kind of active termination.

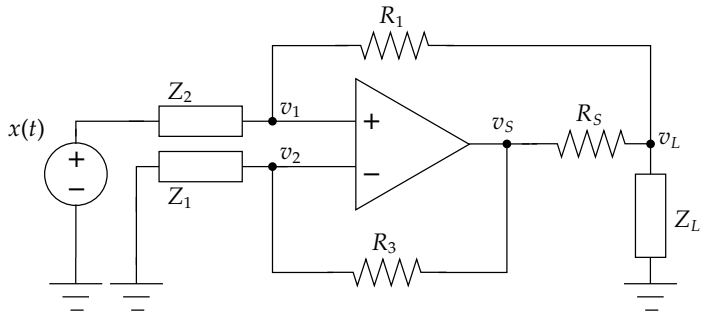

Figure 2: A simplified block diagram of a line driver with active synthesis of the output impedance.

2.1 Selecting a target point

The main goal of PAR-reduction is to lower the power consumption of the line driver. For the class of amplifiers treated here that means lowering the span of the linear amplification region. This is only possible if the signal swing is made smaller, which means reducing the highest peaks in the signal.

The maximum, in terms of voltage, of the signal $v_S(t)$ measured at the point v_S in the line driver is limited by the supply voltage, and it is thus the voltage span at this node that sets the limits on the linear amplification region. PAR reduction should aim at keeping the signal swing of $v_S(t)$ as low as possible. This insight, gained from an investigation of parts of the transceiver that are out of scope in most of the work done on PAR reduction, may be valuable for the study of algorithms and future research.

Line drivers are designed to provide linearity of the signal $v_L(t)$ measured at the point v_L, *not* $v_S(t)$, while PAR reduction should aim at $v_S(t)$, *not* $v_L(t)$. For the passively terminated design, cable dynamics would affect the transfer function to v_L but not to v_S. In actively terminated designs, which are considered here, cable dynamics enter both transfer functions, although in slightly different ways.

The signal $v_S(t)$ differs both from the input signal $x(t)$ of the line driver and from the signal $v_L(t)$ measured at the load. A model of the signal transformation from the input to this node must be included in the PAR reduction algorithm.

With an ideal operational amplifier, the transfer function $H(Z_L)$ of the system with input $x(t)$ and output $v_S(t)$ is given by

$$H(Z_L) = \frac{V_S(f)}{X(f)} = \frac{(R_3 + Z_1)(Z_L R_S + R_1 R_S + Z_L R_1)}{Z_L(Z_1 R_S + Z_1 R_1 - Z_2 R_3) + Z_1 R_S(R_1 + Z_2)}, \qquad (1)$$

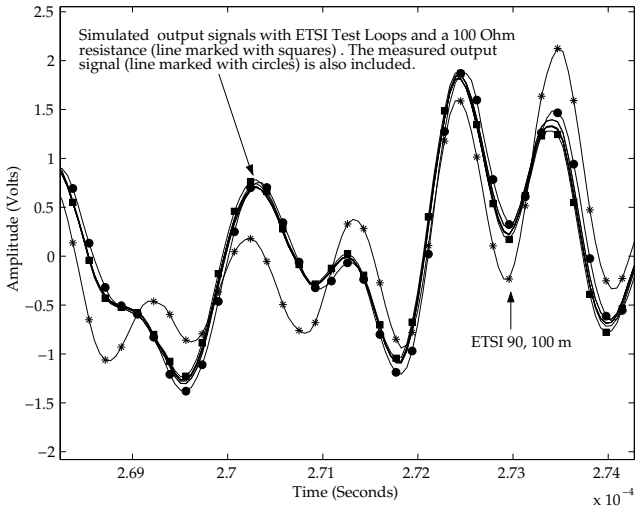

Figure 3: Waveforms of $v_S(t)$: Simulated waveforms for the ETSI loop test cases defined in [8] and for a purely resistive load $Z_L = 100\,\Omega$ (line marked with squares); Measured waveform (line marked with circles) for ETSI40 3.5 km. Significant deviations occur only for the extreme (100m of the ETSI90 cable) loop. The input was identical for all cases.

where $V_S(f)$ and $X(f)$ are the Fourier transforms of $v_S(t)$ and $x(t)$, respectively. The impedances Z_L, Z_1 and Z_2 are complex and frequency dependent. The dynamics of the loop and the transformer enter the transfer function[2] (1) via the impedance Z_L. A similar linear analysis on more detailed circuit schemes for real line drivers yields models that give excellent matches to measured data [2]. These measurements further show that nonlinear effects can be neglected in this application.

2.2 Cable dependency

According to (1), the transfer function $H(Z_L)$ depends on the load impedance Z_L. The characteristics of the load vary with the actual cable attached to the line driver. If the model used for PAR reduction purposes is sensitive to variations of the load impedance, that has to be addressed.

Figure 3 shows simulated waveforms of $v_S(t)$ for different testloops and for a purely resistive load of $Z_L = 100\,\Omega$, as well as a measured waveform.

[2]The transfer function to v_L is dependent on the load characteristics also in the passively terminated design, but as previously stated, $v_S(t)$ is the signal of interest for PAR reduction.

Variation of the cable impedance does not cause large model deviations, except for the comparably short (100m) and thick ETSI90 cable, which causes a more oscillating signal. Simulations and measurements show that, given an accurate model of the transformer, a $100\,\Omega$ resistance approximates the cable impedance with a negligible error, as long as no cables with extreme parameters are used. Hence, as the PAR reduction algorithm can be designed for a single representative load impedance, there is no need to adapt the algorithm to the actual load when installing a system in a new environment.

2.3 Discrete time filter representation

If the impedances Z_L, Z_1 and Z_2 can be approximated as rational functions of $s = j2\pi f$, a closed-form discrete-time representation of (1) can be found using the bilinear transformation $s' = 2(8F_{\text{Nyquist}}) \cdot \frac{z-1}{z+1}$, where $z = \mathrm{e}^{j2\pi f/(8F_{\text{Nyquist}})}$ and F_{Nyquist} is the sampling frequency at the IFFT output. The oversampling factor of eight is recommended in [3] and [4] for a sufficiently accurate representation of an analogue signal for PAR reduction purposes. For the line driver considered here and for the approximation $Z_L = 100\,\Omega$, the resulting discrete-time filter has an IIR form with 9 poles and 9 zeros. We approximate this IIR form with a 20-tap FIR filter $\mathbf{h} = [h[0] \cdots h[19]]$. The filter operation can be represented by the convolution matrix $\mathbf{A}_{ld}$, whose first row is $\mathbf{h} = [h[0]\ 0 \cdots 0]$. This form will be used in the next section.

The transmit filters, including an increase in sampling rate, and the DAC are represented by the matrix $\mathbf{A}_{tx}$. The entire transformation from the space of critically sampled signals just after the IFFT ($x'[n]$ in Figure 1) to the space of oversampled signals in the v_S domain can now be described by the matrix $\mathbf{A} = \mathbf{A}_{ld}\mathbf{A}_{tx}$, which has size 512×4352 for our setup. This representation can be used to extend existing PAR reduction methods in the sense that the PAR reduction criterion is defined for $v_S(t)$ instead of $x'[n]$. In practice, implementations may use the IIR or FIR structure instead.

3 Extension of the tone reservation method

The tone reservation method, a promising PAR reduction scheme suggested by Tellado [3], uses a selected set of tones to modify the signal such that the PAR of the resulting signal is lowered. Finding a low-PAR solution is an optimisation problem, which can be formulated as a linear program. Modifying the algorithm so that it takes into account the line driver dynamics,

we obtain the linear program

$$\begin{array}{ll} \underset{\check{\mathbf{C}}}{\text{minimise}} & \gamma \\ \text{subject to} & \begin{bmatrix} \mathbf{A}\check{\mathbf{Q}} & -\mathbf{1} \\ -\mathbf{A}\check{\mathbf{Q}} & -\mathbf{1} \end{bmatrix} \begin{bmatrix} \check{\mathbf{C}} \\ \gamma \end{bmatrix} \leq \begin{bmatrix} -\mathbf{A}\mathbf{x} \\ \mathbf{A}\mathbf{x} \end{bmatrix}, \end{array} \tag{2}$$

where $\gamma = \sqrt{\text{PAR}}$ is the crest factor. The vector $\check{\mathbf{C}}$ is a length $2U$ vector (where U is the number of tones reserved for PAR reduction) containing the PAR reduction symbols and the matrix $\check{\mathbf{Q}}$ represents a coordinate transform, mapping $\check{\mathbf{C}}$ onto the space of allowed PAR reduction signals. The transformation $\mathbf{A}$ maps signals from $x'[n]$ to the v_S domain in the line driver. With $\mathbf{A} = \mathbf{I}$, (2) corresponds the original problem considered by Tellado [3]. A similar approach to the one presented here considers the transmit filters [6]. Note that, while the criterion for PAR reduction is moved, the actual PAR reduction signal is still added to the critically sampled signal at the output of the IFFT block.

The extension of the model increases complexity significantly, which is mainly due to the oversampling. Even if no line driver model would be used in the algorithm, inter-sample behavior should still be taken into account. Thus, in a fair comparison, the increased complexity caused by the line driver modelling is modest.

The same problem formulation can be kept when using lower complexity active-set based algorithms, proposed in [4]. Here, a good but suboptimal solution will be achieved after a few iterations. Performance results of algorithms both based on linear programming and on the active-set method when focusing on v_S are provided in the next section.

4 Simulation Results

A simulation environment was built around the IIR model of the actively terminated line driver and specifications for digital domain filters given in [9]. Three line driver transfer functions were used in the simulations, corresponding to three different ETSI test loops. The transfer function obtained for the $100\,\Omega$ test loop was used in the PAR reduction algorithm. This illustrates the dependency of the transfer function, and thus the PAR reduction algorithm, to the load connected to the line driver. The effect of these variations are illustrated in Figure 5. The symbols were created using random tone constellations. Ten tones, randomly selected from the transmission band, were reserved for PAR reduction. The tone selection problem is treated in [1].

Three distinct transmit path matrix models were tested. The first model is a pure upsampling $\mathbf{A} = \mathbf{U}_8$, the second model is the digital transmit fil-

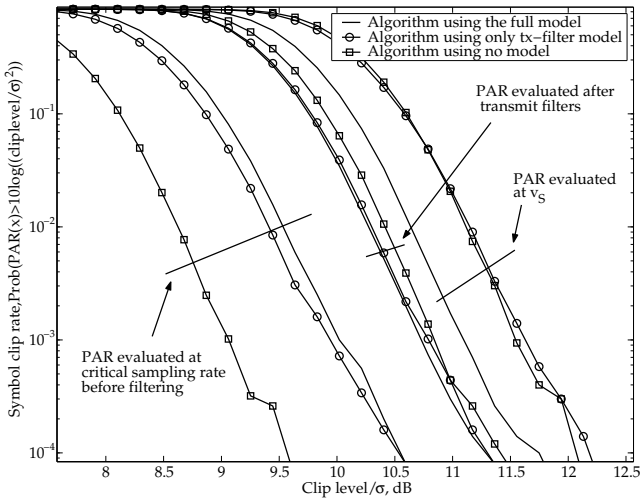

Figure 4: Clip probability as a function of clip level for a signal that is PAR reduced using the three linear programming based methods. The PAR was evaluated at three points in the system; corresponding to $x'[n]$, $x[n]$ and $v_S(t)$ in Figure 1. Evaluating PAR at the critical sampling rate (the three left-most curves), the best performance is achieved when using no filter model. However, when evaluating the physically motivated signal $v_S(t)$, the reduction scheme using the full model performs best.

ter matrix $\mathbf{A} = \mathbf{U}_2\mathbf{A}_{tx}$ (a four times increase in sampling rate is already included in the filter specifications), while the third represents the full model $\mathbf{A} = \mathbf{A}_{ld}\mathbf{U}_2\mathbf{A}_{tx}$. The matrix $\mathbf{U}_i$ is a convolution matrix describing an upsampling operation by a factor i using a sinc impulse response. Note that the comparison is fair in the sense that all three models include the effects of oversampling.

Figure 4 shows the performance of a linear programming based algorithm using the three different models in terms of clip probability evaluated at three different points in the system. The results illustrate an important point: When comparing PAR reduction algorithms, the point in which PAR is evaluated is critical. When PAR is evaluated after the IFFT, the original method with $\mathbf{A} = \mathbf{U}_8$ gives lower PAR than the extended method. Also, when PAR is evaluated at the DAC output, the method with the full line driver model performs worse. Since the goal is to reduce power dissipation in the line driver, the method with the best performance at v_S should be selected. A PAR criterion at the IFFT output or immediately after the DAC

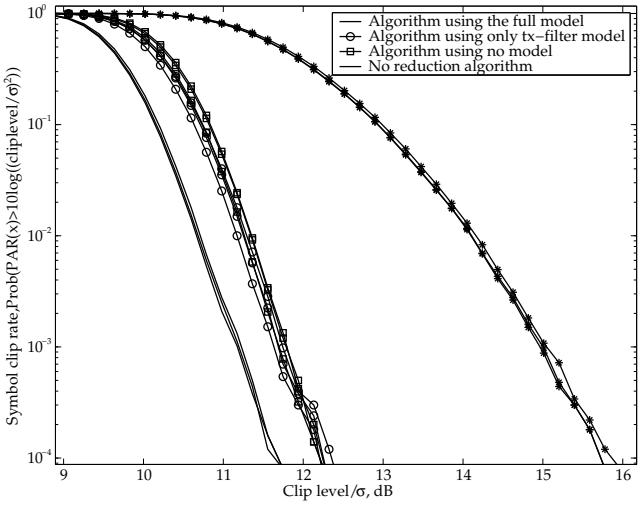

Figure 5: Clip probability as a function of clip level. Three different active set based methods were used. The first uses *no model* but only upsampling by a factor 8 ($\mathbf{A} = \mathbf{U}_8$). The second version has an accurate *transmit filter model*, i.e. $\mathbf{A} = \mathbf{A}_{tx}$, while the third version uses the *full model* including line driver and transmit filters. PAR is evaluated at v_S in all cases. Three line driver models were used in the simulations, corresponding to the three curves in the plot for each method. The line driver models differs only in the load Z_L that is used, corresponding to realistic cable deviations. One of these three models was also used in the design of the PAR reduction algorithm with the full model. The right-most curves correspond to the case when no PAR reduction is employed.

has limited physical motivation. Moving the criterion into the line driver, the PAR at v_S is lowered by approximately 0.5 dB, as shown in Figure 4.

In Figure 5, the results of an active-set based algorithm evaluated at v_S are shown, now also with the unreduced signal. Also for this less complex algorithm, modelling the line driver clearly improves the performance. PAR is about 0.5 dB lower at a symbol clip rate of 10^{-4} when a line driver model is included in the algorithm. The influence of variations of the line driver transfer function due to the different testloops is negligible.

5 Conclusion

A typical line driver structure was analysed and it was concluded that an efficient PAR reduction algorithm should focus on the signal at a specific node inside the line driver that coincides neither with the input signal nor with the output signal. A linear model of the line driver dynamics was developed. Measurements suggest that this model structure is accurate enough for the purpose.

The tone reservation method has been modified to use the new knowledge. Simulations show that improvements of around 0.5 dB are possible. However, note that the gain depends on the algorithm and the transmit filters. The key point of this work is the shift of focus towards a physically motivated PAR reduction criterion.

Bibliography

[1] N. Petersson, "Peak and power reduction in multicarrier systems," Licentiate thesis, Lund University, Lund, Sweden, Nov. 2002.

[2] N. Larsson and K. Werner, "Signal peak reduction for power amplifiers with active termination," Master's thesis, Lund Institute of Technology, Dec. 2002.

[3] J. Tellado-Mourelo, "Peak to average power reduction for multicarrier modulation," Ph.D. dissertation, Stanford University, Stanford, CA, USA, Sept. 1999.

[4] B. S. Krongold, "New techniques for multicarrier communication systems," Ph.D. dissertation, University of Illinois at Urbana-Champaign, Urbana, IL, USA, Nov. 2001.

[5] W. Henkel and V. Zrno, "PAR reduction revisited: an extension to Tellado's method," in *Proc. International OFDM-Workshop*, Hamburg, Germany, Sept. 2001, pp. 31.1–31.6.

[6] A. A. Salvekar, C. Aldana, J. Tellado, and J. Cioffi, "Peak-to-average power ratio reduction for block transmission systems in the presence of transmit filtering," in *Proc. International Conference on Communications*, Helsinki, Finland, June 2001, pp. 175–178.

[7] ITU-T, *Asymmetric digital subscriber line (ADSL) transceivers*. Recommendation G.992.1, June 1999.

[8] ——, *Test procedures for digital subscriber line (DSL) tranceivers*. Recommendation G.996.1, Feb. 2001.

[9] R. Hester, S. Mukherjee, D. Padgett, D. Richardson, W. Bright, M. Sarraj, M. Agah, A. Bellaouar, J. Chaudhry, I. Hellums, K. Islam, A. Loloee, F. Nabicht, J. Tsay, and G. Westphal, "Codec for echo-canceling, full-rate ADSL modems," in *Proc. IEEE International Solid-State Circuits Conference*, Feb. 1999, pp. 242–243.

Paper VII

Paper VII

Implementation Notes for PAR Reduction

Niklas Andgart, Thomas Magesacher, Per Ödling, and Per Ola Börjesson

This report summarizes parts of our work on peak-to-average ratio (PAR) reduction. The main focus is on reduced-complexity tone reservation algorithms. Section 1 proposes a (distortion-free) algorithm that achieves a PAR level of 13.4 dB after the postfilter. A rough complexity estimate yields $63 \cdot 10^6$ relevant operations per second (note that a more accurate complexity assessment should take into account the architecture of the target hardware).

In Section 2, we investigate the idea of introducing a hard-clip device in the DS transmit path together with a "clip-echo canceler". We conclude that modeling the echo path up to 1.1 MHz, as it is usually done, is sufficient, which makes the idea feasible from complexity point of view. We can use the echo canceler that is used now to cancel also the clip-noise echo. Hence, the clip-noise problem is moved from the near-end receiver to the far-end receiver.

Section 3 summarizes our thoughts about the comparison of different PAR reduction algorithms employed in DSL systems. We conclude that it is vital to include the coding in this kind of investigation.

Internal report, Lund University. Dec. 2003

1 Tone reservation

Tone reservation methods reduce PAR by excluding a certain number of tones from the data-carrying set, and using them for PAR reduction instead. We here run the algorithm on the four times oversampled signal, to get better control of the peak regrowth.

1.1 Active-set algorithm

Finding the best solution for the tone weights and phases on the reserved tones is in general a rather complicated operation. The active set algorithm with $O(N)$ complexity exhibits rapid convergence towards a minimax PAR solution [1–3]. Whereas a finite number of iterations will achieve the PAR level γ^*, optimal given the current tone set, a very good suboptimal solution can be achieved in two or three iterations, making this an attractive practical solution.

The active set approach reduces the PAR through the use of the kernel $\mathbf{p}$. Beginning with the sample of largest magnitude γ_0 at location n_0, the peak is reduced by subtracting a scaled version of $\mathbf{p}_{\langle n_0 \rangle}$ until a second peak at some location n_1 is balanced with it at some magnitude $\gamma_1 < \gamma_0$. These two peaks are then reduced equally through a linear combination of $\mathbf{p}_{\langle n_0 \rangle}$ and $\mathbf{p}_{\langle n_1 \rangle}$ until a third peak is balanced. These three peaks are reduced equally until a fourth is balanced, and so forth. When a sample is at the peak magnitude, it signifies an active inequality constraint (i.e., strictly equal), and the active-set approach is therefore building a set of active constraints. Mathematically, the iteration updates can be written as

$$\bar{\mathbf{x}}^{(i)} = \bar{\mathbf{x}}^{(i-1)} - \mu^{(i)} \hat{\mathbf{p}}^{(i)}, \tag{1}$$

where $\bar{\mathbf{x}}^{(i)}$ represents the signal after the ith iteration, $\hat{\mathbf{p}}^{(i)}$ is the descent direction in the ith iteration, and $\mu^{(i)}$ represents the descent stepsize. The stepsize μ is determined by finding the next active-set peak. This can potentially be very time-consuming, and the complexity for this is studied in the following section.

At the start of the ith iteration, there will be i peaks which are balanced at locations $n_0, n_1, \ldots, n_{i-1}$. To keep these peaks balanced, the next iteration descent must satisfy

$$\hat{p}^{(i)}_{n_k} = \operatorname{sign}\left(\bar{x}^{(i)}_{n_k}\right) = S_{n_k}, \quad k = 0, 1, \ldots, i-1, \tag{2}$$

with the assumption that we scale $\hat{\mathbf{p}}^{(i)}$ to have unit magnitude in locations corresponding to the active set of peaks. No matter what value of $\mu^{(i)}$ is

chosen, the magnitudes of the peaks at $n_0, n_1, \ldots, n_{i-1}$ will remain equal. The $\hat{p}_{n_i}$ values can be calculated as

$$\hat{\mathbf{p}}^{(i)} = \sum_{k=0}^{i-1} \alpha_k^{(i)} \, \mathbf{p}_{\langle n_k \rangle}, \tag{3}$$

where the $\alpha_k^{(i)}$ are computed by solving an $i \times i$ system of equations. This requires an $i \times i$ matrix inverse, but in practical implementations, i will typically be at most 3, and the inverse cost is then small relative to the the total iteration complexity.

1.2 Reduced-complexity active set: algorithm, complexity, performance

We have seen that an important property for all algorithms is that the number of operations performed on each sample is held low. By limiting the set of tracked samples to only look at samples which we guess are important, the complexity can be strongly reduced.

The active-set algorithm starts with placing a kernel in counter-phase to the highest peak, and then put so much magnitude on this kernel that it reduces the size on this peak just enough to meet the level of another peak. Then the algorithm continues by having these two peaks as active and searching for a third.

What will affect the location of the next active peak is

- The peaks in the original signal.
- The peaks outside the main peak in the reduction kernel, which then can create new peaks in the signal.

The kernel is precalculated offline. Then the indices of the high samples are stored in a vector. See the left part of Figure 1. Assume that the k_0 highest indices are stored in the set, and also the closest neighboring samples to the k_1 highest. In the figure, $k_0 = 10$ and $k_1 = 0$. The same procedure can be done for the signal. This must be done for each data symbol! In the right part of the figure, it is shown for $s_0 = 30$ and $s_1 = 0$, where s_0 and s_1 specifies the number of peak samples and neighboring samples, respectively.

1.3 Complexity

Notation

N Signal length, i.e., $N = 2048$ if we have 4 times oversampling.

L_d In order to reduce complexity somewhat in the startup phase, only every L_d samples can be viewed when searching for the peak positions.

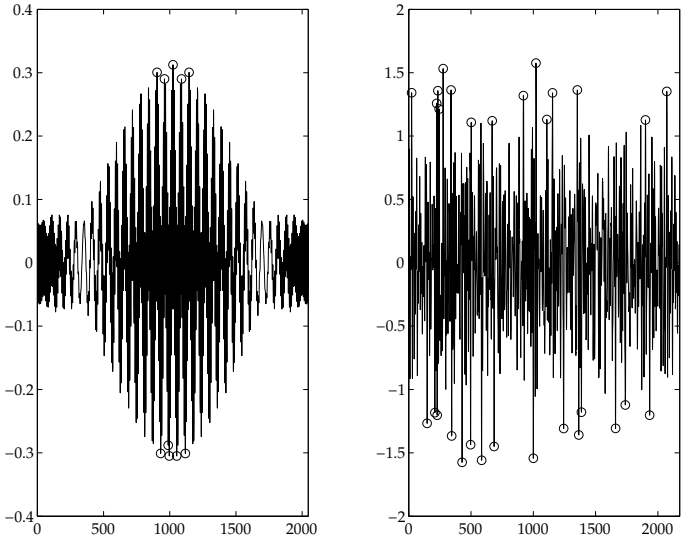

Figure 1: Highest samples in kernel and signal

$B = s_0 + 2s_1$ Number of stored peak positions, including any neighbor samples, in the signal.

$P = k_0 + 2k_1$ Number of stored peak positions, including any neighbor samples, in the kernel.

U Number of tones.

I Number of iterations.

i Current iteration number.

Startup phase

Get the local maxima/minima in the signal. This matlab code gives the indices:

```
idx=find([diff(sign(diff(x([end 1:end 1]))))]);
```

The signal is read through once. Apart from the sign(·), it is basically two subtractions per sample. $\boxed{2N/L_d}$

Keep track of the s_0 largest, and also the neighbors to the s_1 largest. We now have $B = (s_0 + 2s_1)$ samples in the "tracked set". $\boxed{S \approx \frac{B(1+B)}{2} \sum_{n=B+1}^{N/4} \frac{1}{n}}$

Iteration #i

Extending the tracked set Due to the newly balanced peak, we have P new samples in our tracked set.

Update the signal on these samples to include the reduction signal consisting of all kernels so far. $\boxed{iP}$

Sort the indices in the newly added set $\boxed{2P}$

Remove active indices from new set $\boxed{iP}$

Join new and old sets $\boxed{B_i}$

Adding a kernel to the tracked samples Number of tracked samples: $B_i = B + B \cdot i$

Solve $i \times i$ system to get equal height of kernel peaks $\boxed{11i^2}$

Calculate the kernel values on the tracked samples $\boxed{iB_i}$

Calculate stepsize μ for balancing a new peak. $\boxed{10B_i}$

Keep track of the PSD constraint

Calculate the tone weights for balancing the kernel $\boxed{6U}$

Check if any tone violates the PSD constraint $\boxed{40U}$

Update total tone weights $\boxed{2U}$

Add the final reduction signal for this iteration

Update the signal on the tracked set with the resulting kernel $\boxed{B_i}$

Finish

After iterated I times, the whole signal needs to be updated.

Scale&add the kernel to the rest of the samples $\boxed{IN}$

1.4 Complexity example

Let's take an example: $N = 4N_0 = 2048$, $L_d = 1$, $B = 15 + 2 \cdot 5 = 25$, $P = 5 + 2 \cdot 0 = 5$, $U = 12$, $I = 1, 2, 3, 4, 5$.

Iterations	1	2	3	4	5
MIPS	35.0	48.7	63.2	78.6	95.1

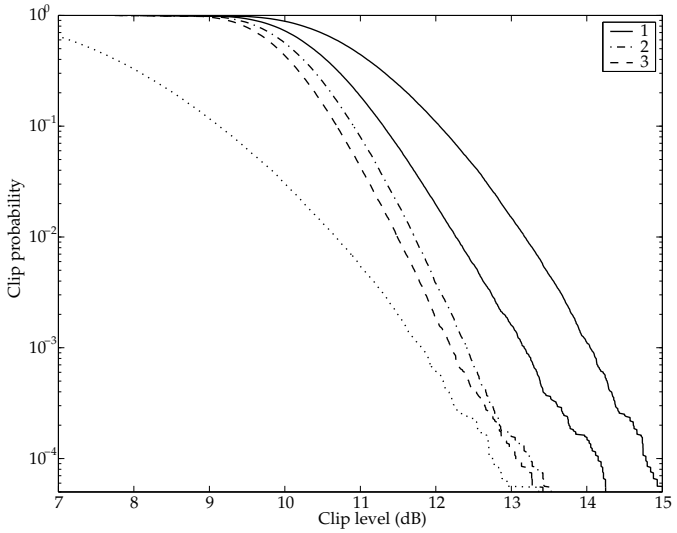

Figure 2: Three active set iterations with 12 tones (4 low, 6 high and 2 middle). PSD constraint is used. The upper solid line shows unreduced signal and the lower dotted line shows bound with this PSD constraint.

1.5 Simulations

Tone selection

Motivated by the low bit allocation of both low and high tones within the data range we choose the tones mainly in the lower or upper part for PAR reduction in our evaluation: 34, 35, 36, 37, 107, 180, 250, 251, 252, 253, 254, 255 (with tone 0 corresponding to DC).

The example above has been simulated. The PAR reducer works after the digital filter chain, and the analog filters after the PAR reduction is modeled with 8 times oversampling and an approximation of D/A and analog filters. In Figure 2, 1–3 iterations are shown for maximum PSD per reduction tone equal to the average PSD on the data tones. We see that it gives PAR reduction down to about 13.4 dB, at a complexity of 63 MIPS.

The lowest line in the plot shows the bound of achievable performance when having this PSD constraint. Since the power on each tone is limited, the reduction signal is limited in magnitude [4, 5].

Figure 3 shows the resulting PSD (evaluated prior to the D/A converter). We see that with increasing number of iterations, the power on the reduction tones increases as well. However, on average it keeps the 10 dB margin to the data tones.

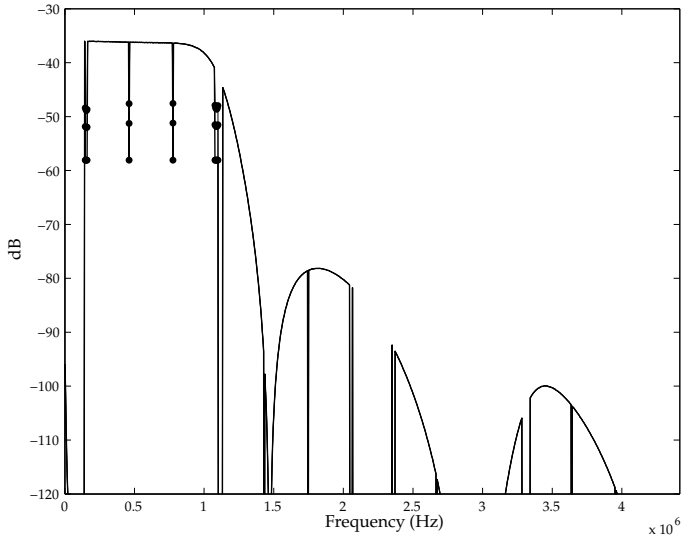

Figure 3: Average PSD measured at the line (PAR tones are marked with dots). Iterations 1–3 are shown, with increasing PSD on the reduction tones. The PSD stays below 10 dB under the signal on average.

2 "Clip echo canceler" system proposal

Consider the DS transmitter (central office side) of an ADSL system. We introduce a clip device that operates at 8.8 MHz and ensures a PAR level at the transmitter output (after the POFI) of 12 dB. The clip noise echo at the US receiver (central office side) is mainly determined by the echo transfer function and the PREFI in the US receiver. The PSDs for a short loop (100 m, ETSI Loop 1) are depicted in Figure 4. We conclude that the clip noise echo at the AD-converter input (after the PREFI) of the US receiver is below the background noise level for frequencies above 400 kHz. The same holds for a long loop (4 km, ETSI Loop 1), as shown in Figure 5. Thus it is possible to downsample the 8.8 MHz-signal, taken from the output of the clip device, to 2.2 MHz and use it as a reference signal for the echo canceler. No relevant aliasing components (relevant in the sense of exceeding the background noise level) that stem from the clip noise echo above 400 kHz will appear after the AD-converter in the US receiver. It is sufficient to model the echo path up to 1.4 MHz, which is roughly the frequency at which the echo of the DS transmit signal drowns in the background noise.

The limit for the clip level is now determined by the SNR required at the

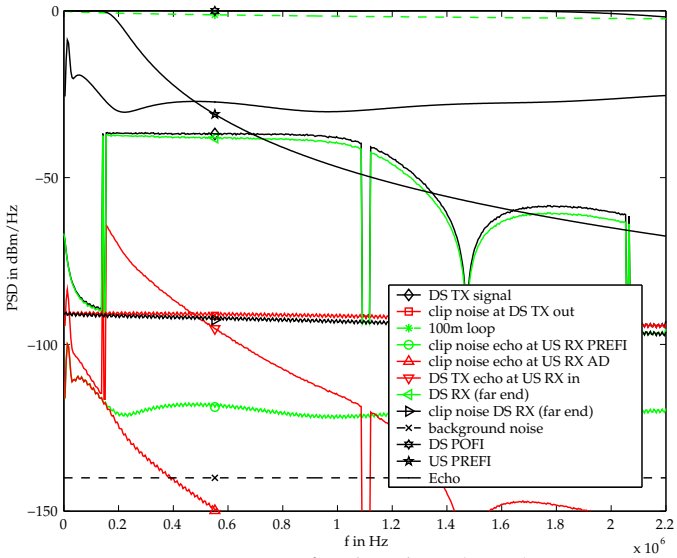

Figure 4: PSDs for short loop (100m).

DS receiver (customer side). The clip noise will become more and more dominant as the loop becomes shorter and the crosstalk noise becomes lower. However, for short loops, PAR reduction should not be necessary since power cut back can be done.

The main point is that we can downsample the 8.8 MHz signal after the clip device to 2.2 MHz and do not have to model the echo path up to 8.8 MHz.

3 Fair comparison of reduction schemes

Since there exist a number of different PAR reduction schemes, it is important to somehow be able to gauge their different performances. Several PAR reduction schemes require knowledge in the receiver about what algorithm the transmitter has implemented, or cannot for some other reason be implemented in a standard-compliant DSL system. We choose not to view them here, and concentrate instead on the transparent reduction schemes, which are more suitable for DSL systems.

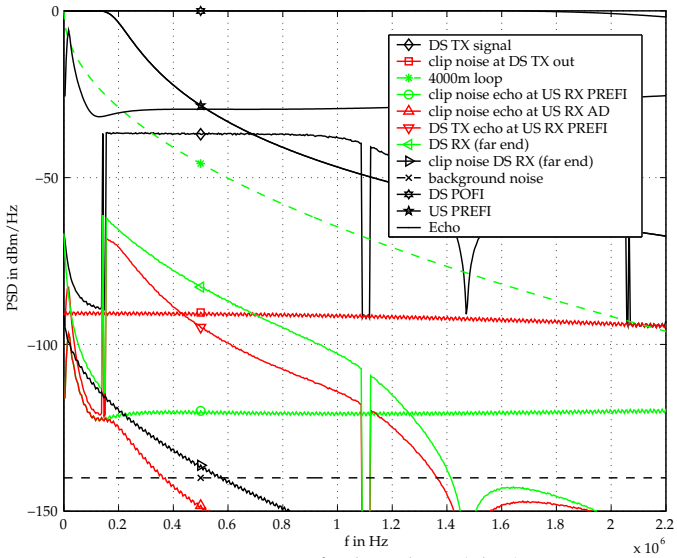

Figure 5: PSDs for long loop (4km).

3.1 Noise frequency characteristics

While both being transparent PAR reduction schemes, a main difference between tone reservation and noise shaping is that the first is a non-distorting method, while the other distorts the signal to achieve the PAR reduction. We are here viewing a way to compare different methods in a fair way.

In Figure 6, the schematic behavior of the distortion using a noise shaper and tone reservation is depicted. The left part shows the resulting noise for four different clip levels when a noise shaper is used. The lower lines correspond to higher clip levels and as the clip level is decreased, the noise level increases, in particular at the higher frequencies.

The right part of the picture shows the behavior for tone reservation; here the noise is concentrated on the unused tones. For the two highest clip levels, there is no noise at the used frequencies — the PAR reduction is non-distorting, but as the clip level decreases, the noise will increase over the whole frequency band.

In this way, we can view both noise shaping and tone reservation as the same thing; we want to concentrate the noise in a desired region. The question is now how to compare the different noise characteristics to each other.

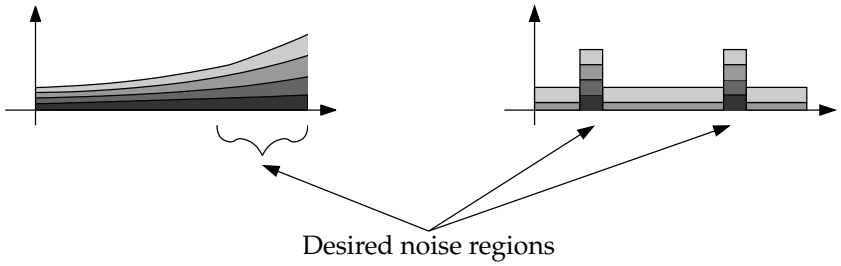

Figure 6: Moving distortion to desired frequency regions. Left: Noise shaping. Right: Tone reservation.

3.2 Main system parameters

We want to condense the performance of a certain PAR reduction scheme to a few parameters:

- A *fixed scenario*, including the loop and noise levels.
- What *supply voltage* is used at the line driver.
- What *bit rate* can be achieved at a certain bit error rate. Here we need also define in which direction we consider the bitrate depending whether we are interested in the near-end loss or the far-end loss.

The goal is to evaluate how much clip noise affects the communication for different schemes, and how much this is compared to for example the loss in bitrate when reserving certain subcarriers for PAR reduction.

We choose not to include the PAR level and clip probability in the set of the essential parameters. The clip probability needs to be defined, example on symbol basis or on sample basis, or as a percentage of the time. When using PAR reduction algorithms, the shape of clips will not be the same as the shape of a clip when viewing an unreduced signal. For reduced signals, the clips will typically be smaller, but may very likely occur more frequently than for an unreduced signal.

The PAR level can still be calculated from the parameters above, as the (square of) supply voltage divided by the signal size as given by the standardized scenario.

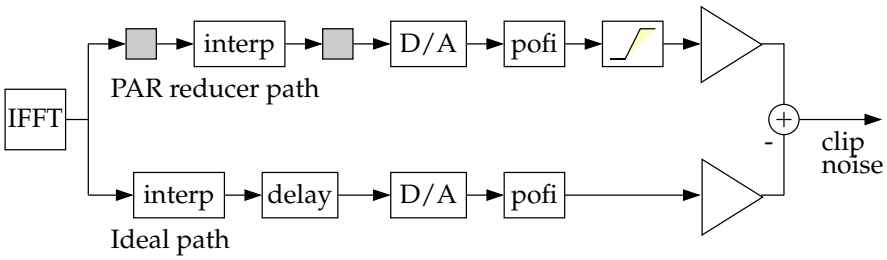

Figure 7: Definition/measurement of distortion signal.

3.3 Comparison setup

To get a measure of the noise introduced by any nonlinearity and different reduction algorithms, we need to define a distortion signal.

- For low-amplitude signals, we assume that the algorithm should give the same output as input. The signal should not be modified unnecessarily.
- A certain delay may be tolerated, to give the algorithms some computing time.

The block scheme in Figure 7 evaluates the distortion introduced by system nonlinearities and reduction schemes. The lower path of the figure, the ideal path, includes the interpolation chain, D/A converter, postfilter and line driver. However, here the nonlinear parts of the line driver are excluded.

In the upper path of the figure, the linedriver nonlinearities are present. The goal is to add PAR reduction in one or both of the square blocks next to the interpolation chain, to reduce the effects of these nonlinearities.

Since the PAR reduction elements are likely to introduce some small delay of the signal, we allow this in the model. We define the distortion signal as

$$d[n] = g(x[n]) - x[n - \Delta], \tag{4}$$

where $g(\cdot)$ is a the model for any nonlinearity after the PAR reducer, before the receiver, and Δ is some defined signal delay. For example, the nonlinearity can be a hard clipper. The signal $d[n]$ as described in the model is a time-continuous signal, but for the evaluation purpose, it can be represented by samples.

3.4 Viewing the clip noise

It is not interesting to view the total energy in the clip signal, since when having tone reservation, some frequencies carry no data bits at all. Noise on these tones does not affect the far-end receiver.

Since different tones have different SNR, and noise shaping tries not do distort the important tones, the noise needs also to be viewed as noise per tone. Taking the FFT of the distortion signal $d[n]$ will view how different tones are affected.

Since the signal is most often not clipped, the clip noise is not stationary. This probably makes it unsuitable to look at the average power of it. Another way of measuring it is to look at the probability of not reaching a certain SDR. The clip probability is then corresponding to the probability of having infinite SNR, since no clip implies no distortion.

3.5 Calculating bit rate

Taking the FFT of the signal as just described and then viewing the probability of not attaining a desired SDR, raises a number of difficulties. The FFT of one or a small number of samples will lead to distortion over several subcarriers; We then introduce correlation among the subcarriers, which may make the problem harder.

One important question is, where to place the "SDR threshold". As just mentioned, one clip affects many tones, so we will not have independent noise over different tones.

The signal is coded both over time and frequency. As an inner code, a trellis code over the tones, which is terminated to the zero state for each DMT frame, is used. The outer code is a RS code with interleaver. There is essentially the same coding for upstream and downstream.

In the ADSL standard, G.992.1, the tone ordering assigns the tones carrying the lowest number of bits to the fast data buffer. The tones with a more dense constellation, higher number of bits, are assigned to the interleaved data buffer. This is however changed in the ADSL2 standard, which uses a new tone ordering, to be more resistant to AM interference.

As seen, there is no obvious and straight-forward correspondence between the clip noise and the effective bit rate. To evaluate how the clips will affect the system, the whole receiver probably needs to be simulated. We might be able to model our clip noise, to plug that into the bitrate simulations.

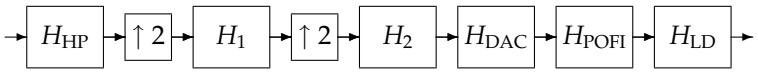

Figure 8: ADSL interpolation path

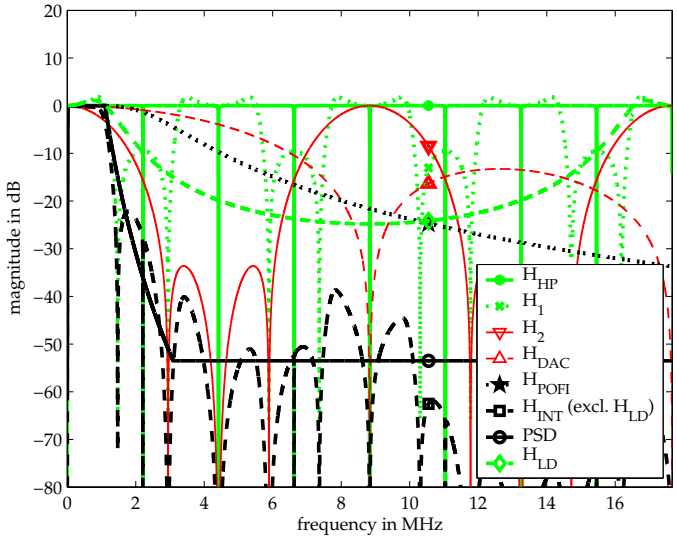

Figure 9: ATU-C interpolation path

A Interpolation path

A.1 Elements

- ... IFFT
- Highpass filter H_{HP} @ $F_{\mathrm{ADSL}} = 2.208\,\mathrm{MHz}$

  This filter corresponds to the filter suggested in [6, p. 81], however, there it was intended to operate at $F_{\mathrm{s1}} = 4.416\,\mathrm{MHz}$ instead of $F_{\mathrm{ADSL}} = 2.208\,\mathrm{MHz}$.

$$H_{\mathrm{HP}}(z) = \frac{129-129z^{-1}}{130-128z^{-1}}, \quad z = \exp\left(\frac{\mathrm{j}2\pi F}{F_{\mathrm{ADSL}}}\right), \quad F_{\mathrm{ADSL}} = 2.208\,\mathrm{MHz}, \quad F \text{ in Hz}, \quad \mathrm{j} = \sqrt{-1}$$

- Expander (↑ 2)

- Interpolation filter H_1 @ $F_{s1} = 4.416\,\text{MHz}$:

$$H_1(z) = \tfrac{1}{2}\tfrac{1+z^{-1}+z^{-2}}{1+\frac{1}{2}z^{-2}}, \quad \begin{array}{l} z = \exp\left(\frac{\mathrm{j}2\pi F}{F_{s1}}\right), \\ F_{s1} = 4.416\,\text{MHz}, \\ F \text{ in Hz}, \\ \mathrm{j} = \sqrt{-1} \end{array}$$

- Expander ($\uparrow 2$)

- Interpolation filter H_2 @ $F_{s2} = 8.832\,\text{MHz}$:

$$H_2(z) = \tfrac{1}{12}(1+3z^{-1}+4z^{-2}+3z^{-3}+z^{-4}), \quad \begin{array}{l} z = \exp\left(\frac{\mathrm{j}2\pi F}{F_{s2}}\right), \\ F_{s2} = 8.832\,\text{MHz}, \\ F \text{ in Hz}, \\ \mathrm{j} = \sqrt{-1} \end{array}$$

- Digital-to-analog converter (DAC) H_{DAC}

  Usually, a zero-order hold stage is a good model. The 'spectral shaping' introduced by the DAC corresponds to the Fourier transform $X(F) = \frac{A}{F_{s2}} \cdot \frac{\sin \pi F/F_{s2}}{\pi F/F_{s2}}$ of a rectangular pulse of width $1/F_{s2}$ and height A.

$$H_{\text{DAC}}(F) = \tfrac{\sin \pi F/F_{s2}}{\pi F/F_{s2}}, \quad \begin{array}{l} F_{s2} = 8.832\,\text{MHz} \\ F \text{ in Hz} \end{array}$$

- Post filter (Pofi) H_{POFI}

  We picked this filter based on our experience—however, it may not be better than just a wild guess without knowledge of the digital-to-analog converter architecture.

$$H_{\text{POFI}}(F) = \frac{3.2761}{3.3140+2.3724\mathrm{j}\,\frac{F}{F_{\text{POFI}}}+\left(\mathrm{j}\,\frac{F}{F_{\text{POFI}}}\right)^2}, \quad \begin{array}{l} F_{\text{POFI}} = 1.4\,\text{MHz} \\ F \text{ in Hz}, \\ \mathrm{j} = \sqrt{-1} \end{array}$$

- Line driver H_{LD}

  The line driver models reported in [6, p. 90] have been found by means of identification exciting the system in the ADSL-band only. Hence the models may not be valid for higher frequencies and have thus been excluded from the interpolation path. The magnitude response

plotted in Figure 9 corresponds to the first of the three models given in [6, p. 90]:

$$H_{\mathrm{LD}}(z) = \frac{-0.1876+1.1773z^{-1}}{1-1.5209z^{-1}+0.6532z^{-2}}, \quad z = \exp\left(\frac{\mathrm{j}2\pi F}{F_{\mathrm{LD}}}\right), \quad F_{\mathrm{LD}} = 17.664\,\mathrm{MHz}, \quad F \text{ in Hz}$$

- ... line

Bibliography

[1] B. S. Krongold and D. L. Jones, "A new method for PAR reduction in baseband DMT systems," in *Proc. Asilomar Conference on Signals, Systems, and Computers*, vol. 1, Pacific Grove, CA, USA, Nov. 2001, pp. 502–506.

[2] ——, "An active-set approach for OFDM PAR reduction via tone reservation," to appear in the *IEEE Transactions on Signal Processing*.

[3] D. G. Luenberger, *Linear and Nonlinear Programming*. Boston, MA, USA: Addison-Wesley, 1984.

[4] N. Petersson, A. Johansson, P. Ödling, and P. O. Börjesson, "A performance bound on PSD-constrained PAR reduction," in *Proc. IEEE International Conference on Communications*, Anchorage, AK, USA, May 2003, pp. 3498–3502.

[5] N. Petersson, "Peak and power reduction in multicarrier systems," Licentiate thesis, Lund University, Lund, Sweden, Nov. 2002.

[6] N. Larsson and K. Werner, "Signal peak reduction for power amplifiers with active termination," Master's thesis, Lund Institute of Technology, Dec. 2002.

Paper VIII

Errata

Middle row in the proof in Appendix A: The factor $-\mathbf{B}\mathbf{A}^{-1}\mathbf{B}\mathbf{A}^{-1}$ is missing. Should read

$$= \mathbf{I} + \mathbf{B}(\mathbf{A}+\mathbf{B})^{-1}\mathbf{B}\mathbf{A}^{-1} + \mathbf{B}\mathbf{A}^{-1}\mathbf{B}(\mathbf{A}+\mathbf{B})^{-1}\mathbf{B}\mathbf{A}^{-1} - \mathbf{B}\mathbf{A}^{-1}\mathbf{B}\mathbf{A}^{-1}$$

Paper VIII

OFDM Frame Synchronization for Dispersive Channels

Daniel Landström, Niklas Petersson, Per Ödling, and Per Ola Börjesson

We address time synchronization in an OFDM system and present an ML estimator that is unbiased also for dispersive channels. The estimator uses the redundancy introduced by the cyclic prefix, and knowledge of the channel. Previously presented estimators based on the cyclic prefix are either biased or have high complexity for this environment. In this paper we show that with proper choice of signal model, the complexity can be reduced considerably while maintaining the performance. Part of the novelty lies in the proper decomposition of correlation matrices that appear in the ML estimator. The new estimator structure consists of a linear filter, followed by an auto-correlating filterbank and a maximization.

1 Introduction

In this paper we focus on the estimation of time offset for *Orthogonal Frequency-Division Multiplexing* (OFDM) symbols for synchronization purposes in a dispersive channel environment. OFDM systems are in general quite sensitive to time and frequency offsets [1]. Not only may synchronization errors cause *intersymbol-interference* (ISI), they can also cause the loss of orthogonality between the subcarriers resulting in *intercarrier-interference* (ICI) [2].

OFDM systems often operate in a multipath environment, and thus under a dispersive channel [3]. In [4] a *maximum-likelihood* (ML) estimator for OFDM systems with a *cyclic prefix* (CP) [5] was derived for an *additive white Gaussian noise* (AWGN) channel. Applying this estimator to a system with a dispersive channel results in an error floor in the time and frequency offset estimation. The error floor stems from the estimator being biased in this environment [6]. In the dispersive channel environment the channel will introduce dependency between the samples, and the simple correlation structure of the received signal used in the AWGN model is not valid any more. In [4] the time offset estimate, $\widehat{\theta}$, is taken as the position of the log-likelihood function's peak. The estimate will be biased if the estimator from [4] is used on a signal that has been transmitted over a dispersive channel. This is because the function where we look for the maximum will be

$$\Lambda_{\mathrm{Disp}}(k) = |h(k)|^2 * \Lambda_{\mathrm{AWGN}}(k)$$

where $\Lambda_{\mathrm{AWGN}}(k)$ is the log-likelihood function from [4], and $\Lambda_{\mathrm{Disp}}(k)$ is the same function calculated on a signal that has been transmitted over the dispersive channel $h(k)$.

The difficulties in the dispersive channel has been observed and addressed before. In [6] an ML estimator for dispersive channels is derived. This estimator is complex to implement, but is suggested as a bound on the achievable performance for ML estimation based on cyclic prefix and channel knowledge.

We now present an ML estimator for use with dispersive channels. This estimator will be unbiased unlike previous cyclic-prefix based ML estimators designed for the AWGN channel. The estimator exploits the redundancy of the received signal introduced by the cyclic prefix and knowledge of the channel impulse response to determine the time offset of the received OFDM symbol. The estimator uses a new structure shown in Figure 1 and can be implemented with lower complexity compared to [6], while essentially maintaining the optimal performance. The basic idea is to have a prefilter collect the information, so that the correlation can be calculated with lower dimension.

Figure 1: Estimator structure

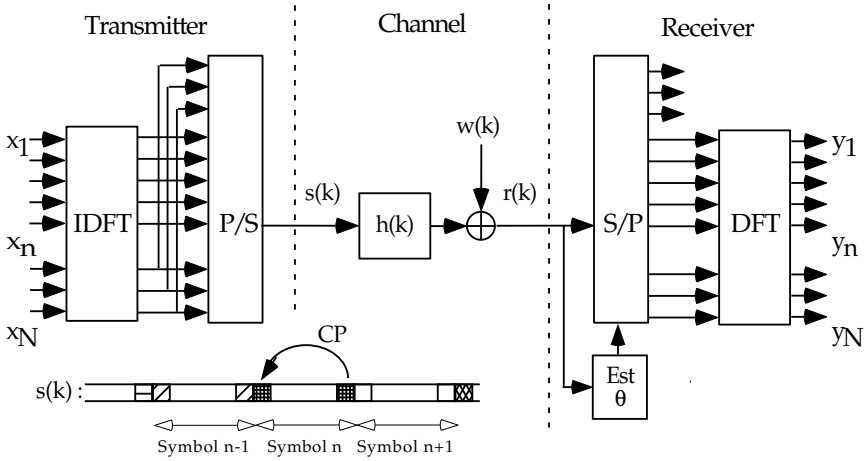

Figure 2: A typical OFDM system. Note the cyclic repetitions in the transmitted signal $s(k)$.

2 The signal model

In an OFDM system [3], complex data symbols are modulated on a large number of carriers by means of an inverse *discrete Fourier transform* (DFT) of size N. Each block of samples is cyclically extended with a prefix of length L before it is transmitted over the channel [5]. In the receiver the cyclic prefix is removed and the data are demodulated by means of a DFT. If synchronization is correct and the cyclic prefix is longer than the length of the channel impulse response, ISI and ICI is avoided [5].

The sensitivity to a symbol-time offset has been investigated in [7]. The requirements on the time offset estimate $\widehat{\theta}$ is determined by the difference in length between the cyclic prefix and the channel impulse response. To avoid ISI and ICI, the time offset estimate needs to be within an interval so that the samples fed to the FFT are not affected by the previous symbol through channel leakage. The time offset will then only appear as phase offsets of the demodulated data symbols. In a coherent system the phase offsets will be compensated for by the channel equalizer and the system performance

depends on the performance of the channel estimator and equalizer. For larger time offsets ISI and ICI occur [7]. Symbol timing requirements can thus be relaxed by increasing the length of the cyclic prefix.

Unlike a real OFDM system, where each symbol is cyclically repeated, we model only one cyclic prefix in our signal model. This way we can derive an estimator that uses information from one symbol only, whereas the observation interval can be longer to handle smearing effects of the dispersive channel. To model our system we assume that the transmitted discrete-time signal $s(k)$ is Gaussian [8]. Because of the cyclic prefix this signal is not white, since L consecutive samples are pairwise correlated with L other consecutive samples, N samples ahead, see Figure 2. By observing this correlation one may find where the OFDM symbol is likely to start. In our model the transmitted signal $s(k)$ has the covariance function

$$\mathbf{C_s}(\theta)_{i,j} = \begin{cases} \sigma_s^2 & \text{if } j-i=0, \\ \sigma_s^2 & \text{if } j-i=N,\ i \in [\theta, \theta+L-1] \\ \sigma_s^2 & \text{if } i-j=N,\ j \in [\theta, \theta+L-1] \\ 0 & \text{otherwise} \end{cases}.$$

We stress that this model only reflects the appearance of one cyclic prefix in the transmitted signal. The simulations will however evaluate the estimator performance for an OFDM system with a stream of symbols, each containing this redundancy.

The system we are targeting is to operate in a dispersive channel. Furthermore we assume the channel impulse response to be known to our estimator. Given the channel impulse response, $h(k)$, we model the received signal $r(k)$ as

$$r(k) = (h * s)(k-\theta) + w(k), \quad k \in I_{obs}, \tag{1}$$

where θ is the time offset, I_{obs} is the observation interval, and $w(k)$ is additive complex white Gaussian noise with variance σ_w^2, with zero mean. In matrix notation we can write this as

$$\mathbf{r} = \mathbf{H}\mathbf{s} + \mathbf{w},$$

where $\mathbf{H}$ is a matrix whose entries have the form $\mathbf{H}_{(i:i+H-1),i} = (h(0), h(1), \ldots, h(H-1))$, and $\mathbf{r}, \mathbf{s}$, and $\mathbf{w}$ are vectors with the samples from $r(k), s(k-\theta)$, and $w(k)$, respectively.

Because of the dispersive channel, $h(k)$, the correlation structure of $s(k)$ is not transferred directly to the received signal $r(k)$. The correlation matrix for the received signal, $r(k)$, will be

$$\mathbf{C_r}(\theta) = \mathbf{H}\mathbf{C_s}(\theta)\mathbf{H}^H + \sigma_w^2\mathbf{I}.$$

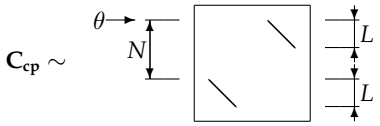

$\mathbf{C_{cp}} \sim$

Figure 3: Schematic figure of the $\mathbf{C_{cp}}$ matrix. The elements in the marked diagonals are all σ_s^2.

3 The ML estimator

The ML estimator for model (1) is [6, 9]

$$\widehat{\theta}_{\mathrm{ML}} = \arg\max_{\theta} \left\{ -\mathbf{r}^H \mathbf{C}_{\mathbf{r}}^{-1}(\theta)\, \mathbf{r} \right\}. \tag{2}$$

We can rewrite $\mathbf{C_r}(\theta)$ as the sum of matrices where one is independent of θ and the other is not,

$$\mathbf{C_r}(\theta) = \mathbf{C_{r0}} + \mathbf{C_{rcp}}(\theta),$$

where $\mathbf{C_{r0}} = \sigma_s^2 \mathbf{H}\mathbf{H}^H + \sigma_w^2 \mathbf{I}$ is a band matrix representing the channel and the noise correlation. The second term $\mathbf{C_{rcp}}(\theta)$ is a matrix representing the total correlation of samples located in the repeated parts, *i.e.*, the cyclic prefix. That is, $\mathbf{C_{rcp}}(\theta) = \mathbf{H}\mathbf{C_{cp}}(\theta)\mathbf{H}^H$, where

$$\mathbf{C_{cp}}(\theta)_{i,j} = \begin{cases} \sigma_s^2 & \text{if } j-i=N,\ i \in [\theta, \theta+L-1] \\ \sigma_s^2 & \text{if } i-j=N,\ j \in [\theta, \theta+L-1] \\ 0 & \text{otherwise} \end{cases},$$

as also illustrated in Figure 3.
Note that only $\mathbf{C_{rcp}}(\theta)$ depends on the unknown θ, and that the dependency lies in the positions of the non-zero values, not in the values themselves.

The ML estimator from Equation (2) can be written as

$$\widehat{\theta}_{\mathrm{ML}} = \arg\max_{\theta} \left\{ -\mathbf{r}^H \left(\mathbf{C}_{\mathbf{r}}^{-1}(\theta) - \mathbf{C}_{\mathbf{r0}}^{-1} \right) \mathbf{r} \right\}, \tag{3}$$

since $\mathbf{C_{r0}}$ is independent of θ and does not affect the maximization [6].

In this paper we choose to perform the maximization over this form, rather than over Equation (2). By choosing this form the estimator can be given a new structure, that will not only reduce the complexity, but also make room for new interpretations. Following Appendix A, we can rewrite

$$\mathbf{r}^H \left(\mathbf{C}_{\mathbf{r}}^{-1}(\theta) - \mathbf{C}_{\mathbf{r0}}^{-1} \right) \mathbf{r} = \mathbf{y}^H \mathbf{Q}(\theta) \mathbf{y},$$

where

$$\begin{aligned} \mathbf{y} &= \mathbf{H}^H \mathbf{C}_{\mathbf{r0}}^{-1} \mathbf{r}, \\ \mathbf{Q}(\theta) &= -\mathbf{C_{cp}}(\theta) + \mathbf{C_{cp}}(\theta) \left(\mathbf{H}^H \mathbf{C}_{\mathbf{r}}^{-1}(\theta) \mathbf{H} \right) \mathbf{C_{cp}}(\theta). \end{aligned}$$

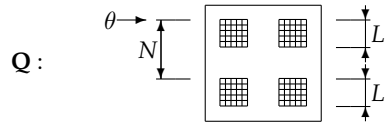

Figure 4: Schematic figure of the $\mathbf{Q}(\theta)$ matrix. All elements outside the marked areas are zero.

The estimator can be written

$$\widehat{\theta}_{\mathrm{ML}} = \arg\max_{\theta} \left\{ -\mathbf{y}^H \mathbf{Q}(\theta)\, \mathbf{y} \right\}. \tag{4}$$

The properties of $\mathbf{Q}(\theta)$ is important for the complexity of the estimator. The first term is just the negative of the $\mathbf{C_{cp}}(\theta)$ matrix. The second term consists of three parts. By multiplying the middle expression with $\mathbf{C_{cp}}(\theta)$ from both sides we will cut out four parts of the middle expression. The $\mathbf{Q}(\theta)$ matrix will be zero in all positions except for in the four areas, see Figure 4.

The location of the non-zero values in the $\mathbf{Q}$ matrix shows that only limited (length $L + L$) intervals of the $\mathbf{y}$ vector has to be known to calculate one point in the log-likelihood function. However, we need to calculate $\mathbf{y} = \mathbf{H}^H \mathbf{C}_{\mathbf{r0}}^{-1} \mathbf{r}$ to know the $L + L$ values. Since the inverse $\mathbf{C}_{\mathbf{r0}}^{-1}$ is not limited to a few diagonals, as the $\mathbf{C_{r0}}$ matrix is, we will need to know $\mathbf{r}$ in a larger interval.

Although $\mathbf{C_{r0}}$ is Toeplitz, $\mathbf{C}_{\mathbf{r0}}^{-1}$ is not. However, for infinite observation interval, $I_{obs} \in (-\infty, \infty)$, the matrix multiplication $\mathbf{y} = \mathbf{G}\mathbf{r} = \mathbf{H}^H \mathbf{C}_{\mathbf{r0}}^{-1} \mathbf{r}$ could be expressed as a convolution, $y(k) = g(k) * r(k)$, with a non-causal filter represented by

$$g(k) = \mathcal{F}^{-1} \left\{ \frac{H^*(f)}{\sigma_s^2 \left| H(f) \right|^2 + \sigma_w^2} \right\}, \tag{5}$$

where $H(f) = \mathcal{F}\{h(k)\}$.

For infinite observation interval it can be shown that the θ-dependency in $\mathbf{Q}(\theta)$ lies in the positions of the non-zero values, not in the values themselves. As the values are independent of θ, we can use a fixed matrix and slide the $\mathbf{y}$ vector to find the log-likelihood function. We write the quadratic

form as

$$\begin{aligned}\Lambda(\theta) &= -\mathbf{y}^H \mathbf{Q}(\theta)\,\mathbf{y} \\ &= -\sum_k \sum_j \mathbf{y}_k^* \mathbf{Q}_{k,j}(\theta)\,\mathbf{y}_j \\ &= -\sum_i \sum_k \mathbf{y}_k^* \mathbf{Q}_{k-\theta,k-\theta+i}(0)\,\mathbf{y}_{k+i} \\ &= -\sum_i \sum_l \mathbf{y}_{l+\theta}^* \mathbf{Q}_{l,l+i}(0)\,\mathbf{y}_{l+\theta+i},\end{aligned}$$

where $\mathbf{Q}(0)$ is the θ-independent matrix $\mathbf{Q}(\theta)|_{\theta=0}$. This result is important because one can now implement the estimator with a bank of time-invariant filters $\widetilde{q}_i(k)$, whose outputs we add.

$$\Lambda(\theta) = \sum_i \sum_k \widetilde{q}_i(\theta - k) y^*(k) y(k+i)$$

where $\widetilde{q}_i(k)$ is the negative of the ith diagonal of $\mathbf{Q}(0)$, time-reversed.

Two properties of $\mathbf{Q}(0)$ are important for further reducing the complexity. First, it is symmetric so that only the upper triangular part of the matrix needs to be evaluated. Secondly, some of the diagonals are zero, and need not to be considered. The estimator can be expressed as

$$\widehat{\theta}_{\mathrm{ML}} = \arg\max_\theta \left\{ \sum_{i \in I} \gamma_i(\theta) \right\}, \tag{6}$$

where $I = \{0, \ldots, L-1, N-L+1, \ldots, N+L-1\}$,

$$\gamma_i(m) = \Re \left\{ \sum_{k=-\infty}^{\infty} q_i(m-k) y(k) y^*(k+i) \right\}, \tag{7}$$

and

$$q_i(k) = \begin{cases} \tilde{q}_i^*(k) & \text{if } i = 0 \\ 2\tilde{q}_i^*(k) & \text{otherwise.} \end{cases}$$

The $q_i^a(k)$ and $q_i^b(k)$ in Figure 5 refers to the first and the second half of the $q_i(k)$ filters.

Estimator (6) suggests the implementation structure shown in Figure 5. First the products $y(k)y^*(k+i)$ are formed. These are fed into the filterbank where the outputs are summed, and the real part gives the log-likelihood function. The peak in the log-likelihood yields the time offset estimate.

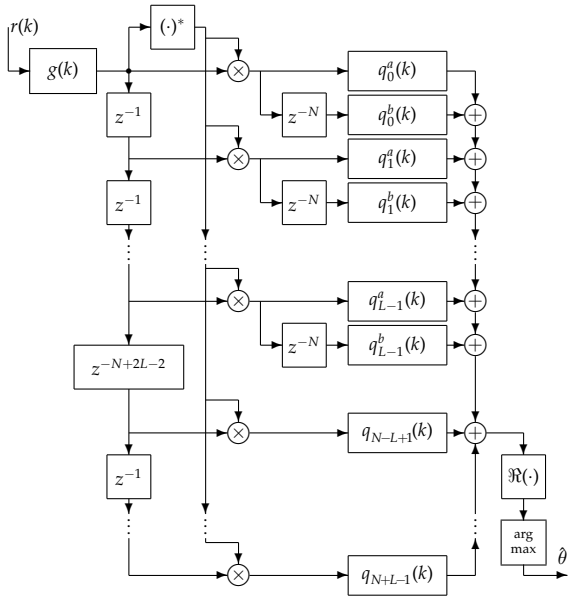

Figure 5: Structure of the estimator for dispersive channels.

4 Simulations

To compare the performance of the different estimators, a number of simulations have been performed. Although the estimator was derived with only one cyclic repetition, we now simulate it in an OFDM system with multiple cyclically extended symbols. The simulation system is an OFDM system with symbol length $N = 128$ and cyclic prefix length $L = 16$. The observation interval I_{obs} is of length $4N + 2L$, because θ has $N + L$ possible values, $\mathbf{Q}$ has dimension $N + L$ and the we choose a prefilter length of $2N$. In each simulation 50000 symbols are transmitted over a channel $h(n)$, which is assumed to be time-invariant, with impulse response

$$h(n) = \frac{1}{\sqrt{2.13}} \left(\delta(n) + 0.7\delta(n-6) + 0.8\delta(n-12)\right)$$

which has normalized energy.

We have simulated three estimators. As a reference we have the estimator from [4] which is designed for an AWGN channel (denoted AWGN in the figure). The second estimator is from Equation (3) which does the full matrix multiplication in the quadratic form (denoted Disp in the figure). The last estimator, from Equation (6) and shown in Figure 5, uses a prefilter and has a filterbank implementation of the quadratic form. For the simulations,

the prefilter in Equation (5) is calculated by a $2N$-point FFT, and thereby constrained to a total length of $2N$ samples. The impulse response is delayed with N samples, making the first N samples of the impulse response correspond to the non-causal filter taps.

In Figure 6, the errors in the estimated time offsets, $\widehat{\theta} - \theta$, are shown in histograms. The top subfigure shows the ML estimator for an AWGN channel [4]. The estimate $\widehat{\theta}_{\text{AWGN}}$ shows a considerable bias because of the dispersive channel. The two tops at -25 and 25 represent outliers that are more than 24 samples from the true θ. The center subfigure shows the estimates from Equation (3) (Disp). This estimator shows an unbiased behaviour. The bottom part, which shows the estimator in Figure 5, also shows an unbiased behaviour.

The mean square error, MSE, of the estimates for the different estimators is shown in Figure 7. Simulations were performed with SNR in the range 0 to 20 dB. The AWGN-based estimator has as expected the highest MSE. The two dispersion-based estimators shows a considerable smaller MSE, and are almost identical in performance up to SNR values of about 16 dB. There the prefilter-based estimator seems to reach an error floor, whereas the matrix-based estimator continues to give better performance. For such high SNR, where $\sigma_w^2 \ll \sigma_s^2$, the prefilter $g(k)$ in Equation (5) approaches the inverse filter to $h(k)$. Since the filter, $g(k)$, is limited to a length of $2N$, the impulse response is cut off at a point where the filter coefficients are not negligible, which causes the degradation in performance.

5 Summary

In this paper we derive the ML estimator for time offsets in a dispersive channel environment. The estimator is based on the redundancy introduced by the cyclic prefix and assumes knowledge of the channel impulse response.

By the proper structuring of the calculations and some approximations where the observation interval goes to infinity, we end up with a new estimator structure. The new structure consists of a linear prefilter and a correlating filterbank. By introducing a prefilter the dimension of the estimation problem can be reduced. Letting the observation interval go to infinity suggests a filterbank implementation of the estimator's quadratic form.

Simulations show that although we make some approximations, the performance of the new estimator structure is virtually indistinguishable from the performance of the estimator without approximations, for a large range of SNR's.

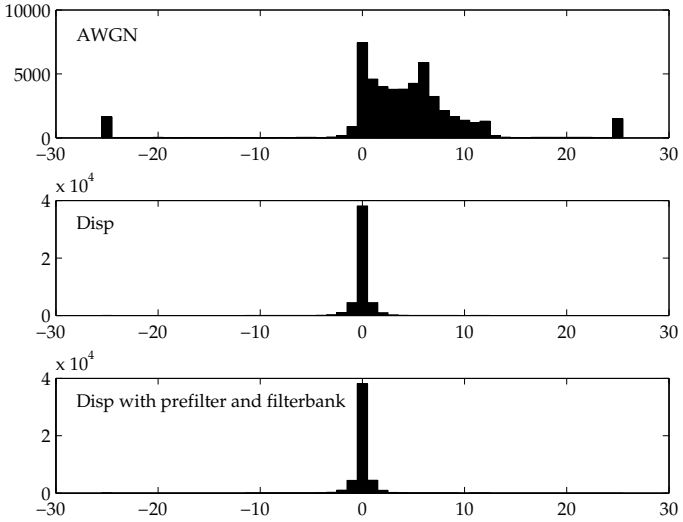

Figure 6: Histogram over the time offsets at SNR = 10 dB. Please note the difference in the vertical scale.

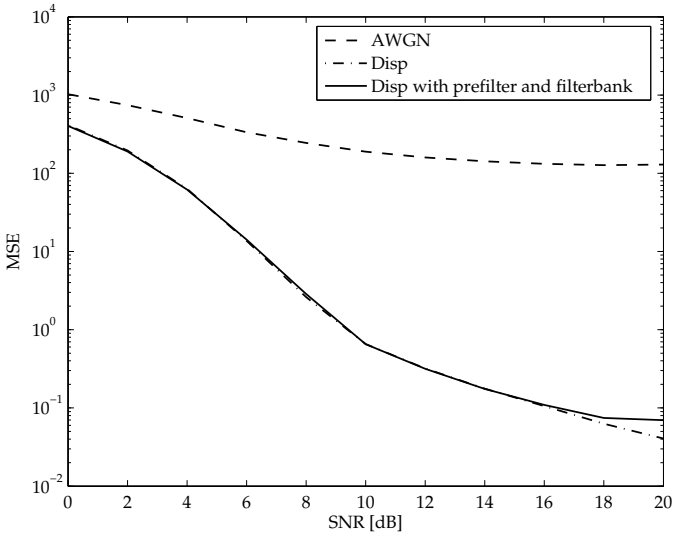

Figure 7: Estimators mean-square error as a function of SNR.

A Appendix

Inverse of $(\mathbf{A}+\mathbf{B})$

$$(\mathbf{A}+\mathbf{B})^{-1} = \mathbf{A}^{-1} - \mathbf{A}^{-1}\left(\mathbf{B} - \mathbf{B}(\mathbf{A}+\mathbf{B})^{-1}\mathbf{B}\right)\mathbf{A}^{-1}$$

Proof: (Note that only A needs to be invertible.)

$$\begin{aligned}
&(\mathbf{A}+\mathbf{B})\left(\mathbf{A}^{-1} - \mathbf{A}^{-1}(\mathbf{B} - \mathbf{B}(\mathbf{A}+\mathbf{B})^{-1}\mathbf{B})\mathbf{A}^{-1}\right) \\
&= \mathbf{I} + \mathbf{B}(\mathbf{A}+\mathbf{B})^{-1}\mathbf{B}\mathbf{A}^{-1} + \mathbf{B}\mathbf{A}^{-1}\mathbf{B}(\mathbf{A}+\mathbf{B})^{-1}\mathbf{B}\mathbf{A}^{-1} \\
&= \mathbf{I} + \mathbf{B}\mathbf{A}^{-1}(\mathbf{A}+\mathbf{B})(\mathbf{A}+\mathbf{B})^{-1}\mathbf{B}\mathbf{A}^{-1} - \mathbf{B}\mathbf{A}^{-1}\mathbf{B}\mathbf{A}^{-1} = \mathbf{I}
\end{aligned}$$

Bibliography

[1] T. Pollet, M. van Bladel, and M. Moeneclaey, "BER sensitivity of OFDM systems to carrier frequency offset and Wiener phase noise," *IEEE Transactions on Communications*, vol. 43, no. 2/3/4, pp. 191–193, Feb/Mar/Apr 1995.

[2] T. Pollet and M. Moeneclaey, "Synchronizability of OFDM signals," in *Proc. Globecom*, vol. 3, Singapore, Nov. 1995, pp. 2054–2058.

[3] J. G. Proakis, *Digital communications*, 3rd ed. New York, USA: Prentice-Hall, 1995.

[4] J.-J. van de Beek, M. Sandell, and P. O. Börjesson, "ML estimation of time and frequency offset in OFDM systems," *IEEE Transactions on Signal Processing*, vol. 45, no. 4, July 1997.

[5] A. Peled and A. Ruiz, "Frequency domain data transmission using reduced computational complexity algorithms," in *Proc. IEEE International Conference on Acoustics, Speech, and Signal Processing*, Denver, CO, USA, 1980, pp. 964–967.

[6] J.-J. van de Beek, P. O. Börjesson, M.-L. Boucheret, D. Landström, J. M. Arenas, P. Ödling, and S. K. Wilson, "Three non-pilot based time- and frequency estimators for OFDM," *Signal Processing*, vol. 80, no. 7, pp. 1321–1334, July 2000.

[7] M. Gudmundson and P.-O. Andersson, "Adjacent channel interference in an OFDM system," in *Proc. IEEE Vehicular Technology Conference*, vol. 2, Atlanta, GA, USA, Apr. 1996, pp. 918–922.

[8] P. Billingsley, *Probability and Measure*, 2nd ed. New York, NY, USA: John Wiley and Sons, 1986.

[9] S. M. Kay, *Fundamentals of Statistical Signal Processing: Estimation Theory*. Upper Saddle River, NJ, USA: Prentice-Hall, 1993.

Paper IX

Paper IX

The Cyclic Prefix of OFDM/DMT – An Analysis

Werner Henkel, Georg Tauböck, Per Ödling, Per Ola Börjesson,
Niklas Petersson, and Albin Johansson

We address the impact of a too short cyclic prefix on multicarrier systems such as Orthogonal Frequency Division Multiplex (OFDM) and Discrete MultiTone (DMT). The main result is that the intersymbol interference (ISI) and intercarrier interference (ICI) may be spectrally concentrated and analytical expressions showing this are given. A practical implication is, *e.g.*, that the cyclic prefix in some xDSL systems can be surprisingly short, as shown in one example of ADSL transmission.

 This work was partially financed by the Telecommunications program of the Swedish National Board for Industrial and Technical Development (NUTEK) and by the Austrian K*plus* program. It was initiated by Per Ödling while being with ftw.

1 Introduction

In this paper, we address the impact of a too short cyclic prefix in multicarrier systems [1]. The cyclic prefix removes the intersymbol interference (ISI) and intercarrier interference (ICI) [2]. The introduction of the cyclic prefix of length L, see Figure 1, gives a constant capacity loss, since the channel does no longer carry data for short periods of time. As such, one would like to minimize the length of the cyclic prefix, preferably maintaining performance. Common wisdom is to choose the cyclic prefix to be of roughly the same length as the channel (or system) impulse response, thus eliminating ISI and ICI. It is also well established that, if the tail of the impulse response contains only very little energy, it has little impact and can be considered zero allowing a shorter cyclic prefix. We show that, furthermore, the ISI and ICI can be spectrally concentrated and sometimes have limited or even zero impact on performance. Although this is not completely unknown among designers of DMT digital subscriber loop (DSL) systems, it has rarely been given a thorough analysis. Our attempt here is to provide an intuitive and immediate understanding of the mechanisms involved.

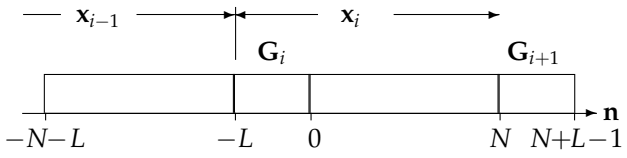

Figure 1: Symbol structures

We give a mathematical analysis of the ISI and ICI for a system with insufficient length of the cyclic prefix for the case when all the tones are used to transmit data in one direction, for instance in simplex communication or for a time-division duplex (TDD) system. This is done in Section 2. In Section 3, we present an example where the interference is strikingly concentrated in frequency.

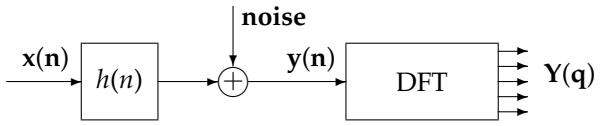

Figure 2: The system under analysis: the receiving end of a multicarrier system

2 Signal model and Interference Calculation

The interference that we are studying consists of two parts: the intersymbol interference (ISI) and the intercarrier interference (ICI). We start with analyzing the ISI, which can be derived in a more intuitive fashion. We will also see that the ICI is of very similar structure, and can be described with the same mathematics under our present assumptions.

Consider the transmission of symbols $x_i(n)$ through a channel with the impulse response $h(n)$ of length L_h. We extend our notations with an index i on the input sequence $x_i(n)$ as we need to distinguish between the input corresponding to the present symbol $y_i(n)$, which gives rise to the ICI, and the previous data $x_{i-1}(n)$ which causes the ISI[1]. The signal $x(n)$ is assumed to be zero mean with a variance of σ_x^2 and $x(L+1), x(L+2), \ldots, x(L_h-1)$ are assumed to be pairwise uncorrelated. The received signal, which is to be processed by the FFT,

$$y_i(n) = h(n) * x(n) = \sum_{\nu=0}^{L_h-1} h(\nu)x(n-\nu), \tag{1}$$

where $x(n)$ denotes the concatenation of all $x_i(n)$ up to the present symbol. A part of this signal will then be ISI from the previous symbol. Figure 3 illustrates the tails of the impulse response that are not covered by the cyclic prefix. Note that in contrast to Figure 1 not only the guard interval but also its counterpart at the end of the frame is highlighted (hatched) and labeled with **G**. The ISI that affects a symbol i from a symbol $i-1$ is

$$y_{\mathrm{ISI}}(n) = \sum_{\nu=L+1+n}^{L_h-1} h(\nu)x(n-\nu), \text{ with } 0 \le n \le L_h - L - 2\,. \tag{2}$$

In (2), we actually used the concatenated symbols in order to simplify the description.
The signal after the DFT, $Y_i(q)$, then becomes

$$\begin{aligned} Y_i(q) &= \sum_{n=0}^{N-1} y_i(n) e^{-j\frac{2\pi}{N}nq} \\ &= \sum_{n=0}^{N-1} \sum_{\nu=0}^{L_h-1} h(\nu)x(n-\nu)e^{-j\frac{2\pi}{N}nq}. \end{aligned} \tag{3}$$

[1]We do not consider the case where the evaluation frame at the receiver is positioned such that it has post- and precursors from both neighboring frames. In a real system, this could be the case. However, this would make the math lengthy and difficult to follow. Thus, in order to outline the fundamental properties, we decided to restrict this presentation to only postcursors from a preceding frame.

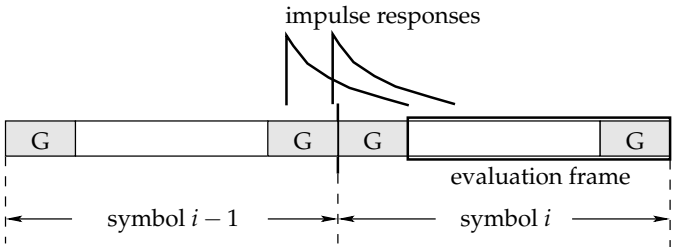

Figure 3: ISI from symbol $i-1$ to symbol i

With a cyclic prefix of length L, the residual ISI is determined as

$$\Upsilon_{\mathrm{ISI}}(q) = \sum_{n=0}^{N-1} \sum_{\nu=L+1+n}^{L_h-1} h(\nu)x(n-\nu)e^{-j\frac{2\pi}{N}nq} \tag{4}$$

$$= \sum_{n=0}^{N-1} \sum_{m=L+1}^{L_h-1-n} h(m+n)x(-m)e^{-j\frac{2\pi}{N}nq}\,. \tag{5}$$

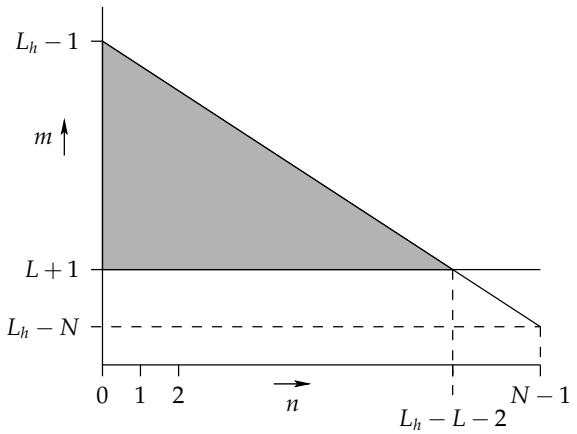

Figure 4: Summation area in (5)

Next, we interchange the two sums. Due to the dependence of n in the inner sum, we have to investigate the summation over the pair (n, m) in some more detail. Figure 4 shows the effective pairs that are used in the two sums. There, we assume that $L_h - N \leq L+1$, i.e., $N \geq L_h - L - 1$. This is a reasonable assumption. One would certainly not design a DMT (OFDM) system with a frame length shorter than the channel impulse response. While n

is increased, the upper limit of the inner sum $L_h - 1 - n$ is decreased accordingly. The lower limit $L + 1$ is reached ($L_h - 1 - n = L + 1$) when $n = L_h - L - 2$. If we now take the sum over m as outer sum, we obtain the upper limit for the inner sum over n as $L_h - L - 2 - (m - (L + 1)) = L_h - m - 1$ and thus,

$$Y_{\mathrm{ISI}}(q) = \sum_{m=L+1}^{L_h-1} x(-m) \sum_{n=0}^{L_h-m-1} h(m+n) e^{-j\frac{2\pi}{N}nq} \,. \tag{6}$$

Substituting $m + n = \mu$ yields

$$\begin{aligned} Y_{\mathrm{ISI}}(q) &= \sum_{m=L+1}^{L_h-1} x(-m) \sum_{\mu=m}^{L_h-1} h(\mu) e^{-j\frac{2\pi}{N}(\mu-m)q} \\ &= \sum_{m=L+1}^{L_h-1} x(-m) e^{+j\frac{2\pi}{N}mq} \cdot \underbrace{\sum_{\mu=m}^{L_h-1} h(\mu) e^{-j\frac{2\pi}{N}\mu q}}_{=:H_m(q)} \,. \end{aligned} \tag{7}$$

Note that the expression for $H_m(q)$ is actually the DFT of the tail of the impulse-response. The power spectral density $N_{\mathrm{ISI}}(q)$ after the FFT due to the intersymbol interference follows to be

$$N_{\mathrm{ISI}}(q) = E\{Y_{\mathrm{ISI}}(q) Y^*_{\mathrm{ISI}}(q)\} \tag{8}$$

$$= \sum_{m_1=L+1}^{L_h-1} \sum_{m_2=L+1}^{L_h-1} H_{m_1}(q) H^*_{m_2}(q) \; E\{x(-m_1)x^*(-m_2)\} \, e^{j\frac{2\pi}{N}(m_1-m_2)q} \tag{9}$$

$$= \sigma_x^2 \sum_{m=L+1}^{L_h-1} |H_m(q)|^2 \tag{10}$$

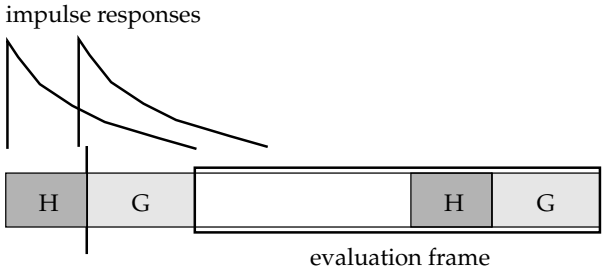

Figure 5: Hypothetic extension "H" of the guard interval "G" for computing the ICI

Remains now to calculate the ICI term. ICI would not be an issue if the guard interval would be big enough to fake the channel convolution as a

cyclic convolution within the frame that is evaluated by the receiver. Thus we just assume an extension of the guard interval that would null the ICI and compute its impact on the evaluation frame. Its negative would then be the ICI signal. The hypothetic frame extension is shown in Figure 5. The negated ICI signal is then similar to (2) and can be written as

$$y_{\mathrm{ICI}}(n) = -\sum_{\nu=L+1+n}^{L_h-1} h(\nu) x_i\left((n-\nu) \bmod N\right), \qquad 0 \le n \le L_h - L - 2\,. \tag{11}$$

Note that this time, (11) refers to only one input signal block x_i from which the hypothetical guard interval is taken. Correspondingly, we count modulo N to stay within this frame. In DFT domain, we obtain

$$Y_{\mathrm{ICI}}(q) = -\sum_{n=0}^{L_h-L-1} \sum_{\nu=L+1+n}^{L_h-1} h(\nu) x_i\left((n-\nu) \bmod N\right) e^{-j\frac{2\pi}{N}nq} \tag{12}$$

which corresponds to (4). If we further follow the steps in the derivation of the ISI result down to (10), we see that the only differences are the minus sign and that we count modulo N, staying within the same frame. The minus sign disappears with the squaring when computing the power spectral density. If we consider x_i instead of x, does not change the result, either, so that we obtain

$$N_{\mathrm{ICI}}(q) = N_{\mathrm{ISI}}(q) \tag{13}$$

and

$$N_{\mathrm{ICI+ISI}} = 2 \cdot \sigma_x^2 \sum_{m=L+1}^{L_h-1} |H_m(q)|^2\ . \tag{14}$$

ISI and ICI have the same power spectral density. This is an important first result that has relevance for practical time-domain equalizer algorithms (see, e.g., [3]).

3 Example

As a practical example we choose an ADSL transmission with an FFT length of $N = 512$ and a guard interval of $L = 32$ samples. We select the impulse response of a 4 km long loop of German 0.4 mm cables, which is shown in Figure 6, cutting non-causal precursors that are due to the underlying cable model. We see that it certainly has a portion exceeding the guard interval. If we compute the ICI and ISI components according to (10) and (13), we see in Figure 7 that the noise is predominantly disturbing low-frequency components. It has long been realized that the signal-to-noise ratio decreases

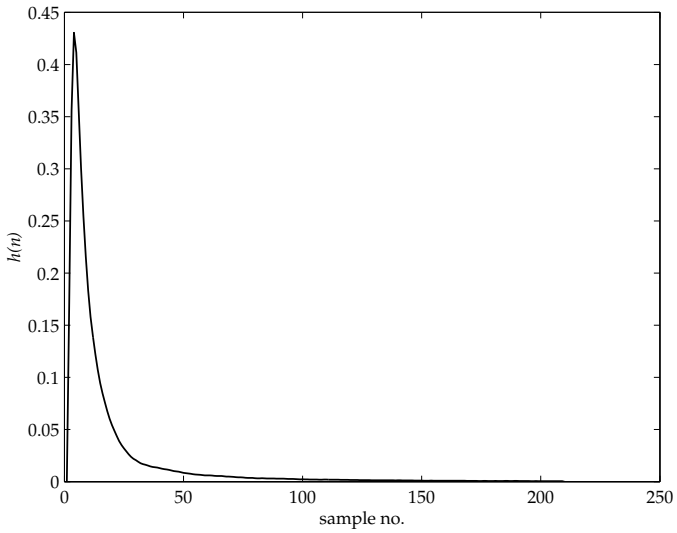

Figure 6: Impulse response of a 4 km, 0.4 mm loop

near DC, which was considered partly to be due to the leakage effect of the DFT which folds high-frequency noise components into the low-frequency range. The results in here now show that noise due to ISI and ICI is concentrated around DC as well.

4 Conclusions

We derived closed formulas for the intersymbol and interchannel interference power spectral density and found that they are actually the same. From a typical example we concluded that this noise will be concentrated around DC.

Bibliography

[1] J. A. C. Bingham, "Multicarrier modulation for data transmission: An idea whose time has come," *IEEE Communications Magazine*, vol. 28, pp. 5–14, May 1990.

[2] A. Peled and A. Ruiz, "Frequency domain data transmission using reduced computational complexity algorithms," in *Proc. IEEE International*

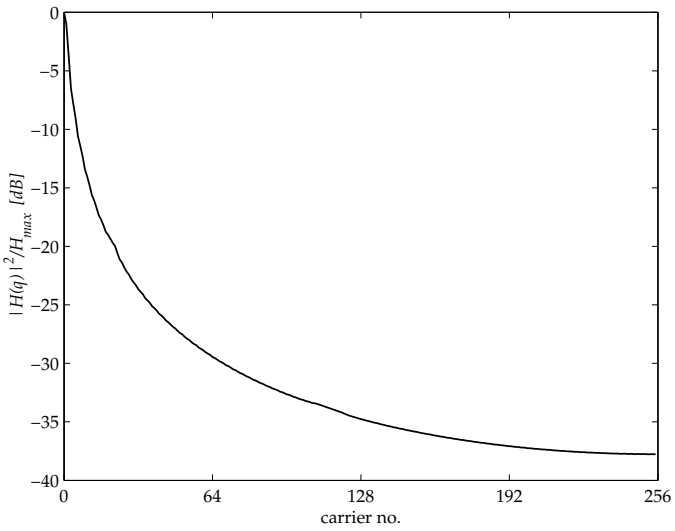

Figure 7: ISI and ICI power spectral density according to (10) and (13) normalized to its maximum ($|H(q)|^2 = \sum_{m=L+1}^{L_h-1} |H_m(q)|^2$)

Conference on Acoustics, Speech, and Signal Processing, Denver, CO, USA, 1980, pp. 964–967.

[3] W. Henkel and T. Kessler, "Maximizing the channel capacity of multicarrier transmission by suitable adaptation of the time-domain equalizer," *IEEE Transactions on Communications*, vol. 48, no. 12, pp. 2000–2004, Dec. 2000.